

A PROPOSED PRELIMINARY DESIGN FOR A SECOND  
GENERATION OF THE M.I.T. ROBOT, DATA COL-  
LECTING, SUBMARINE

James Standish Bunce

DUDLEY KNOX LIBRARY  
NAVAL POSTGRADUATE SCHOOL

A PROPOSED PRELIMINARY DESIGN FOR A SECOND GENERATION  
OF THE M.I.T. ROBOT, DATA COLLECTING, SUBMARINE

by

JAMES STANDISH BUNCE

B.S.M.E., TUFTS UNIVERSITY  
(1970)

SUBMITTED IN PARTIAL FULFILLMENT  
OF THE REQUIREMENTS FOR THE  
DEGREE OF OCEAN ENGINEER AND THE  
DEGREE OF MASTER OF SCIENCE IN  
NAVAL ARCHITECTURE AND MARINE ENGINEERING

at the  
MASSACHUSETTS INSTITUTE OF TECHNOLOGY

May, 1977

THESE  
B848



A PROPOSED PRELIMINARY DESIGN  
FOR A SECOND GENERATION OF THE M.I.T. ROBOT,  
DATA COLLECTING, SUBMARINE

by

JAMES STANDISH BUNCE

Submitted to the Department of Ocean Engineering on May 12, 1977, in partial fulfillment of the requirements for the Degrees of Ocean Engineer and Master of Science in Naval Architecture and Marine Engineering.

ABSTRACT

Students at M.I.T., under the supervision of Professor A. Douglas Carmichael, have developed a small, low cost, computer controlled, robot submarine, which is intended to follow preprogrammed course and depth instructions and collect subsurface oceanographic data. Since the first summer of testing in 1974, the submarine has undergone considerable further testing and improvement, mainly in its electronic control systems.

This work systematically re-examines the design of the robot submarine, placing particular emphasis on the Ocean Engineering aspects of the design. The intent is to determine how and where changes could be made to improve the robot's performance. The investigation leads to the presentation of a proposed preliminary design for a second generation of the M.I.T. robot, which incorporates these improvements.

Thesis Supervisor: A. Douglas Carmichael

Title: Professor of Power Engineering



## ACKNOWLEDGEMENTS

The author wishes to express his appreciation to Professor A. Douglas Carmichael, whose guidance and suggestions have contributed significantly to this thesis.

Thank you, also, to Teri and Jim Baskerville, whose work in typing this thesis was invaluable.



## TABLE OF CONTENTS

	<u>PAGE</u>
TITLE PAGE	1
ABSTRACT	2
ACKNOWLEDGEMENTS	3
TABLE OF CONTENTS	4
LIST OF FIGURES	6
LIST OF TABLES	9
NOMENCLATURE	12
INTRODUCTION	16
1. DESIGN APPROACH AND DESIGN CONSTRAINTS	22
1.1 Proposed Operating Scenario	22
1.2 Design Requirements	24
1.3 Design Philosophy	27
1.4 Design Approach	28
2. PRESENTATION OF THE PROPOSED PRELIMINARY DESIGN FOR THE SECOND GENERATION ROBOT SUBMARINE	31
2.0 General	31
2.1 Envelope	31
2.2 Propulsion System	35
2.2.1 Propulsor	35
2.2.2 Prime Mover and Drive Train	39
2.3 Energy Storage System	41
2.4 Pressure Hull and Structural Design	43
2.5 Control System	49
2.6 Robot Control Payload	50



## TABLE OF CONTENTS (Cont'd.)

	<u>PAGE</u>
2.7 Data Collection Payload	51
2.8 Auxiliary Systems	52
2.9 Submarine Integration	54
2.10 Summary of the Characteristics of the Proposed Second Generation Robot Submarine	56
3. OBSERVATIONS, CONCLUSIONS AND RECOMMENDATIONS	61
APPENDIX I SUMMARY OF THE CHARACTERISTICS OF THE ORIGINAL MIT ROBOT SUBMARINE	63
APPENDIX II ENVELOPE FORM TRADE OFF STUDY	71
APPENDIX III PROPULSION SYSTEM TRADE OFF STUDY	101
APPENDIX IV ENERGY STORAGE SYSTEM TRADE OFF STUDY	138
APPENDIX V PRESSURE HULLS CONFIGURATION TRADE OFF STUDY	157
APPENDIX VI CONTROL SYSTEM TRADE OFF STUDY	191
APPENDIX VII PRIMARY CONTROL PAYLOAD EQUIPMENT STUDY	200
APPENDIX VIII DATA COLLECTION PAYLOAD STUDY	207
APPENDIX IX TRIM AND BUOYANCY AUGMENTATION SYSTEM STUDY	211
APPENDIX X ROBOT SIZING ROUTINE	219
REFERENCES	251





## LISTING OF FIGURES

- Figure 1 Submarine Design process
- Figure 2-1 Resistance versus Speed for 9 foot Series 58 Form 4165
- Figure 2-2 Optimum speed through the Water versus opposing current velocity for constant auxiliary loads
- Figure 2-3 Inboard profile of proposed second generation robot configuration
- Figure 2-4 Cross section of Battery Compartment
- Figure 2-5 Cross section of Propulsion Motor Compartment
- Figure A1-1 Cutaway view of the first generation MIT Robot Submarine
- Figure A1-2 Inboard profile and section views of the first generation MIT Robot Submarine
- Figure A2-1 Profile of a Typical Laminar Flow Body
- Figure A2-2 Profile of Form 4165
- Figure A2-3 Profile of Form 4173
- Figure A2-4 Profile of Form 4166
- Figure A2-5  $v_p/v_E$  versus  $D_p/L$  for Series 58 Form 4165
- Figure A2-6  $v_p/v_E$  versus  $D_p/L$  for Series 58 Form 4173
- Figure A2-7  $v_p/v_E$  versus  $D_p/L$  for Series 58 Form 4166
- Figure A2-8 Resistance comparison between the first generation robot and the Form 4165 equivalent forms
- Figure A3-1 Contra-Rotating Propellers Driven by a Single Motor Through a Set of Epicyclic Reduction Gears
- Figure A3-2 Optimum Kaplan Propeller Series in Duct 19A Selection with Propeller RPM specified Using the Propeller Torque



## LISTING OF FIGURES (Cont'd.)

- Figure A3-3 Optimum Kaplan Propeller Series in Duct 19A  
Selection with Propeller RPM Specified  
using the Propeller Thrust
- Figure A3-4 Optimum Kaplan Propeller Series in Duct 19A  
Selection with Propeller Diameter Specified
- Figure A3-5 Propeller Duct for Ka 3-65 Screw Series in  
Nozzle No. 19A
- Figure A3-6 Typical Propeller Blade of Ka 3-65 Series
- Figure A3-7 Profile of Nozzle 19A
- Figure A3-8 Comparison of  $l-t$ ,  $l-w$ , and  $\eta_H$  as Calculated  
by Jackson's Formula and  
Formula Derived from Alternate data
- Figure A3-9 Propeller Optimization Curves for B 3-45  
Propeller with Propeller RPM Specified
- Figure A3-10 Propeller Optimization Curves for B 3-45  
Propeller with Propeller Diameter Specified
- Figure A3-11 Typical Motor Efficiency for a Pressure  
Compensated DC Motor
- Figure A3-12 Performance Curves for First Generation Robot  
Propulsion Motor
- Figure A5-1 Typical Pressure Hull Configuration and  
Nomenclature
- Figure A5-2 Typical Stiffening Frame Nomenclature
- Figure A6-1 Inboard Detail of Proposed Steerable Ducted  
Propeller
- Figure A6-2 Cross section views of Proposed Steerable  
Ducted Propeller
- Figure A9-1 Schematic Diagram of Proposed Automatic Trim  
System
- Figure A9-2 Schematic Diagram of Proposed Buoyancy Augmenta-  
tion System



## LISTING OF FIGURES (Cont'd.)

Figure A10-1 Relationships Between Cylindrical Pressure  
Hull Parameters and Form 4165 Envelope  
Length



## LISTING OF TABLES

Table 2-1	Offsets for 9 foot series 58 Form 4165
Table 2-2	Summary of Main Pressure Hull Dimensions
Table 2-3	Preliminary weight and Moment Balance for the proposed Second Generation Submarine
Table 2-4	Summary of the characteristics for the proposed Second Generation Robot Submarine
Table A2-1	The Geometrical Parameters for Models of Series 58
Table A2-2	Net Residual-Resistance Coefficients for Series 58 Forms at Deep Submergence
Table A2-3	Offsets for Form 4165
Table A2-4	Offsets for Form 4173
Table A2-5	Offsets for Form 4166
Table A2-6	Resistance Comparison for Series 58 Form 4165, 4173, and 4166 on the Basis of Envelope Volume
Table A2-7	Resistance Comparison for Series 58 Form 4165, 4173, and 4166 on the Basis of Pressure Hull Volume
Table A3-1	Propeller Blade Data for Ka Series Propellers
Table A3-2	Propeller Blade Offsets for Ka Series Propellers
Table A3-3	Use of Optimum B 3-45 Screw Selection Data
Table A3-4	Tabulated Data of $P/D$ , $J$ , and Propeller Efficiency versus $K_T/J^4$ or $K_Q/J^5$ , for Optimum Diameter of B 3-45 Screw Series at a Reynold's Number of $2 \times 10^6$ if Propeller RPM is Specified





## LISTING OF TABLES (Cont'd.)

Table A3-5	Tabulated Data of P/D, J, and Propeller Efficiency versus $K_T/J^4$ , or $K_Q/J^5$ , for Optimum Diameter of B 3-45 Screw Series at a Reynold's Number of $2 \times 10^7$ if Propeller RPM is Specified
Table A4-1	Characteristics of Candidate Batteries
Table A4-2	Characteristics of Various Production Silver-Zinc Batteries
Table A4-3	Characteristics of Various Production Silver-Cadmium Batteries
Table A4-4	Characteristics of Various Production Nickel-Cadmium Batteries
Table A4-5	Characteristics of Various Production Deep Discharge Lead-Acid Batteries
Table A4-6	Characteristics of Various Production Sealed Lead-Acid Batteries
Table A5-1	Characteristics of available 6160-T6 Aluminum Alloy Pipe
Table A5-2	Stiffened Cylindrical Pressure Hull Program Listing
Table A5-3	Sample Output from Cylindrical Pressure Hull Program
Table A8-1	Size and Weight of Various Models Edgerton Deep Sea 35mm Photographic Systems
Table A10-1	Speed versus Power and Optimum Speed Calculations Program Listing



LISTING OF TABLES (Cont'd.)

Table A10-2 Sample output from Speed versus Power and  
Optimum Speed Calculation Program

Table A10-3 Summary of Robot Sizing Routine Steps



## NOMENCLATURE

$A_e / A_o$	Propeller Expanded Area Ratio
$B$	Total Submarine Buoyancy
$B_{PH}$	Pressure Hull Buoyancy
$B_R$	Residual Buoyancy = $B - B_{PH}$
$C_T$	Total Drag Coefficient = $\frac{R_T}{\frac{1}{2} \rho V^2 S}$
$C_f$	Frictional Drag Coefficient
$\Delta C_f$	Surface Roughness Correction
$C_r$	Residual Resistance Coefficient
$C_p$	Prismatic Coefficient
$D_p$	Maximum Diameter of Pressure Hull
$D_{pr}$	Propeller Diameter
$D = D_{shell}$	Inside Diameter of Main Pressure Hull
$D_x$	Maximum Envelope Diameter
$E$	Hull Material Modulus of Elasticity
$EHP_{BH}$	Bare Hull Effective Horsepower
$EHP$	Appended Hull Effective Horsepower
$E_T$	Total Energy Storage Capacity
$g$	Acceleration Due to Gravity
$J$	Propeller Advance Ratio = $\frac{V_A}{n D_{pr}}$
$K_T$	Propeller Thrust Coefficient
$K_Q$	Propeller Torque Coefficient
$L$	Envelope Length



$L_p$	Length of Cylindrical Section of the Pressure Hull
$L_{FWD}$	Length of Forward Compartment
$L_{BAT}$	Length of Battery Compartment
$L_{AFT}$	Length of Aft Compartment
$L_f$	Pressure Hull Stiffening Frame Separation
$N$	Propeller RPM
$n$	Propeller RPS
$P$	External Pressure
$P/D$	Propeller Pitch Diameter Ratio
$P_o$	Auxiliary Electric Load
$PC$	Propeller Propulsive Coefficient $= \eta_H \times \eta_o \times \eta_{rr}$
$Q$	Propeller Torque
$Re$	Reynold's Number
$R_T$	Bare Envelope Drag
$R_{TA}$	Appended Envelope Drag
$SHP$	Shaft Horsepower
$S$	Bare Hull Wetted Surface
$S_t$	Appendage Wetted Surface
$T$	Propeller Thrust
$t$	Thrust Deduction Coefficient
$t_{shell}$	Wall Thickness of Cylindrical Pressure Hull





$t_{\text{bulk}}$	Thickness of Internal Pressure Hull Bulkheads
$V = V_R$	Submarine Speed Through the Water
	$V_R = V_T - V_C$
$V_T$	Submarine Speed Over Ground
$V_C$	Ocean Current Velocity
$V_A$	Propeller Speed of Advance
	$= (1-w) V$
$V_E$	Envelope Volume
$V_P$	Subtended Pressure Hull Volume
$V_R$	Envelope Volume Not Enclosed by the Pressure Hull
$W$	Submarine Dry Weight
$w$	Wake Fraction
$X$	Distance Measure From Submarine Nose
$Y$	Offset From Body Axis of Symmetry
$z$	Number of Propeller Blades
$\eta_o$	Propeller Open Water Efficiency
$\eta_{rr}$	Propeller Relative Rotative Efficiency
$\eta_H$	Hull Efficiency $= \frac{1 - t}{1 - w}$
$\eta_{oa}$	Overall Propulsion System Efficiency
$\eta_{\text{drive train}}$	Drive Train Efficiency
$\eta_{\text{motor}}$	Propulsion Motor Efficiency
$\mu$	Poisson's Ratio or Permeability
$\nu$	Fluid Kinematic Viscosity



$\rho$	Fluid Mass Density
$\sigma_y$	Yield Stress of Hull Material



## INTRODUCTION

Man has plied the sea's surface for thousands of years, using it as a source of food and wealth and as an avenue of transportation. The sea's surface, however, has been a barrier to the search and exploitation of the vast expanse of water which lies below. References [1] and [2] detail the history of man's attempts to penetrate beneath the surface. This history recounts the use of crude underwater breathing apparatus by Alexander the Great as early as 334 B. C. Development was slow, though, for it was not until 1932, when Otis Burton dove to 900 meters, that men had explored below 300 feet. This development pace is in sharp contrast to the history of powered flight, which proceeded from Kittyhawk to the first lunar landing in only 66 years.

Since 1932 research submersible development proceeded steadily through the gasoline filled ocean balloons of the late 1950's such as Trieste, to the more mobile self-propelled submarines such as Alvin [3] or Aluminaut [4]. These vehicles were designed to carry men to the depths so they could get a first hand look and with the use of various devices, such as mechanical arms and television cameras, could begin to collect samples, record data, or even work at depths where man had been unable to previously. These submersibles are very sophisticated, with life support systems, communications, highly trained crews, and extensive surface support vehicles. As a result, they are very expensive to



operate and maintain. Current costs for work submersibles used by the oil industry are in the neighborhood of \$20,000 per day. These submarines are also limited in speed and range and many were designed for specific missions and their usefulness outside of this area is severely limited as noted in [5]. Originally these submersibles were intended for research, but the recent interest in the ocean depths as a source of resources, especially in the search for oil deposits, has led to the use and further development of submersible vehicles as work vessels.

The costs, limitations, and various other factors involved with manned submersibles led to development of various tethered submersibles such as CURV III [6] or the RCV developed by Tetra Tech. These vehicles are tethered by cable to a surface ship where an operator controls the vehicle remotely. Self propelled and towed designs have been developed and they are capable of tasks which range from picture taking to work performed by remote control mechanical arms. They vary in size from the 400,000 pound (dry) Sea Probe to the very small RCV.

These tethered submersibles do have certain advantages and disadvantages. They do not carry men and thus, do not have to carry the life support systems, but this can also work to their detriment, since control of the vehicle must be accomplished remotely from the surface, which can result in a certain amount of degradation. These





vehicles also must carry the necessary cable around on large drums which get larger and heavier as the depth increases. These requirements introduce significant limitations on the use of these vehicles.

In part in response to the previously mentioned need for data collecting submersibles, the limitations of the manned and tethered vehicles and advancing technology a new type submersible has entered the picture, the robot submarine. This is a vehicle which has some of the better attributes of each of the aforementioned types without some of the drawbacks.

The robot submarine is an unmanned, computer controlled, mobile, submarine which is either preprogrammed or guided by prepositioned acoustic transmitters. These vehicles are untethered free swimmers whose mission is usually underwater data collection, though they could certainly be employed to transport tools, etc., to divers operating at depths. Generally the mission is only limited by the degree of control one can exercise over the vehicle.

The concept of an unmanned robot submersible is certainly not new. U. S. Patent No. 1,868,948, dated April 4, 1931, details a locomotor for conveying items such as cables beneath ice [2]. The computer technology required to control the vehicles has, however, just recently progressed to the point where computer control of a submersible has become feasible and practical.



Reference [7] provides a listing of the non-military undersea vehicles in use throughout the world as of 1976. The report lists 100 manned submersibles and 55 unmanned in operation or under construction. Of the unmanned vehicles, only five (5) are of the untethered "robot" variety. [8] and [9] describe two of these vehicles which have been or are being developed. In addition, [10] provides a discussion of a vehicle currently being designed by the Navy Research Laboratories (NRL) for long range collection of data in the oceans. This last vehicle is certainly the most ambitious of all robot vehicles considered to date.

Of particular interest to this thesis, however, is the robot submarine originally developed by MIT as an undergraduate summer project. Appendix I provides a brief introduction to the design and capabilities, while [11], [12], [13], [14] and [15] give a more detailed account of the MIT robot.

Briefly, the MIT robot is a small (250 pound, dry weight) computer controlled vehicle designed to operate in a marine environment according to preprogrammed instructions, collecting and recording various sorts of data as it proceeds.

The MIT robot is of particular interest to this thesis since the goal of this work is to develop a preliminary design for a second generation of this data collecting robot submarine. This preliminary design shall be based in



part on experience gained during the design and operation of the first generation MIT robot submersible, "Albertross", and also on studies of the various aspects associated with the submarine's subsystems. The preliminary design presented will be complete in sufficient detail to establish the feasibility of the proposed vehicle, but will not necessarily include sufficient detail to allow production of all the vehicle's components.

The major effort of the following design is in the Ocean Engineering related areas of the vehicle. These areas specifically include the following:

- 1) External hull form
- 2) Propulsion System (propulsor, transmission, and primemover)
- 3) Pressure hull and overall structural design
- 4) Energy storage system
- 5) Auxilliary Systems (ballasting and emergency systems)
- 6) Vehicle control
- 7) Overall Vehicle Integration (Hydrostatics, weight and moment computations, etc.)

Details of the onboard computer design and operation will not be investigated, nor will the specifics of other internal electronic components such as the autopilot or various sonar systems. These areas will be studied only to establish reasonable size, weight, and power requirement



estimates for these components which will then be used to size the vehicle. A similar approach will be used to evaluate prospective data collection payload items such as side scan sonars or photographic equipment. Candidate components will be evaluated for their impact on vehicle size and configuration and the feasibility and suitability of their inclusion into the design.

In summary, the intention of this thesis is not to expound on the theories of robotics, the possibility of incorporating artificial intelligence concepts into the control of a submerged robot vehicle, nor to enter into the manned versus unmanned debate which is raised in [2], but rather to reevaluate the naval architectural and marine engineering aspects of such a vehicle. The end result of this thesis shall be the presentation of a feasible preliminary design for a second generation of the MIT robot submarine which meets the established design requirements and thus is able to carry out various data collection missions in the hydrospace environment. The proposed design is not intended to be the end all of all robot submarines, but will essentially be a reevaluation and improvement on the first generation design.





## CHAPTER 1

## DESIGN APPROACH AND DESIGN CONSTRAINTS

Before commencing the development of a design there must be a good picture of the problem at hand. This will lead to the establishment of a design approach and to development of a consistent method for making the required decisions which will eventually result in a well balanced design.

For the specific problem at hand it is necessary to first understand the intended use of the proposed vehicle. This is accomplished by first establishing specific design goals or requirements which constrain and guide the design process. Finally, a design philosophy should be evolved which aids in making trade off decisions. The statements of these three initial design facets follow:

## 1.1 Proposed Operating Scenario

The second generation robot submarine is intended to operate in a fashion very similar to the first generation robot. Changes will principally consist of improvements in the capabilities over those of the original robot.

The second generation robot is intended to be a small, easily transportable, untethered, unmanned, computer controlled submersible designed to collect various types and forms of data in an aquatic environment. The submersible may be operated from a shore or waterborne launch platform in either fresh or salt water. Mission instructions are fed



to the vehicle's onboard computer via a physical data link between the robot and the launch station. This process may be performed while the vehicle is either wet (in the water) or dry. Upon mission commencement the submarine will use its autopilot controller to navigate using dead reckoning techniques in accordance with the previously loaded instructions. Detailed navigation and tracking of the submarine's position will be accomplished by equipment at the launch site with the aid of a time synchronized pinger located on the vehicle. The launch site is assigned the tracking function since it is better suited to accomplish the navigation task than the robot is itself. To assist the navigation process and to provide better control to the submarine, a command data link shall be incorporated which allows update commands from the tracking station to be transmitted to the submarine. This capability enables the operators to change the onboard instructions during a mission and even order mission termination should conditions warrant. This command capability becomes more and more important as the mission durations increase. Data collected by the robot need not in turn be transmitted to the operator by remote return data link, but will be offloaded at the end of a mission.

For a particular mission the robot may be fitted with a variety of data collection components which could include side scan sonar, photographic equipment or oceanographic data collectors as determined necessary for a



particular mission. This concept of equipment flexibility allows one hydroframe to be used for a variety of tasks, thus enhancing the vehicle's overall usefulness. The data collection function is, after all, the reason for the submarine's existence, and flexibility in this area means the robot will not outlive its usefulness should the one function it was designed to perform change.

The submarine is designed to be launched manually by a team of four men or with mechanical assistance, but will not require special launch apparatus. Additionally, launching will only be performed in relatively calm seas and during daylight. Accordingly, mission durations will not exceed approximately fifteen hours.

## 1.2 Design Requirements

The original MIT robot submarine was conceived as a small, easily transportable, untethered, unmanned submersible. Its mission was to carry data sensors and recorders to the depths. The submarine was intended to be launched and recovered by four men, and therefore, the vehicle would be easily transported. These size and weight limitations add flexibility to the robot's use, but also place limitations on the submarine's capabilities.

The aforementioned aspects of the original robot's design will be retained as design requirements for the second generation robot. Additionally, the following specific design requirements are intended to better define the con-



straints on the design.

1. Vehicle gross weight dry shall be less than 350 pounds.
2. Payload capability devoted to data collection equipment shall be at least 50 pounds dry.
3. The vehicle shall be designed to operate at depths down to 1,000 feet (continental shelf) with a factor safety for pressure vessel collapse of 1.5.
4. Maximum operating speed; 3 to 7 knots.
5. Fifteen (15) hours maximum submerged endurance.
6. The vehicle shall be capable of operation in salt or fresh water.
7. The exterior hull form (envelope) shall be selected to provide reduced drag and also provide extensive use of its enclosed volume for mission related functions and not just as free flooded volume.
8. Pressure hulls shall be able to be opened and resealed readily to provide easy access to installed equipment.
9. No mechanical linkages shall penetrate large pressure hulls. Components which require a pressure housing through which a mechanical linkage must penetrate should have their own pressure housings to reduce flooding, should





the mechanical seal fail.

10. All pressure hulls and housings shall be equipped with sensors to detect water leaks and signal mission termination.
11. The vehicle shall be designed to be slightly positively buoyant at design operating depth.
12. The vehicle shall be able to increase its buoyancy at depths down to 1.5 times the maximum operating depth to enable the submarine to surface in an emergency.
13. The vehicle shall be able to be readily trimmed to zero degrees roll or pitch during constant speed straight line motion. This system must be able to perform this function in any operating environment.
14. The robot shall not have to make rapid course changes, hence directional stability of the vehicle shall be stressed.
15. Space weight and power allocations shall be made for a collision avoidance sonar compatible with the submarine's maneuvering characteristics.
16. An alternative power source shall be provided to supply power to vital systems such as the computer in case of primary power source failure.



### 1.3 Design Philosophy

The following elements of design philosophy are provided to offer guidance in addition to the design requirements which may prove useful in making trade off decisions.

1. Survivability of the submarine in the event of component failure shall be strongly stressed
2. Conservative design predictions should be used in selecting components. This should lead to a final design which is at least as capable as predicted.
3. An effort shall be made to reduce risks of failure when selecting components and developing designs.
4. Component capabilities must be viewed with a critical eye to their impact on the overall design. Small, low power, lightweight components are the most desirable.
5. An effort shall be made to keep the center of gravity low to improve surfaced and submerged righting moments.
6. Symmetry of the envelope shall be stressed to reduce undesirable hydrodynamic effects. Also, envelope openings and other drag increasing factors should be minimized.
7. Simplicity should be stressed as much as



possible in the design to eliminate complex systems with multiple failure modes.

#### 1.4 Design Approach

The operating scenario, design requirements and design philosophy have defined the problem. The next phase is to develop a method to solve the design problem in an orderly fashion which yields the best feasible design. The problem must be divided into smaller parts for study and then the studies reintegrated to yield the final overall design. The individual parts, however, are not always independent, and the best solution in one area is not always compatible with the best in another area. The designer must then go back and resolve the conflict, but in turn, this can cause another conflict which must be resolved, and so on and so forth. The designer must perform an iterative procedure going through all the phases of the design in turn and resolving conflicts until he has a solution which is satisfactory. This iterative design process is illustrated by Figure I. As represented, this process does not always have a well defined starting point.

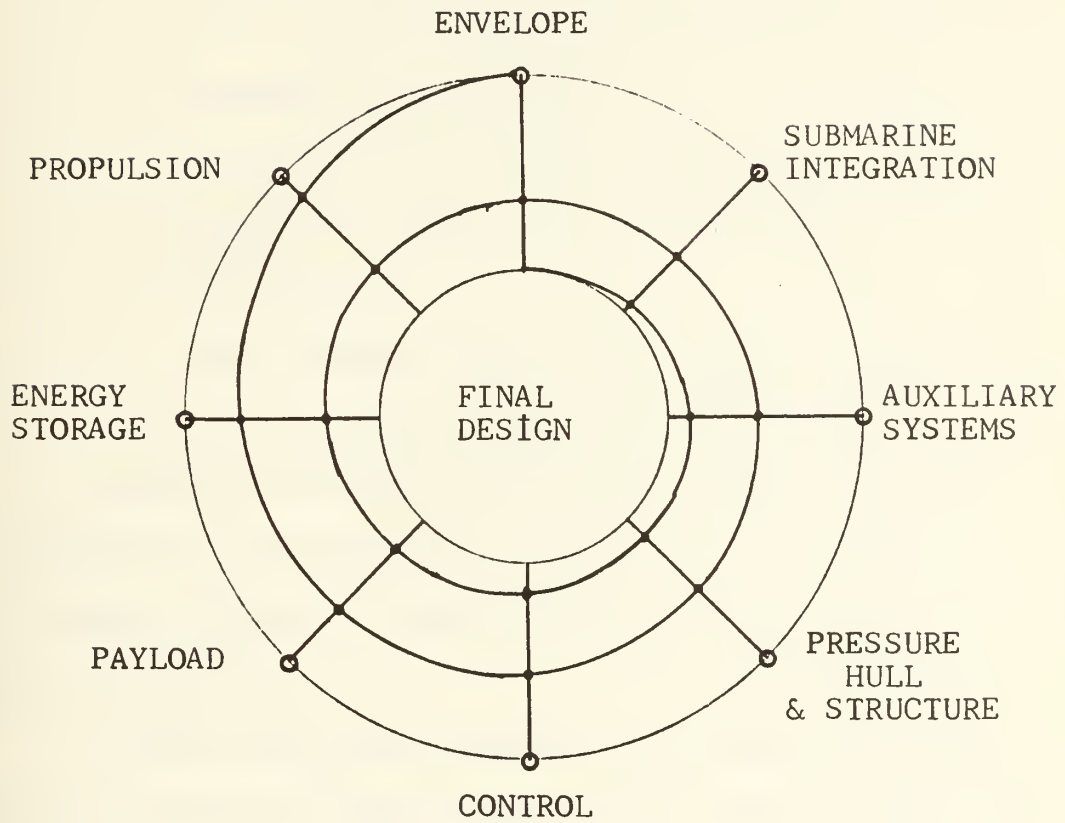
For the purpose of this design the problem was divided into nine parts as follows:

1. Envelope - the external hull form
2. Propulsion System - includes propulsor, transmission, and prime mover
3. Energy Storage System - the storage method



FIGURE 1

## SUBMARINE DESIGN PROCESS







for energy required by onboard electronics and the propulsion system

4. Pressure Hull and Structural Design
5. Control System - brief evaluation of vehicle controllability and control system
6. Control Payload Equipments - those equipments vital to control of the robot such as the computer and autopilot
7. Data Collection Payload Equipments - those equipments which are related solely to data collection
8. Trim, Ballast and other Auxilliary Systems
9. Overall Submarine Systems Integration.

Supporting studies conducted in these nine areas are presented in Appendices II through IX. The results of these studies led to the chosen configuration which is presented in Chapter Two.

During the development of the design, techniques employed by military submarine designers shall be employed where practical, since that problem is quite similar to the one at hand and those techniques have been developed during many years in the development of new military submarines.



CHAPTER 2  
PRESENTATION OF THE PROPOSED PRELIMINARY DESIGN  
FOR THE  
SECOND GENERATION ROBOT SUBMARINE

2.0. The configuration presented here is based on the results of the trade off studies and design methods presented in Appendices II through X. The proposed design is discussed in sections which correspond to the key design elements identified in Figure 1. Detail drawings of the selected configuration are presented in Section 2.10.

2.1. Envelope

The envelope is the external hull form which determines the drag and overall size of the vehicle. The envelope selection was made on the basis of the trade off studies presented in Appendix II. Three hull form types were originally considered.

1. Torpedo hull form
2. Laminar flow hull form
3. Fully turbulent flow hull form.

The attributes of these three categories were investigated and the fully turbulent flow Series 58, Form 4165 hull form was selected as the best envelope for this application. The comparison was based on resistance of different forms with the same total envelope volume and with the same volume



cylindrical pressure hull carrying capability. The Form 4165 was best in both respects.

After selection of the form, the sizing of the envelope posed a considerable problem. It was decided that the enclosed volume in a single cylindrical pressure hull would be the most desirable quality to try to optimize. For the Form 4165, at the very best, a cylindrical pressure hull could only occupy fifty seven per cent of the envelope volume. It was felt that this larger pressure hull volume would allow maximum space for the various electronics which perform the robot's tasks, and still leave sufficient space in the wet sections of the envelope for any desired instruments.

With the previous goal in mind, several envelope pressure hull combinations were considered. An envelope length of nine feet would hold a cylindrical pressure hull, constructed as discussed in Appendix V, which would occupy the greatest percentage of the envelope volume possible. This configuration would allow the minimum sized envelope for a given enclosed pressure hull volume to be used. A check of the required pressure hull volume, as discussed in Appendices III and VII, indicated the proposed configuration would be sufficient. Additionally, an estimate of the dry weight of the vehicle indicated such a configuration would be just under the maximum weight limit of 350 lbs. The nine foot size was, therefore, selected.



The hull form parameters for the selected Series 58 Form 4165 are as follows:

$$L = 9.0 \text{ ft.}$$

$$D_x = 1.29 \text{ ft.}$$

$$L/D_x = 7.0$$

$$C_p = .60$$

$$V_E = 7.01 \text{ ft.}^3$$

$$S = 26.81 \text{ ft.}^2$$

The offsets for the envelope are presented in Table 2-1.

The envelope will be constructed of fiberglass reinforced plastic laid up in a female mold. The mold will only be built for one half side of the envelope, since the two sides are identical. This construction method is widely used by commercial kayak and boat manufacturers. It yields a remarkably strong shell with a good surface finish quite easily.

The appended drag of the envelope, assuming nine per cent additional wetted surface due to appendages, was calculated using the computer program presented in Appendix X.





TABLE 2-1 OFFSETS FOR 9 FOOT SERIES 58 FORM 4165

X	Y	X	Y
0.00	0.000	4.68	0.618
.18	.183	4.86	.609
.36	.260	5.04	.600
.54	.318	5.22	.589
.72	.367	5.40	.577
.90	.409	5.58	.564
1.08	.445	5.76	.549
1.26	.477	5.94	.534
1.44	.505	6.12	.518
1.62	.530	6.30	.500
1.80	.548	6.48	.481
1.98	.571	6.66	.461
2.16	.587	6.84	.440
2.34	.601	7.02	.417
2.52	.613	7.20	.393
2.70	.622	7.38	.368
2.88	.630	7.56	.341
3.06	.636	7.74	.312
3.24	.640	7.92	.282
3.42	.642	8.10	.250
3.60	.643	8.28	.215
3.78	.642	8.46	.178
3.96	.640	8.64	.137
4.14	.636	8.82	.080
4.32	.631	9.00	0.000
4.50	.625		

X Distance in Feet from the Forward Perpendicular

Y Distance in Feet from the Axis of Symmetry



The predicted sea water drag versus speed for this appended envelope is presented in Figure 2-1.

## 2.2 Propulsion System.

The propulsion system is made up of the propulsor, drive train, and prime mover. These elements were studied in detail as presented in Appendix III.

### 2.2.1 Propulsor.

Three alternative propulsors were considered:

1. Contra-rotating propellers
2. Ducted propellers
3. Conventional open screw

The contra-rotating propellers were eliminated from contention due to the complexity of their drive train, and problems associated with the design of the screws.

The accelerating inflow ducted propeller offered the prospect of propeller protection provided by the duct and reduced propeller induced vibration. The efficiency of this alternative, however, was low in comparison with the open water propeller. The possibility does exist, though, to use a steerable version of the ducted propeller for steering. In this configuration, the normal control surfaces, and their drag, could be partly eliminated. A comparison between the steerable ducted propeller and an open screw with conventional control surfaces showed the



FIGURE 2-1 RESISTANCE VERSUS SPEED FOR 9 FOOT SERIES 58 FORM 4165





ducted propeller will require less power when compared with the open propeller driving a body with forward diving planes and tail control surfaces. If the forward driving planes could be removed, however, and the open screw propelled vehicle operated with only the tail control surfaces, then the open screw requires less power.

The selection required a study of the control problem as presented in Appendix VI. This study concluded that the forward diving planes could be eliminated. It also determined that the steerable ducted propeller involved a complex mechanical arrangement with a considerable risk. The open B-45 screw was, therefore, chosen as the best propulsor for the robot.

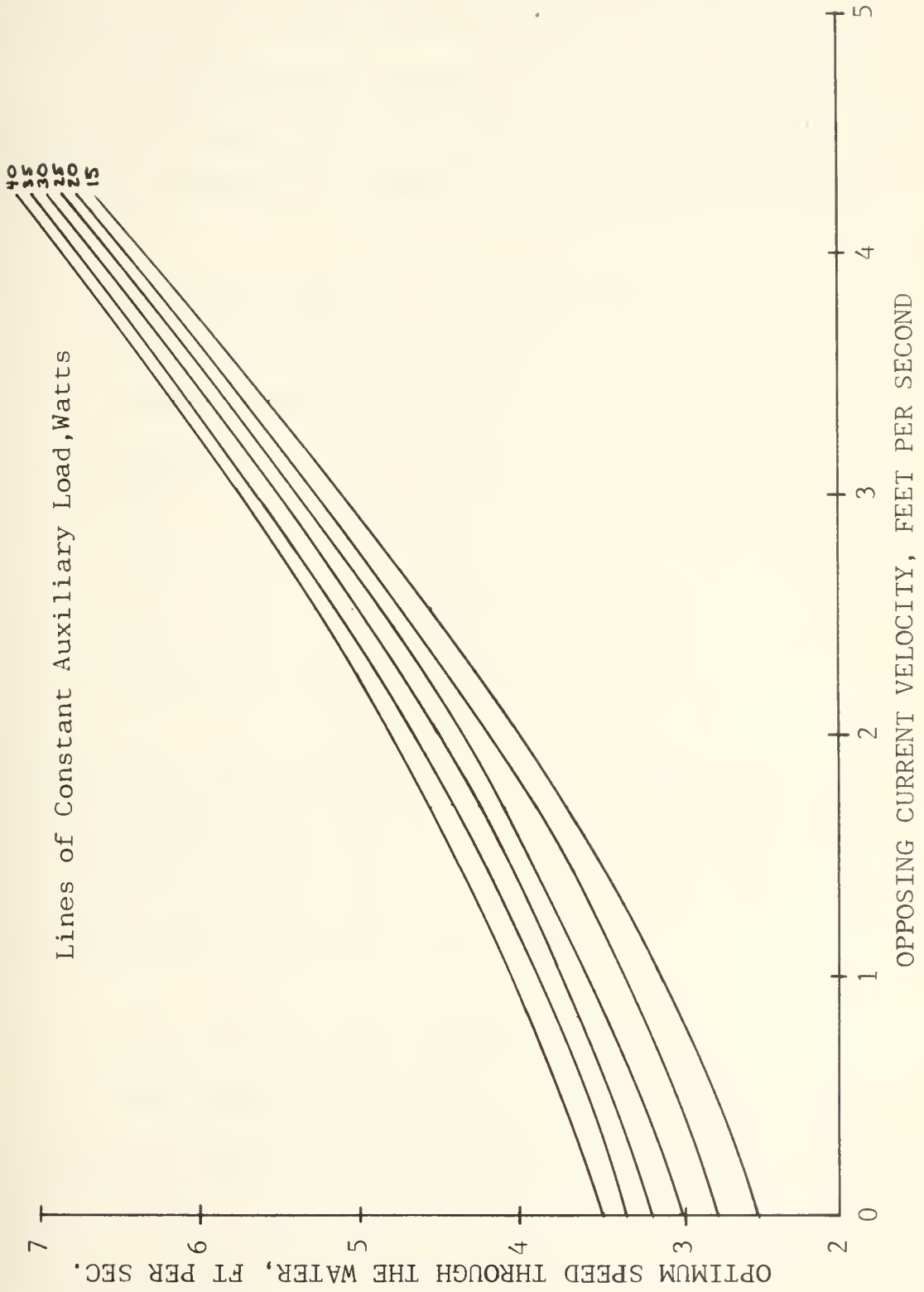
In order to select the propeller, the desired operating speed has to be known. Appendix X presents a computer program which calculates the most economical speed for the robot based on vehicle drag criteria, auxiliary electric load, and ocean current velocities. These data were run through the program for several assumed auxiliary loads and different current velocities. The results are shown in Figure 2-2. It is very evident that the optimum speed is more dependent on the opposing current velocity than the auxiliary load. Unfortunately, the opposing current velocity is also the more variable of the two parameters.

To make the best speed prediction, an opposing current of two knots and auxiliary load of 30 watts were





FIGURE 2-2 OPTIMUM SPEED THROUGH THE WATER VERSUS  
OPPOSING CURRENT VELOCITY FOR CONSTANT AUXILIARY LOADS





assumed. With these assumptions, the optimum speed was determined to be 3.5 knots, which was felt to be realistic.

With the design operating speed chosen, the propeller selection was made using the method from Appendix III. The selected propeller characteristics are as follows:

Screw designation: B Series 3-45

Number of Blades: 3

Expanded area ratio: .45

Diameter: .9 ft.

P/D: 1.2

Design RPM: 100

$\eta_o$ : .70

$\eta_{rr}$  assumed: 1.00

An attempt was originally made to select a propeller to operate with the first generation submarine's propulsion plant. The efficiency of such a screw was very poor in comparison with this screw selected, however.

### 2.2.2 Prime mover and Drive Train.

Two configurations were considered. The first was a pressure compensated motor manufactured by the Hoover Electric Company. The other was the propulsion motor used in the first generation robot. The attributes of these two systems are discussed in Appendix III.



Considering all the qualities of each alternative, it was decided to use the pressure compensated motor, due to its better efficiency and the fact it can not be flooded, since it is filled with oil. These motors, however, are custom built for individual applications, and the exact specifications for this motor are not available. Similar size and power output motors have been built by Hoover, and this data was used for estimating the size and weight of the unit.

The required output of this motor is determined as follows:

$$\text{SHP required} = \frac{\text{EHP}}{\text{PC} \times \eta_{\text{Drive Train}}}$$

$$\text{where: } \text{PC} = \eta_o \times \eta_H \times \eta_{rr}$$

$$\eta_o = .70$$

$$\eta_H = \frac{(1-t)}{(1-w)} = 1.19$$

$$\eta_{rr} \text{ assumed to be } = 1.0$$

$$\eta_{\text{Drive Train}} = \eta_{\text{reduction gears}} \times \eta_{\text{seals}}$$

$$\eta_{\text{reduction gears}} \text{ assumed } = .9$$



$$\eta_{\text{seals}} \text{ assumed} = .9$$

Therefore: SHP required = .0745 horsepower.

Figure A3-10 shows the typical motor efficiency for the chosen motor. If it is assumed the motor will be well matched to the load, a motor efficiency of .70 seems fully reasonable. The overall propulsion plant efficiency is, therefore:

$$\begin{aligned} \text{Propulsion Plant Efficiency} &= \text{PC} \times \eta_{\text{Drive Train}} \times \eta_{\text{motor}} \\ &= .47 \end{aligned}$$

The estimated motor and reduction gear parameters are as follows:

Input Voltage	= 24 volts
Nominal Diameter	= 4 inches
Length	= 8 inches
Weight (Dry)	= 8 lbs.
Output RPM	= 100

### 2.3 Energy Storage System.

Several candidate batteries were studied, including Lithium-chloride, silver-zinc, silver-cadmium, zinc-air,





nickel-cadmium, and lead-acid, as discussed in Appendix IV. For this application, a battery with a high energy to weight ratio and flexibility in configuration was desirable. The silver-zinc battery was chosen for these reasons, which were felt to outweigh its cost and short life span. The lead-acid battery, which was the other candidate, simply impacted the design too greatly. Additionally, the lead-acid system is not flexible enough to provide a reasonably sized 24 volt system, which is required for the chosen propulsion unit.

The characteristics of the chosen main battery selected from Table A4-2 are as follows:

Four LR4/80 series wired modules were selected as the main battery.

Dimensions of the four module unit:

Length = 13.28 inches

Depth = 5.35 inches

Height Overall = 7.12 inches without cover

Total Weight = 38 lbs.

Energy rating = 1920 Whr @ 40 degrees F

Design Voltage = 24 volts

For the emergency battery located in the aft compartment, a sealed rechargeable battery with good stand life was required. The sealed lead-acid batteries manufactured by Gates Energy systems, as listed in Table A4-6, were considered the most suitable alternative. A 12 volt design was chosen to provide power to the computer, pinger, and



the emergency systems in case of main battery failure. The emergency battery characteristics are as follows:

Model number 0810-0008

Length = 4.2 inches

Depth = 2.8 inches

Height = 2.7 inches

Energy Capacity = 30 Whr

Weight = 2.5 pounds

The power supplies which make up the third element of the energy storage system are located in the aft compartment to supply regulated voltages for the computer and other functions. The voltages are as follows:

10 volts autopilot

5 volts servos

5 volts instrument

±12 volts computer interface

±5 volts computer power and tape recorder

#### 2.4 Pressure Hull and Structural Design.

The pressure hull design trade off study is presented in Appendix IV. A configuration using one main pressure housing with no mechanical linkage penetrations and three much smaller pressure housings to contain the control servos is employed. These pressure housings will be constructed from 6061-T6 aluminum alloy pipe selected from Table A5-1.



This aluminum alloy was chosen because it is readily available in seamless extruded pipes up to twelve inch diameter, has good corrosion resistance properties, is non magnetic, is manufactured to tolerances suitable for pressure hull applications, and is easily worked. Steel was considered unacceptable because of its magnetic properties. Filament wound fiberglass was also very attractive, but requires very specialized equipment to construct.

A straight cylindrical form was chosen for the main pressure hull shape as a compromise to the more efficient spherical shape or the stepped cylindrical shapes.

To aid in the pressure hull design, a computer program was developed to perform the stiffened cylindrical hull calculations. This program is presented in Appendix V.

The size of the main pressure hull is determined by the size of the envelope and the total payload volume contained inside. The selected configuration characteristics are presented in Table 2-2. The forward compartment is intended to house the data collection payload electronics. The middle compartment houses the main battery and the aft compartment houses the robot control payload electronics, including the computer, autopilot, power supplies, emergency battery, magnetic heading compass, and data tape recorder. The sizes of these compartments were determined by requirements estimated in Appendices III and VII.

The main pressure hull also forms the primary



TABLE 2-2 SUMMARY OF MAIN PRESSURE HULL DIMENSIONS

Refer to Figure A4-1 for Definations

$L_p$	=	55.0 inches	$L_{fwd}$	=	16.0 inches
$L_{bat}$	=	15.0 inches	$L_{aft}$	=	24.0 inches
$D_{shell}$	=	10.192 inches	$D_p$	=	12.25 inches
$t_{shell}$	=	0.279 inches	$t_{bulk}$	=	0.25 inches
$t_{end\ cap}$	=	0.279 inches			

## Stiffening Frame Dimensions

$t_{web}$	=	0.50 inches	$h_{web}$	=	0.75 inches
-----------	---	-------------	-----------	---	-------------

## Connecting Flange Dimensions

$t_{web}$	=	1.00 inches	$h_{web}$	=	0.75 inshes
-----------	---	-------------	-----------	---	-------------

## Complete Pressure Hull Characteristics

Volume in Cylinder	=	4487 in <sup>3</sup>
Volume in End Caps	=	277 in <sup>3</sup>
Total Enclosed Volume	=	4764 in <sup>3</sup>
Displaced Volume	=	5470 in <sup>3</sup>
Displaced Weight Sea	=	205 lbs.
Displaced Weight Fresh	=	200 lbs
Hull Weight Total	=	79 lbs





structural member of the submarine. The largest bending moments the pressure hull will experience occur during lifting, when the hull is out of the water, suspended by its ends. The maximum total weight the pressure hull can carry, and still be positively buoyant, is 205 pounds, which is equal to the buoyancy of the hull in salt water. Using the bending moment equation:

$$\sigma = \frac{M y}{I}$$

where:  $\sigma$  = Stress psi

$M$  = Bending Moment

$y$  = Distance to the extreme fiber from neutral axis

$I$  = Moment of Inertia

with  $\sigma_y$  and  $I$  of the aluminum pipe, the cylinder could support a point load of almost 30,000 pounds at its midpoint without yielding due to the bending moment stresses. It will, therefore, provide more than adequate support for its enclosed maximum load.

The pressure hull's flanges provide surfaces to bolt the sections of the pressure hull together. The height of these flanges was chosen as .75 inches to help keep the



maximum diameter small, and this height was felt to offer sufficient bolting surface. The sections are held together by twelve one-quarter-inch diameter stainless steel bolts. The bolts are stressed during handling, but at depth they will align the sections which are forced together by the 444 psi external operating pressure. These connecting flanges also serve in conjunction with the one-quarter-inch bulkheads to strengthen the hull against general instability failure.

During fitting out of the pressure hull, the materials used must be carefully chosen. Copper, brass, nickel, monel, tin, lead and carbon steel should be avoided, since they can form a galvanic couple, causing serious corrosion of the aluminum. Stainless steel and zinc or zinc-coated steel are satisfactory.

Several penetrations of the hull are required for electrical and other connections. The electrical connections penetrate the hull in the end caps on the axis. Sufficient connections should be fitted to handle any requirement, and the unused capped. The end caps are almost three times as thick as required to allow for these penetrations.

Additional penetrations are required through the battery compartment. One leads from the high pressure air bottles to the buoyancy augmentation enclosure. The battery compartment should also be fitted with plugged openings to allow venting of the compartment without disconnecting the



flanges. A pressure relief valve should also be fitted to the battery compartment to prevent an unwanted buildup of gas if one of the high pressure bottles should start to leak. This relief should be mounted internally, if possible.

The selected pressure hull configuration is designed to operate at 1000 feet; however, an additional weight of ten pounds would allow operation to 2500 feet. This modification involves halving the stiffening frame separations.

The other pressure housings which contain the servo motors are constructed from unstiffened aluminum pipe with flat end closures whose thickness is determined by the following formula:

$$t = d \sqrt{(0.3 P) / \sigma_y}$$

$t$  = thickness of flat end plate

$d$  = diameter of the plate

$P$  = 1.5 design operating depth pressure

For the 1.99 inch O.D. servo motor housings, the end caps then have to be 0.15 inches thick.

Structural support in the tail section is provided by an aluminum support framing working in conjunction with



the envelope. The nose is supported by the envelope alone.

## 2.5 Control System.

A horizontal and vertical set of fins with movable control surfaces are fitted as far aft on the tail as possible. The movable parts of the control surfaces are of the balanced design and are activated by three servo motors in the same arrangement as used on the original robot.

The control surfaces themselves are larger than those used on the original robot, and are higher aspect ratio, which gives better lift and drag performance. The surfaces consist of a movable part and a nonmovable support part. The control surface configuration shown in Figure 2-3 is intended to be representative of this design. The actual configuration will be dependent on fabrication and more specific control requirements.

A detailed analysis of the controllability of the submarine was not performed, due to time constraints. This analysis would be conducted using the methods of [15]. In any case, at this point, the analysis would only be an approximation, since the physical characteristics, such as moment inertia, have to be known, and these would be based on estimates, at best.

From previous experience with the envelope form, the directional stability characteristics of the vehicle are expected to be very good.





## 2.6 Robot Control Payload.

The robot control payload items are considered those electronics which control the robot's actions. These electronics form the heart of the robot. Included in this category are the computer, autopilot, location pinger, and heading sensor, among others.

The control electronics onboard the present MIT robot has received a great deal of design and development since the inception of the robot. This group is continuing to receive a great deal of attention since improvements in this area vastly increase the operational capabilities of the present robot.

A detail study of the control equipment was not undertaken. However, these functions were investigated, as presented in Appendix VII, to obtain an estimate of the required space they will occupy onboard. Generally, these electronics are very low density, and their volume is more important than the weight.

A volume of 2100 cubic inches has been made available in the aft compartment of the proposed design. An additional space of 1300 cubic inches is available in the forward compartment, but this volume is earmarked for data collection payload items. The compartments were divided up this way so data collection payload electronics could be removed or replaced without affecting the robot control payload.



The battery compartment separates the two compartments. Bulkheads seal the battery compartment and any necessary electrical connections between the two compartments pass through the overhead of the battery compartment and are sealed at the bulkhead with gas tight connectors.

## 2.7 Data Collection Payload.

The data collection payload is composed of those equipments which relate to the data collection mission. In Appendix VIII, two high impact data payload items were considered, a side scan sonar and a still camera. The side scan sonar was eliminated as a contender because there presently is no method, suitable for robot operation, to store the data onboard.

The still camera was considered as a high impact system which would be very desirable. However, a vehicle would have to be designed to perform only that one function; and even then, it is debatable if the high exposure camera could be accommodated in a vehicle with the size and weight limitations established.

With the two high impact data collection payloads eliminated, a multitude of lower impact sensors, such as temperature, or salinity sensors, are left. The forward compartment is dedicated to house any electronics associated with these functions. A total of 1300 cubic inches is provided in this compartment.



## 2.8 Auxiliary Systems.

The auxiliary systems include the buoyancy augmentation system, trim system, and the emergency systems.

The emergency systems include the flooding sensors in the main and servo pressure housings, an excess depth sensor, and a switching system to switch the acoustic locator to auxiliary power. These functions are the same as those employed in the original robot, except here they are located in the aft compartment.

The trim system is an attempt to eliminate the timely process of hand ballasting each time the operating environment is changed. This system is discussed in Appendix IX. At this point, it can only be considered conceptual, since the actual design must be developed and tested to prove its feasibility. Space and weight allocations were made for this system onboard, however.

The two trim tanks shown in Figure 2-3 are not the same size. The rear tank has a volume of 61.1 cubic inches, and the forward tank has a volume of only 35.6 cubic inches. The tanks are sized this way due to space limitations; also, the forward tank is further from the center of buoyancy of the vehicle than the rear tank, and accordingly, can exert a greater moment using less weight.

The trim tanks are not sized to be able to compensate for the buoyancy change between fresh and salt water. This must be accomplished by adding ballast weights and then



performing final trimming with the trimming system.

A buoyancy augmentation system is also installed. This is a buoyancy augmentation system, rather than a ballast system, because it does not do any ballasting. When the robot is placed in the water, this system is vented to expell any air. When coming up, the system is used to augment the buoyancy by discharging compressed air into an open enclosure surrounding the battery compartment. A schematic is presented in Table A9-2 of Appendix IX.

The air system was chosen over a dropping weight for several reasons. First, weights are a one shot affair, whereas this system can be used repeatedly. Second, vehicles of this sort tend to have a vertical center of gravity very close to the vertical center of buoyancy. When the weight is dropped, this distance is shortened considerably, and the vehicle becomes less stable, or even unstable.

A lightweight enclosure open to the sea at the bottom is fitted around the battery compartment into which compressed air is blown. This enclosure has a total volume of 400 cubic inches, which will allow 14.6 pounds of buoyancy. The location of the enclosure is slightly forward of the LCB, so that the vehicle will nose up slightly when the water is expelled from the enclosure. This system is very compatible with the hull form and vehicle configuration chosen.

This system is only presented at this point as a





concept, however. A detailed design and testing would have to be accomplished before the system is installed.

## 2.9 Submarine integration.

With the final configuration determined, the parts must fit together and operate as a unit. The most critical of these requirements is the ability to float upright in near neutral buoyancy. Table 2-3 presents a weight and longitudinal moment study for the various robot weight groups. At this point, only the longitudinal center of buoyancy and gravity were calculated. The vertical center of gravity was not calculated because it is a strong function of the arrangement of equipment inside the pressure hull, and this arrangement could not be determined with any accuracy. The location of the battery is low, which will certainly help to lower the center of gravity.

As can be seen from Table 2-3, the submarine does balance. The data presented in this table is calculated for fresh water. The submarine is, however, intended to be operated slightly positively buoyant, which is not accounted for in this calculation.

The amount of positive buoyancy was originally intended to be determined so the vehicle would remain positively buoyant at operating depth. A calculation to determine the effect of the external pressure on the pressure hull showed the hull lost about 0.081 pounds of buoyancy due to



TABLE 2-3 PRELIMINARY WEIGHT AND MOMENT BALANCE FOR THE  
PROPOSED SECOND GENERATION SUBMARINE

<u>Weight Group</u>	<u>Weight</u>	<u>X</u>	<u>Buoyancy*</u>	<u>X</u>
Envelope and Support Structure	31.38	4.53	19.50	4.36
Propulsion System	13.20	7.82	5.05	7.71
Main Battery	39.00	3.50	-	-
Pressure Hull	79.43	3.82	197.40	3.82
Control	12.58	7.55	5.23	7.62
Trim & Buoyancy	14.40	3.97	7.16	4.30
Misc.	8.70	4.70	3.61	4.77
Wet Payload Nose	10.00	0.67	4.00	0.67
Fwd. Compt. Payload	19.25	2.17	-	-
Aft. Compt. Payload	27.45	4.50	-	-
Syntactic-Foam	<u>18.55</u>	<u>6.08</u>	<u>31.95</u>	<u>6.08</u>
TOTAL:	273.94	4.24	273.9	4.24

\* Fresh Water

X Distance in Feet from the Forward Perpendicular



compression at depth. This is, obviously, not significant enough to worry about.

#### 2.10 Summary of the Characteristics of the Proposed Second Generation Robot Submarine

Table 2-1 summarizes the characteristics of the proposed second generation of the MIT robot submarine.

Figures 2-3 through 2-5 show various views of the proposed design.



TABLE 2-4 SUMMARY OF THE PROPOSED SECOND GENERATION  
ROBOT SUBMARINE'S CHARACTERISTICS

Envelope Form: Series 58 Form 4165

$L = 9.0 \text{ ft.}$        $D_x = 1.28 \text{ ft.}$

Design Operating Speed: 3.5 knots

Endurance : 20 hours

Range : 70 NM with zero current

Main Battery : Silver-Zinc 24 volt 1920 Wh

Emergency Battery : Sealed Lead-Acid 12 volt  
30 Wh

Dry Weight : 274 lbs.

Required SHP : 0.0745

Propeller : B 3-45  $D_{pr} = 0.9 \text{ ft.}$

Pressure Hull Material: 6061-T6 Aluminum Alloy

Design Operating Depth: 1000 ft.

Design Crush Depth : 1500 ft.

Maximum Pitch Angle : 30 degrees limited by  
the compass gimbaling

Total Enclosed Payload

Volume : 3400 in<sup>3</sup>

Data Collection

Payload Capacity : 29.25 lbs. (depends on  
volume)





FIGURE 2-3 INBOARD PROFILE OF THE PROPOSED SECOND  
GENERATION ROBOT CONFIGURATION

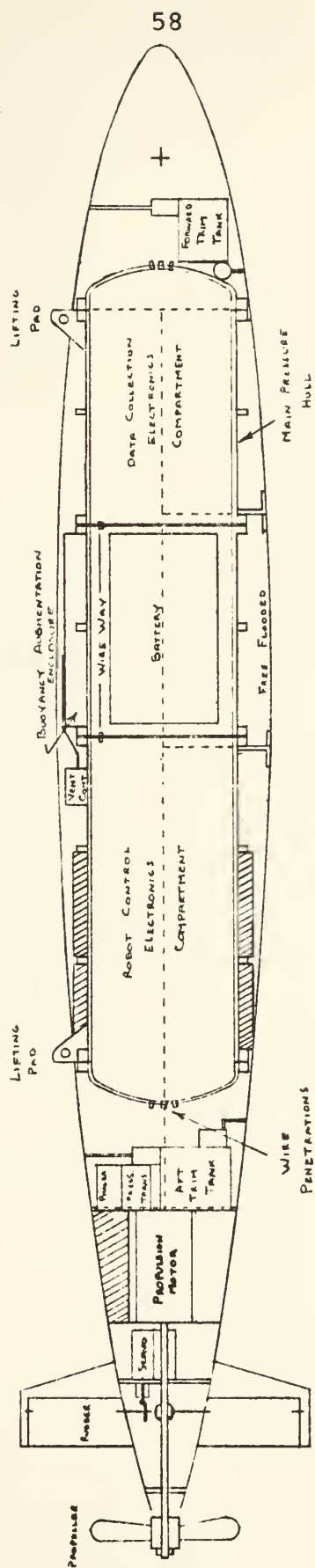
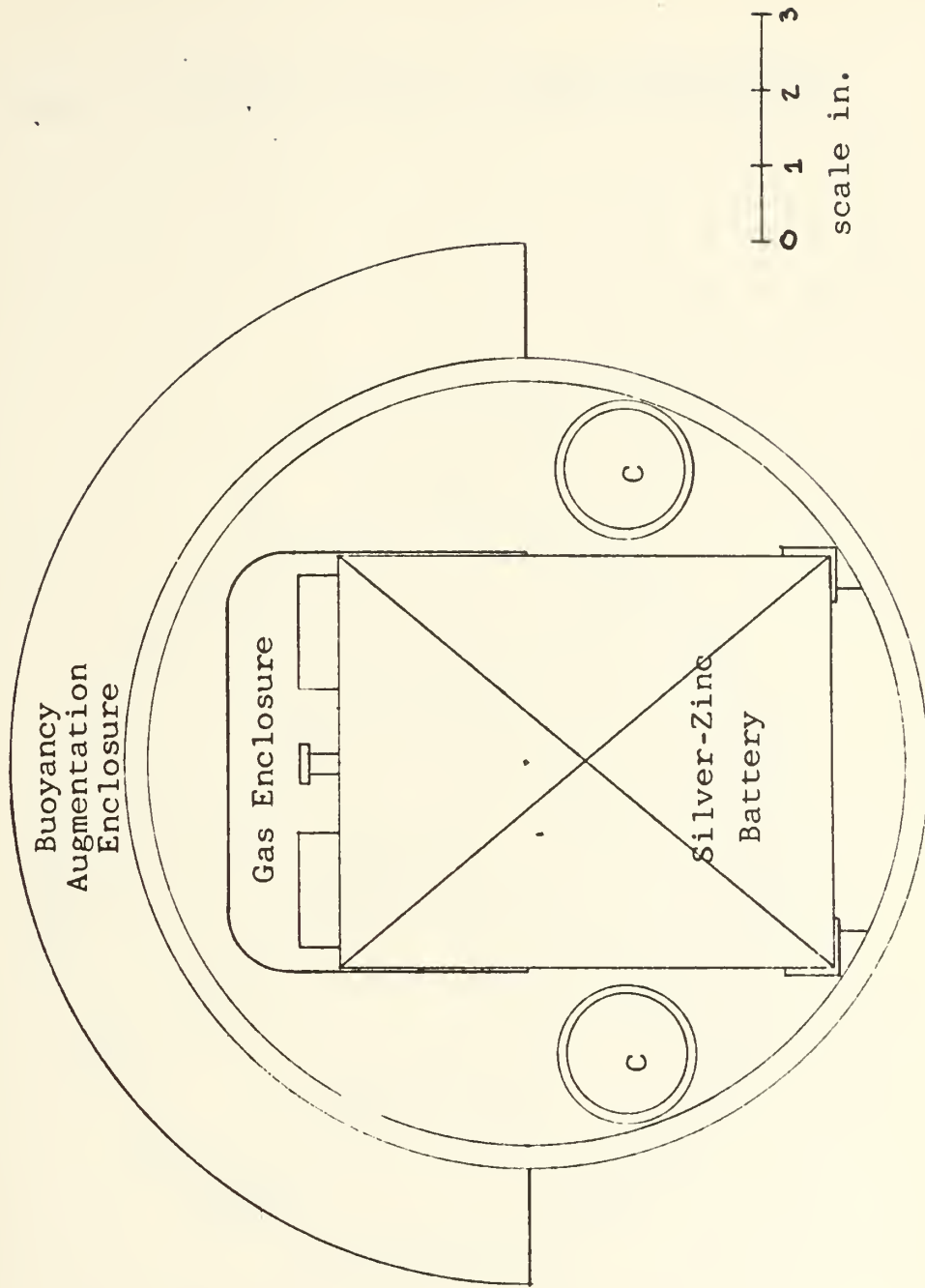




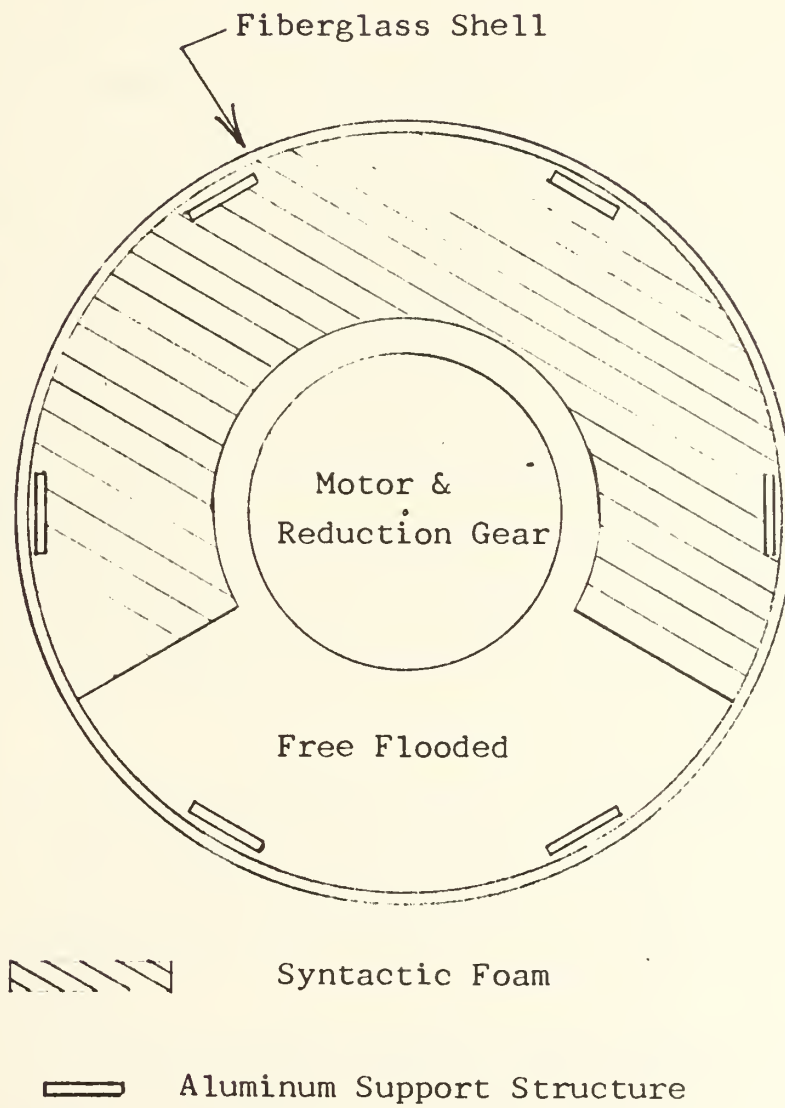
FIGURE 2-4 CROSS SECTION OF BATTERY COMPARTMENT



C - 1500 psi Compressed Air Flasks



FIGURE 2-5 CROSS SECTION OF MOTOR COMPARTMENT





## CHAPTER 3

## OBSERVATIONS, CONCLUSIONS AND RECOMMENDATIONS

The design process does not really have a definite ending. Sometimes there are forced periods of dormancy due to deadlines or other factors, but usually various aspects of a design reappear to be reviewed and refined again. Such is the case with this preliminary design. It was not intended to be the end-all of robot submersibles, but merely an opportunity to take a systematic look at the various elements which make up the robot submarine, to see where and how improvements were possible, and could be implemented. In this respect, it seems to have succeeded.

This analysis focused on the ocean engineering aspects of the submersible robot problem. But of perhaps greater importance, are the electronics aspects of the design. As new technologies in these areas are advanced and refined, the capabilities of the robot will be vastly improved.

The design presented here has met nearly all of the design requirements stipulated at the beginning of the project. Several specific aspects are, however, worthy of special mention.

The first is the pressure hull weight, which greatly affects the buoyancy and load carrying capability. In the present design, the pressure hull thickness is greater than is required. In fact, an increase in pressure





hull weight of about 13 per cent (10 pounds), due to halving the stiffening frame spacing, will allow a design operating depth of 2500 feet, rather than the present 1000 feet. This additional weight was unavoidable, however, since the pressure hull material was not available with thinner wall dimensions.

The second aspect of note is the battery selection. The silver-zinc battery selection allows use of the ten inch diameter pressure hull vice a twelve inch diameter required for a lead-acid battery. This selection also greatly improves the endurance of the vehicle and allows the more flexible twenty four volt battery system.

The final point is the use of the 4165 envelope form with the double hull configuration. This envelope significantly reduces the vehicle drag and propulsion plant power required. The use of the double hull configuration also allows the more easily installed external stiffening frames to be used, and the space between the two hulls provides room for functions such as flotation foam and the buoyancy augmentation system.

In the final analysis, the project appears to have achieved most of its goals; but, this is only a preliminary design. A detailed design would certainly have to be conducted before this proposed configuration were actually constructed.



APPENDIX I  
SUMMARY OF THE CHARACTERISTICS  
OF THE  
ORIGINAL MIT ROBOT SUBMARINE

### A1.0

A small robot submarine designed to collect oceanographic data was originally developed as part of an undergraduate laboratory in the summer of 1974 by students at MIT. It has since undergone considerable further development and refinement. Detailed descriptions of the vehicle through the various phases of its development and testing are contained in [11], [12], [13], [14], and [15].

Figures A1-1 and A1-2 present general views of the robot showing the exterior and internal arrangement.

The general characteristics of the robot are as follows:

Speed through the water . . .	2.2 knots
Design range . . . . .	13 NM
Design Operating Depth . . .	200 ft.
Weight (dry) . . . . .	240 lbs.
Payload . . . . .	25 lbs.
Length . . . . .	7.52 ft.
Maximum Diameter . . . . .	1.23 ft.

### A1.1 Envelope

The robot's envelope is a modified torpedo form with a 4 foot aluminum cylindrical midsection and fiberglass



FIGURE A1-1 CUTAWAY VIEW OF THE FIRST GENERATION MIT ROBOT SUBMARINE

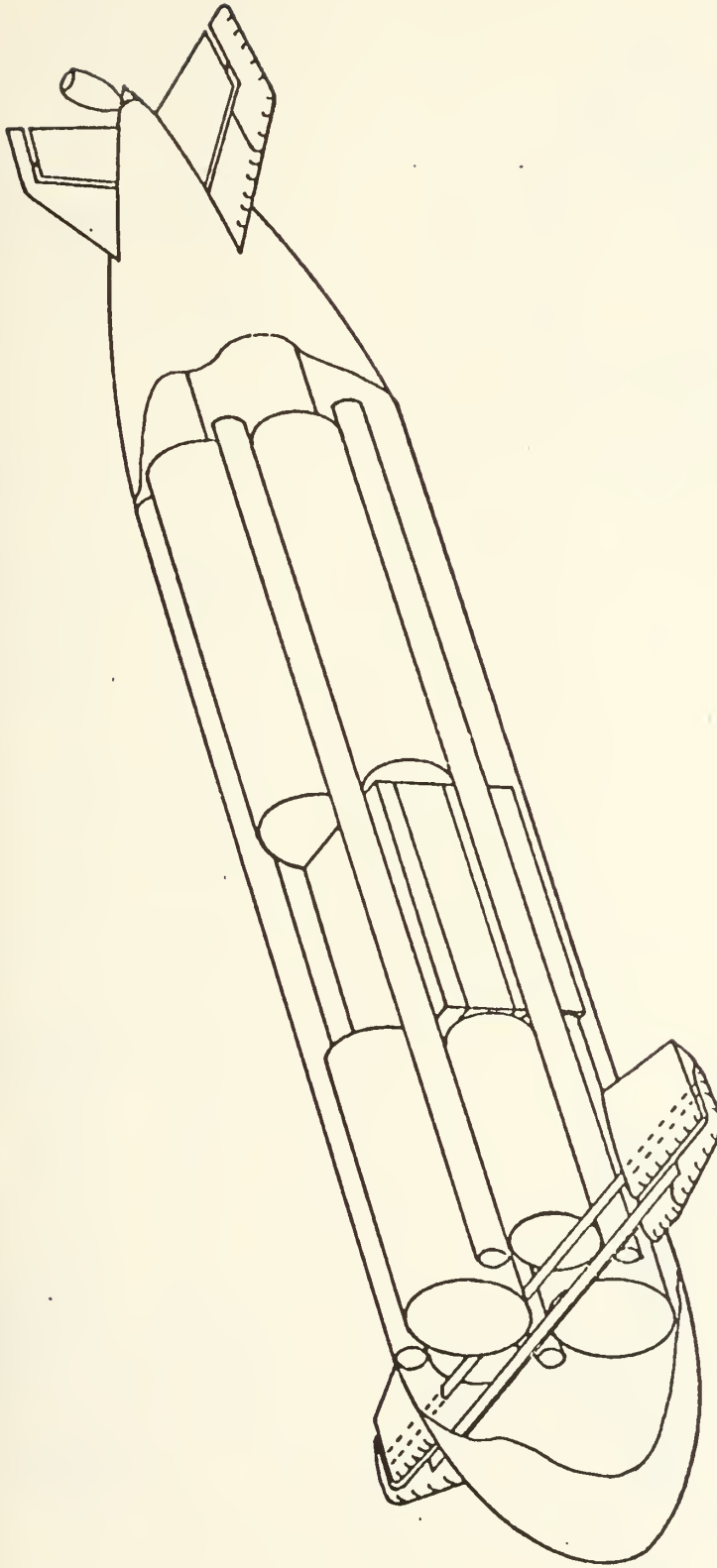
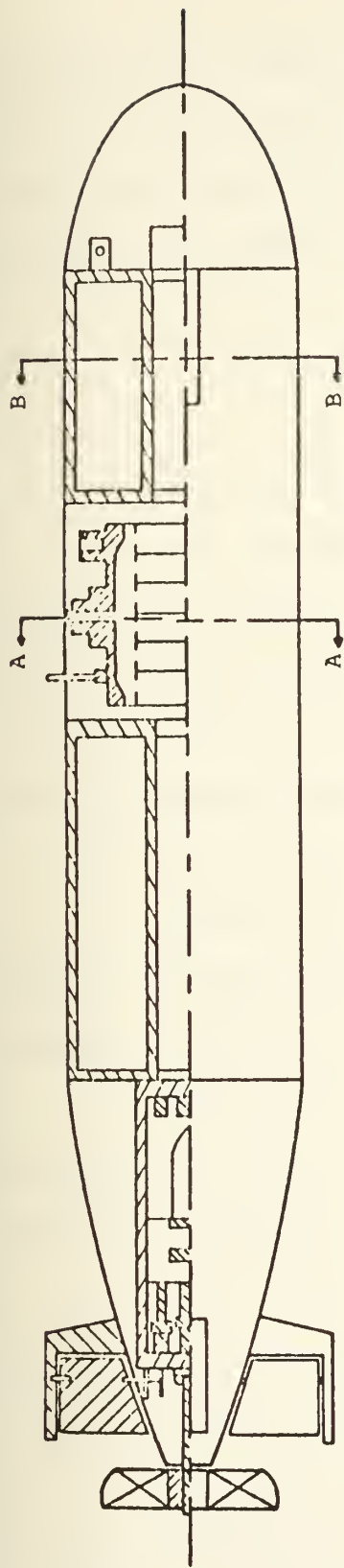
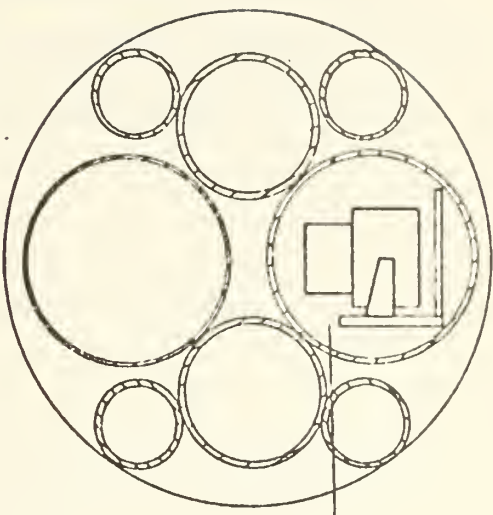




FIGURE A1-2 INBOARD PROFILE AND SECTION VIEWS OF FIRST GENERATION MIT ROBOT SUBMARINE

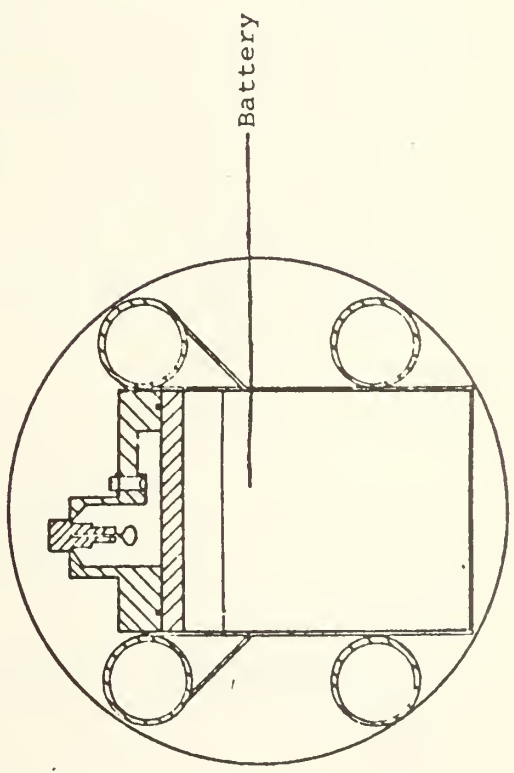


Section B-B



Autopilot  
Tube

Section A-A



Battery





nose and tail cones fitted on the ends for streamlining. These fairings are all removable to provide internal access. Towing tank tests with the actual vehicle measured the appended drag coefficient,

$$C_T = \frac{R_{TA}}{\frac{1}{2} \rho L^2 V^2}, \text{ as } 6.0 \times 10^{-3}.$$

### Al.2 Propulsion System

The propulsion system consists of a twelve inch diameter two bladed propeller driven by a twelve volt D. C. trolling motor through a 10:1 reduction gear. The motor and reduction gears are housed in a 6 inch poly vinyl chloride (PVC) pressure housing.

### Al.3 Energy Storage System

Electrical power is supplied by a 96 AH automobile battery equipped with a pressure compensating cover which allows the battery to operate fully immersed in water.

The battery supplies electrical power directly to the propulsion motor, but other regulated power supplies provide the following voltages:

10 V to autopilot;

5 V for servo's, and instruments;

±12V & ±5V to the Computer;

9.1V for auxilliary.

Emergency power is provided to the computer by small rechargeable batteries.



#### A1.4 Pressure Hull and Structural Design

Four 5.91 inch (15 cm) diameter PVC tubes with flat PVC end caps make up the pressure housings for installed electronic components. These cylinders are arranged as shown in Figures A1-1 and A1-2. Another tube of the same diameter is located on the centerline aft to provide the pressure housing for the propulsion motor, reduction gear, and the aft fin control servos. Additional 3.91 inch (10 cm) tubes are fitted next to the main pressure housings to provide additional buoyancy as shown in Figure A1-2. The total enclosed volume for electronics amounts to about 2,000 in<sup>3</sup>.

The structural members of the robot are four 2.0 inch PVC tubes which run the entire length of the cylindrical section. These support tubes are, in turn, supported by four aluminum bulkheads which divide the main cylinder into three compartments.

#### A1.5 Control System.

Vehicle control is provided by six control surfaces operated by small electric servo motors with integral position feedback potentiometers.

The forward pair of control surfaces act together and are positioned by a single servomotor. This pair of control surfaces operate in conjunction with another servo controlled pair of fins located at the tail to control the robot's depth and pitch.

Yaw control is provided by another pair of movable



control surfaces mounted vertically at the tail and controlled by a separate servo.

The operation of the control surfaces is coordinated by an autopilot whose function and operation are discussed in the following section.

#### A1.6 Robot Control Payload Equipment

The brain of the robot is a mini computer located in the lower aft six inch pressure housing which controls all the functions of the robot. The computer is comprised of three main parts:

1. The Central Processing Unit (CPU)
2. Memory
3. Interfaces.

The CPU is a 16 bit microprocessor built using low power usage CMOS integrated circuits and requiring only 200 mW of power.

The computer's memory is 4K by 16 bit with a power consumption of 1.5 - 2.5 w.

Three interfaces are provided. The first uses a D→A and A→D conversion between the computer and the autopilot. The second interfaces the teletype and cassette tape recorder to store digital data. The remaining interface is to the control panel which is used for detailed manual control of the computer and the submarine.

Information is passed to and from the computer through an optical coupler. An array of light emitting



diodes (LEDs) and phototransistors in the coupler provide the signal path and eliminate the need for making and breaking electrical corrections so that data can be fed in with the robot in the water.

An autopilot provides real time control of the robot. It carries out the computer's depth and course instructions and controls the pitch attitude of the vehicle. The autopilot has three sections:

1. Sensors which sense depth, attitude, and vehicle heading.
2. Analog controller, which provides control signals to instruct the control surfaces.
3. Servo Amplifiers, which use the analog controller's signals to provide the necessary power to drive the servomotors.

The sensors provide pitch, depth, and heading information to the autopilot. Pitch is obtained from an oil damped pendulum attached to a potentiometer. Depth is determined by an absolute pressure transducer. Heading is determined from a magnetic compass using photo-potentiometers placed below a compass card on which a spiral is scratched.

The analog controller is a proportional-derivative controller which utilizes the differences between the command signals and the sensor output to generate the control signals. Depth and heading commands come from the computer





while the attitude command requires the robot to remain horizontal.

The servo amplifiers compare the voltages on the command lines with the position feedback voltages from the servomotors and provide power to move the motors until the voltages match.

#### A1.7 Data Recording Payload Equipment.

The only oceanographic data the robot currently records is temperature. The major work to date has been concerned with perfecting the control of the submarine and not adapting new data collecting equipment.

#### A1.8 Auxilliary Systems.

Each pressure housing is equipped with sensors to detect the presence of water which would indicate a leak in the housing.

The robot is not equipped with any buoyancy augmentation devices or automatic trimming system.

A 10 KH transducer which emits a 4 ms burst every second is located in the nose of the robot. The vehicle is tracked by the use of this "pinger" in conjunction with a sonar receiving system coupled to two hydrophones and a wet paper recorder with a precise one second sweep.



## APPENDIX II

## ENVELOPE FORM TRADE OFF STUDY

A review of the envelope design of many of the present robot submersibles shows they all have significant cylindrical midbody with various degrees of nose and tail streamlining, much the same as a torpedo. This allows the outside shell of a cylindrical pressure hull to be the outside of the envelope. Many modern military submarines are also designed for part of their length with this so called single hull configuration. A torpedo shape may, however, not be the most efficient from the standpoint of resistance; after all, torpedoes have cylindrical midsections so they can be launched easily from cylindrical tubes and this is not a requirement for the robot.

For the purposes of this design an envelope form is required which has the following characteristics:

1. Low drag for a given measure of enclosed volume, either total enclosed volume or volume enclosed in a particular size and configuration of pressure hulls.
2. A form which enhances maneuvering characteristics.
3. A form which is compatible with pressure hull design.
4. A form which is compatible with the control surface and propulsor configuration.



One attribute common to any envelope form to be considered is they shall be bodies of revolution since this type of body displays better hydrodynamic performance than forms which are not. Any other common attribute among possible candidates is not so well defined. Three candidate envelope forms will be considered and evaluated. These are as follows:

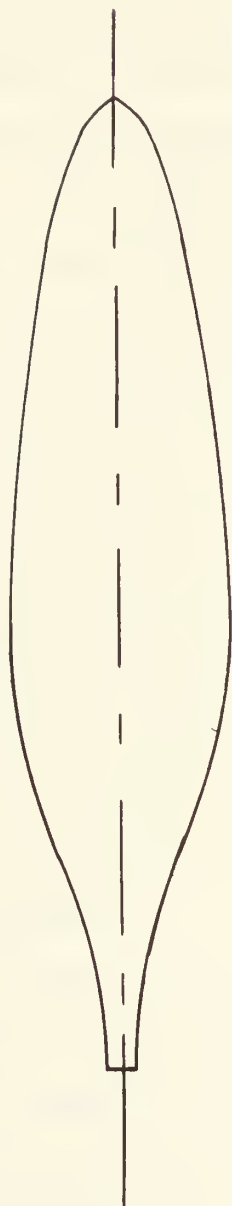
1. Torpedo form with streamlined nose and tail sections
2. Laminar flow form
3. Fully turbulent flow form

The first alternative, the modified torpedo form, is the envelope used in the first generation robot submarine. At this point, no additional evaluation of this form will be performed, but the data and assumptions from that vehicle will be used to help measure the effectiveness of other proposed envelope forms.

The second alternative, the laminar flow form, was first presented in [16] by Carmichael in his work with the Dolphin hull form. An example of this type hull form is presented in Figure A 2-1. The theory behind this shape is that by proper choice of shape a hull form may be designed which promotes laminar flow over a considerable length of the body, even at high Reynold's numbers. By promoting laminar flow the drag can be reduced considerably. Carmichael claimed drag reductions in the range of 40 per cent over a



FIGURE A2-1  
PROFILE OF A TYPICAL LAMINAR FLOW BODY







conventional torpedo hull form of equal volume at 45 knots.

In [17], Parsons and Goodson carried Carmichael's work further and developed a method to study optimum laminar flow designs for minimum drag at various Reynold's numbers. This work developed a series of forms for different Reynold's numbers, all of which show significant drag reductions over non laminar flow bodies. This study was, however, conducted on unpowered mathematical models with no assumed surface roughness operating in modeled fluids. The authors express significant doubt, however, over whether the laminar flow can be maintained as predicted in an actual marine environment. Factors such as hull surface roughness and vibrations imparted to the hull by the propulsion system both may trip the laminar boundary layer, and with a turbulent boundary layer these hull forms are far from optimum. In fact, in their final conclusions, the authors state they believe that laminar flow over these bodies in a real environment will be prevented by surface roughness.

Despite these reservations concerning the practicality of sustaining laminar boundary layer flows in an operational environment, Johnson, et al, [10] selected a laminar flow hull form for the Naval Research Laboratory's proposed smart multi-mission unmanned free swimming submersible, claiming drag reductions of about one third over other hull form designs. They also stipulate that hull roughness heights must be less than .0005 inches in order to maintain



the laminar flow characteristics.

All factors considered, it is doubtful that surface roughnesses of the magnitude stipulated in [10] can be maintained over time with the handling a vessel such as this receives. Also, they have not addressed the question of propulsion system induced vibrations which will tend to trip the laminar layer. It, therefore, has been concluded for this study that the laminar flow hull forms, though they offer the possibility of considerable drag reductions, are not realistic for the robot vehicle. Their selection would introduce a serious risk into the design. In [10], the authors indicate NRL is planning to build a laminar flow envelope form for their vehicle to be tested in FY 78. The results of these tests should prove most informative.

Having eliminated the laminar flow form from further evaluation, consideration turns to the third alternative, the fully turbulent flow hull form. Parsons and Goodson also studied this flow situation. The best body of this type which they studied proved to be nearly identical to the series 58 form number 4165 tested by Gertler and reported in [18]. Gertler also concluded the form 4165 was the best of those he tested.

To arrive at his conclusions, Gertler towed models of 24 bodies of revolution which had five systematically varied hull parameters, to determine the impact of changing each parameter on the drag. Table A 2-1 lists these



TABLE A2-1

The Geometrical Parameters for Models of Series 58

Model	m	$r_o$	$r_1$	$C_p$	$L/D_x$
4154	0.40	0.50	0.10	0.65	4.0
4155	0.40	0.50	0.10	0.65	5.0
4156	0.40	0.50	0.10	0.65	6.0
4157	0.40	0.50	0.10	0.65	7.0
4158	0.40	0.50	0.10	0.65	8.0
4159	0.40	0.50	0.10	0.65	10.0
4160	0.36	0.50	0.10	0.65	7.0
4161	0.44	0.50	0.10	0.65	7.0
4162	0.48	0.50	0.10	0.65	7.0
4163	0.52	0.50	0.10	0.65	7.0
4164	0.40	0.50	0.10	0.55	7.0
4165	0.40	0.50	0.10	0.60	7.0
4166	0.40	0.50	0.10	0.70	7.0
4167	0.40	0.00	0.10	0.65	7.0
4168	0.40	0.30	0.10	0.65	7.0
4169	0.40	0.70	0.10	0.65	7.0
4170	0.40	1.00	0.10	0.65	7.0
4171	0.40	0.50	0.00	0.65	7.0
4172	0.40	0.50	0.05	0.65	7.0
4173	0.40	0.50	0.15	0.65	7.0
4174	0.40	0.50	0.20	0.65	7.0
4175	0.40	0.50	0.10	0.60	5.0
4176	0.40	0.50	0.10	0.55	5.0
4177	0.34	0.50	0.10	0.65	7.0

m - Position Maximum Section

 $r_o$  - Nose Radius  $\frac{R_o L}{D^2}$ 
 $r_1$  - Tail Radius  $\frac{R_1 L}{D^2}$ 
 $C_p = \frac{V_E}{\frac{\pi D^2}{4} L}$ 

Reference (18)



parameters for the 24 models Gertler tested.

To better evaluate the series 58 form, it is necessary to understand and develop a method to calculate the drag on the bodies of this series.

To calculate the drag of the series 58 envelope forms, the resistance is first broken down into three components:  $C_f$ , frictional resistance due to viscous drag;  $C_r$ , the residuary resistance; and,  $\Delta C_f$ , a correction factor to account for hull roughness. The total resistance coefficient is then the sum of these three components.

$$C_T = C_f + C_r + \Delta C_f$$

also,

$$C_T = \frac{R_T}{[1/2]\rho V^2 S}$$

where:

$\rho$  = mass density of fluid  
 = 1.99 slugs/ft<sup>3</sup> for sea water @ 60°F

$V$  = Velocity

$S$  = Wetted surface area of body

Gertler used a value of  $0.4 \times 10^{-3}$  for  $\Delta C_f$ , however, he notes this value may be low even for clean bottomed vessels. In [19] Jackson recommends a range for  $\Delta C_f$  of  $0.5 \times 10^{-3}$  to  $1.2 \times 10^{-3}$  due to holes in the hull, construction imperfections, etc. The employment intended for the robot involves removal from the water when not in operation, and





it should easily be possible to fabricate a fairly smooth model. For this analysis then, a value of  $0.5 \times 10^{-3}$  for  $\Delta C_f$  is selected as suitable. The major reason for dividing the resistance coefficient into three components is to separate the frictional resistance, which varies as the Reynold's number, from the residuary resistance which is directly proportional to the velocity squared for a particular hull form. The values of  $C_r$  which Gertler determined by experiment for the various forms of Series 58 are shown in table A 2-2.

The remaining element necessary for calculating the resistance is to determine  $C_f$ . Gertler used the Schoenherr formula for this calculation.

$$\frac{.242}{\sqrt{C_f}} = \log_{10} [(Re) (C_f)]$$

$$\text{where } Re = \frac{V L}{\nu}$$

and  $L$  = length overall

$V$  = Speed

$\nu$  = Kinematic viscosity of fluid medium

However, the solution of this formula has to be determined by combersome iteration. In [19], Jackson presents an alternate formula which does not require an iterative solution:



Table A2-2

Net Residual-Resistance Coefficients for Series 58 Forms  
at Deep Submergence

Model	Net Coefficient	Model	Net Coefficient
4154	$0.58 \times 10^{-3}$	4166	$0.28 \times 10^{-3}$
4155	0.36	4167	0.16
4156	0.22	4168	0.14
4157	0.13	4169	0.14
4158	0.09	4170	0.18
4159	0.075	4171	0.13
4160	0.12	4172	0.13
4161	0.15	4173	0.13
4162	0.17	4174	0.10
4163	0.19	4175	0.32
4164	0.37	4176	0.41
4165	0.07	4177	0.16

Reference (18)



$$C_f = \frac{0.472}{[\log Re]^{2.58}}$$

$$\text{where } Re = \frac{V L}{\nu}$$

This is easier but it's accuracy must be questioned.

A comparison of the results of the two formula at Reynold's numbers of  $10^6$  and  $10^7$  indicate the Jackson formula yields solutions for  $C_f$  which are five percent and six percent greater, respectively, than those calculated using the Schoenherr formula. Since a larger value of  $C_f$  is more conservative, the Jackson formula will be used to determine  $C_f$ .

A summary of the resistance calculation procedure follows:

$$\text{Bare hull resistance} = R_T$$

$$R_T = [C_f + C_r + \Delta C_f] (1/2) \rho V^2 S$$

$$C_f = \frac{0.472}{[\log Re]^{2.58}}$$

$$C_r \rightarrow \text{from table A2-2}$$

$$\Delta C_f = 0.5 \times 10^{-3}$$

$\rho$  = mass density of fluid

= 1.99 slugs/ft<sup>3</sup> for sea water @ 60°F

= 1.93 slugs/ft<sup>3</sup> for fresh water @ 60°F

S = Wetted surface



$V$  = Velocity relative to fluid

$$Re = \frac{V L}{\nu} \quad \nu = 1.2641 \times 10^{-5} \text{ ft}^2/\text{sec salt water}$$

$$= 1.2100 \times 10^{-5} \text{ ft}^2/\text{sec fresh water}$$

$$EHP_{BH} = \frac{R_T V}{550} \text{ horsepower}$$

This is, however, only a method for determining the bare hull resistance. The appended hull resistance is of more interest. For this purpose, Gertler used an empirical formula:

$$R_{T(\text{appended})} = R_T \left[ 1 + 2.3 \frac{S_t}{S} \right]$$

where:

$S_t$  = wetted surface area of appendages

$S$  = bare hull wetted surface

2.3 = an empirical factor determined from various actual submarine data

also:  $EHP_{(\text{appended})} = EHP_{BH} \left[ 1 + 2.3 \frac{S_t}{S} \right]$

With the means to calculate the resistance of the forms established, the problem remains to develop a means of measuring the merit of one form over another. Gertler did this by comparing forms of equal enclosed volume. On this basis, he determined that form 4165 had the lowest drag for a given enclosed volume,  $V_E$ . With the robot, however, the





concern is with the volume which can be enclosed inside the envelope in a pressure hull. This could prove to be a more adequate measure of an envelope's usefulness. According to the pressure hull study, Appendix V, a uniform diameter cylindrical shape is the best shape for the intended purpose. Therefore, an envelope form's resistance should be evaluated in relation to the volume inside which can be enclosed in a cylindrical pressure hull. On this basis, the 4165 form may no longer be the best selection.

In looking for more suitable forms for comparison among the Series 58, consideration was given to forms which have a higher  $C_p$ , since these will be more able to accomodate a larger cylindrical pressure hull. As additional candidate forms the form 4173 with a  $C_p = 0.65$  and the form 4165 with a  $C_p = 0.70$  have been selected. The remaining parameters of these two forms remain unchanged from those of the Form 4165 with the exception of the tail radius of the Form 4173 which is 0.15 vice the value of 0.10 for the form 4165. Gertler, however, found this parameter had very little effect on the resistance. Tables of offsets and profile views of these three envelope forms are presented in tables A 2 - 3 through 5 and figures A 2-1 through 3.

To evaluate the cylindrical pressure hull carrying capability of each candidate form, determination must first be made of the largest cylindrical volume which can be contained within a given envelope. This task was performed



TABLE A2-3  
Offsets for Form 4165

X/L	Y/D	Formula:
0.00	0.0000	$Y^2 = a_1 X + a_2 X^2 + a_3 X^3 + a_4 X^4 + a_5 X^5 + a_6 X^6$
.02	.1423	
.04	.2020	<p>where <math>a_1 = + 1.000000</math></p> <p><math>a_2 = + 0.837153</math></p> <p><math>a_3 = - 8.585996</math></p> <p><math>a_4 = + 14.075954</math></p> <p><math>a_5 = - 10.542535</math></p> <p><math>a_6 = + 3.215422</math></p>
.06	.2476	
.08	.2855	
.10	.3179	
.12	.3462	
.14	.3710	
.16	.3930	
.18	.4123	
.20	.4260	
.22	.4439	
.24	.4565	
.26	.4674	
.28	.4765	
.30	.4841	
.32	.4900	
.34	.4944	
.36	.4976	
.38	.4994	
.40	.5000	Wetted Surface = $.33094 L^2$
.42	.4995	Volume = $.9617 \times 10^{-2} L^3$
.44	.4978	LCB = $\frac{X}{L} = .4484$
.46	.4950	Length Diameter Ratio = $\frac{L}{D} = 7$
.48	.4911	
.50	.4864	Prismatic Coefficient = $C_p = .60$
.52	.4806	
.54	.4739	
.56	.4665	
.58	.4580	
.60	.4486	
.62	.4384	
.64	.4273	
.66	.4154	
.68	.4026	
.70	.3890	
.72	.3743	
.74	.3588	
.76	.3422	
.78	.3245	
.80	.3059	
.82	.2861	
.84	.2652	
.86	.2429	
.88	.2193	
.90	.1941	
.92	.1672	
.94	.1383	
.96	.1065	
.98	.0699	
1.00	0.0000	

Reference (18)



FIGURE A2-1

Profile of Form 4165

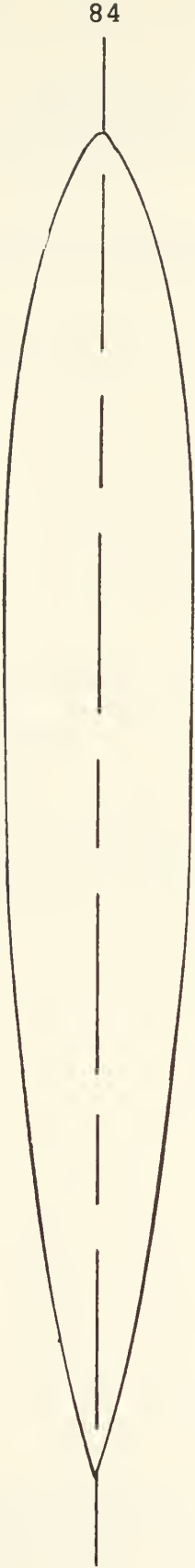




TABLE A2-4  
Offsets for Form 4173

X/L	Y/D	Formula:
0.00	0.0000	$Y^2 = a_1 X + a_2 X^2 + a_3 X^3 + a_4 X^4 + a_5 X^5 + a_6 X^6$
.02	.1438	
.04	.2055	where $a_1 = + 1.000000$ $a_2 = + 1.999633$ $a_3 = - 16.679052$ $a_4 = + 33.862413$ $a_5 = - 30.386285$ $a_6 = + 10.203269$
.06	.2530	
.08	.2925	
.10	.3262	
.12	.3554	
.14	.3807	
.16	.4026	
.18	.4215	
.20	.4378	
.22	.4517	
.24	.4634	
.26	.4731	
.28	.4810	$\text{Wetted Surface} = .34827 L^2$ $\text{Volume} = 1.0418 \times 10^{-2} L^3$ $\text{LCB} = \frac{X}{L} = .4657$ $\text{Length Diameter Ratio} = \frac{L}{D} = 7.$ $\text{Prismatic Coefficient} = C_p = .65$
.30	.4874	
.32	.4923	
.34	.4958	
.36	.4982	
.38	.4995	
.40	.5000	
.42	.4996	
.44	.4985	
.46	.4966	
.48	.4942	
.50	.4912	
.52	.4876	
.54	.4836	
.56	.4790	
.58	.4737	
.60	.4680	
.62	.4615	
.64	.4542	
.66	.4463	
.68	.4373	
.70	.4274	
.72	.4163	
.74	.4039	
.76	.3901	
.78	.3747	
.80	.3576	
.82	.3386	
.84	.3175	
.86	.2940	
.88	.2683	
.90	.2397	
.92	.2081	
.94	.1729	
.96	.1334	
.98	.0871	
1.00	0.0000	

Reference (18)





FIGURE A2-2

Profile of Form 4173

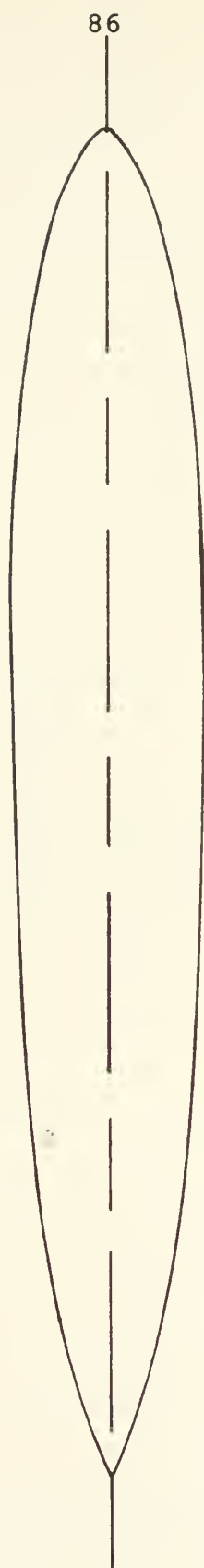




TABLE A2-5  
Offsets for Form 4166

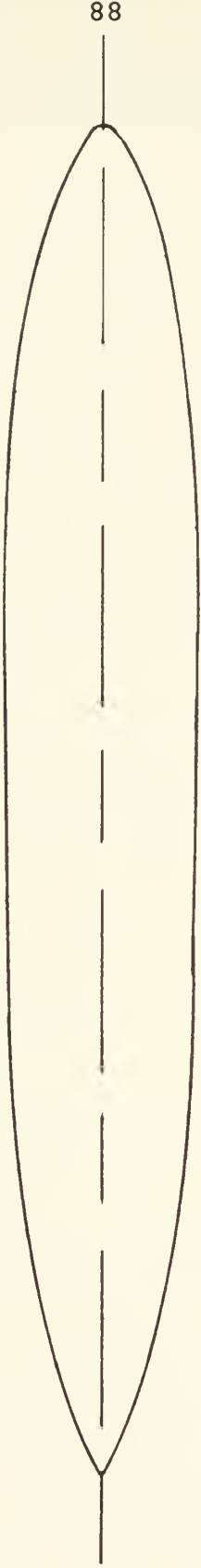
X/L	Y/D	FORMULA:
0.00	0.0000	$Y^2 = a_1 X + a_2 X^2 + a_3 X^3 + a_4 X^4 + a_5 X^5 + a_6 X^6$ <p>where <math>a_1 = + 1.000000</math>  <math>a_2 = + 3.462153</math>  <math>a_3 = - 26.960996</math>  <math>a_4 = + 59.35721</math>  <math>a_5 = - 56.48003</math>  <math>a_6 = + 19.62167</math></p> <p>Wetted Surface = <math>.36325 L^2</math>  Volume = <math>1.1219 \times 10^{-2} L^3</math>  LCB = <math>\frac{X}{L} = .4781</math>  Length Diameter Ratio = <math>\frac{L}{D} = 7</math>  Prismatic Coefficient = <math>C_p = .70</math></p>
.002	.1455	
.04	.2097	
.06	.2596	
.08	.3010	
.10	.3362	
.12	.3664	
.14	.3922	
.16	.4141	
.18	.4327	
.20	.4483	
.22	.4611	
.24	.4716	
.26	.4799	
.28	.4865	
.30	.4915	
.32	.4950	
.34	.4974	
.36	.4990	
.38	.4998	
.40	.5000	
.42	.4998	
.44	.4994	
.46	.4986	
.48	.4978	
.50	.4968	
.52	.4958	
.54	.4945	
.56	.4930	
.58	.4912	
.60	.4890	
.62	.4862	
.64	.4825	
.66	.4780	
.68	.4723	
.70	.4651	
.72	.4565	
.74	.4460	
.76	.4333	
.78	.4185	
.80	.4010	
.82	.3807	
.84	.3573	
.86	.3306	
.88	.3004	
.90	.2663	
.92	.2280	
.94	.1853	
.96	.1376	
.98	.0837	
1.00	0.0000	

Reference (18)



FIGURE A2-3

Profile of Form 4166





graphically for the three candidates. Cylindrical volumes of varying diameters were drawn inside the envelopes, the maximum lengths of these cylinders determined and the enclosed volumes in the cylinders calculated. The volume of the cylinder was then normalized by the total volume enclosed in the hull form. This fraction was plotted versus  $D_p/L$ , the maximum diameter of the pressure hull over the length of the form. Several data points were calculated for each form and then a least squares fit drawn through the points. These plots are presented in figures A 2 - 4, A 2 - 5, and A 2 - 6 for the three bodies.

The largest pressure hull volume for a given envelope volume for the three forms are therefore as follows:

$$\text{Form 4165} \quad \left( \frac{V_p}{V_E} \right)_{\text{Max}} = 0.56 \quad @ \quad \frac{D_p}{L} = 0.116$$

$$\text{Form 4173} \quad \left( \frac{V_p}{V_E} \right)_{\text{Max}} = 0.58 \quad @ \quad \frac{D_p}{L} = 0.12$$

$$\text{Form 4166} \quad \left( \frac{V_p}{V_E} \right)_{\text{Max}} = 0.61 \quad @ \quad \frac{D_p}{L} = 0.126$$

A comparison of envelope resistance on the basis of both the total envelope volume and the volume of an optimum cylindrical pressure hull enclosed in each form can now be made. These calculations were performed for envelope





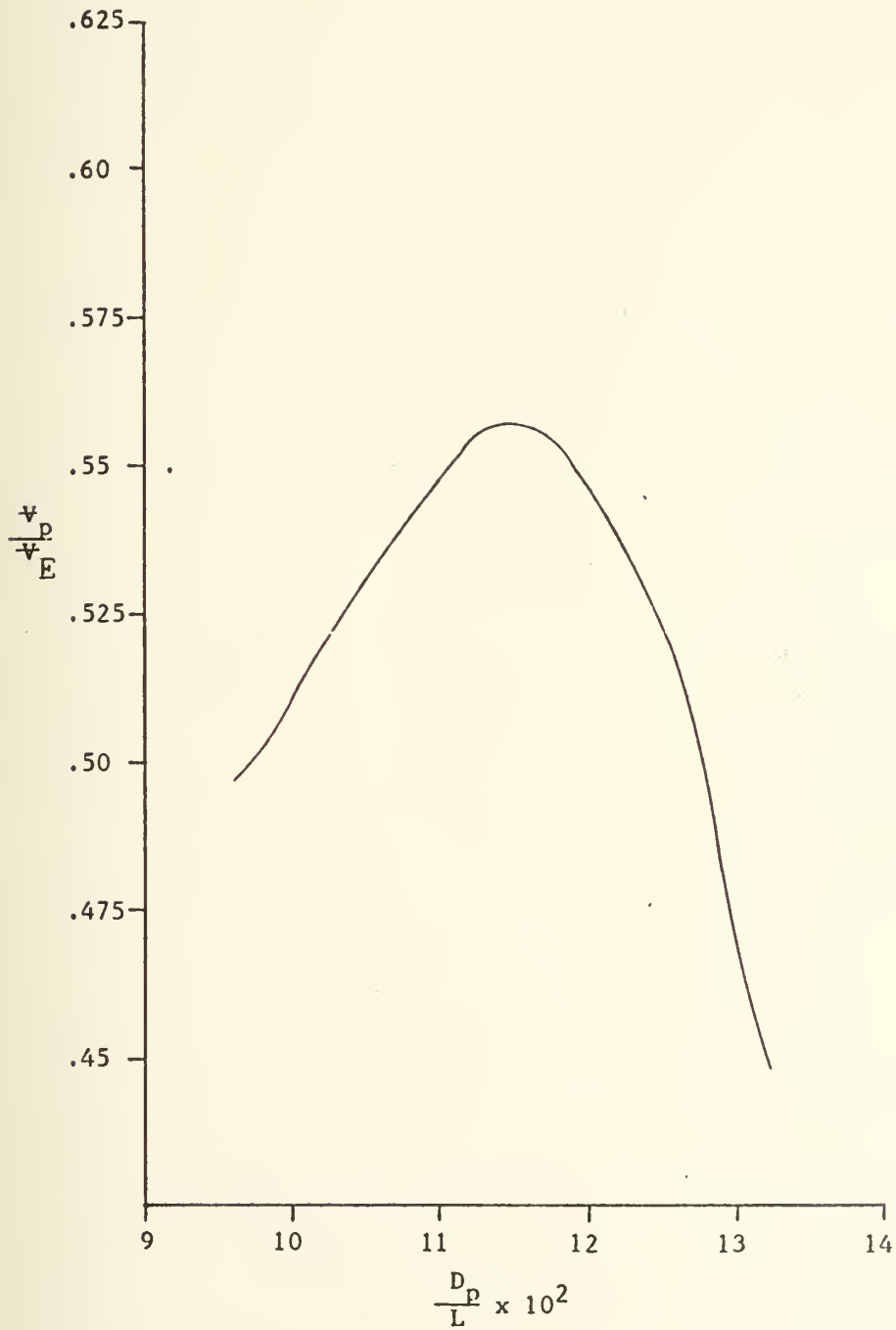
FIGURE A2-4  $v_p/v_E$  versus  $D_p/L$  FOR SERIES 58 FORM 4165



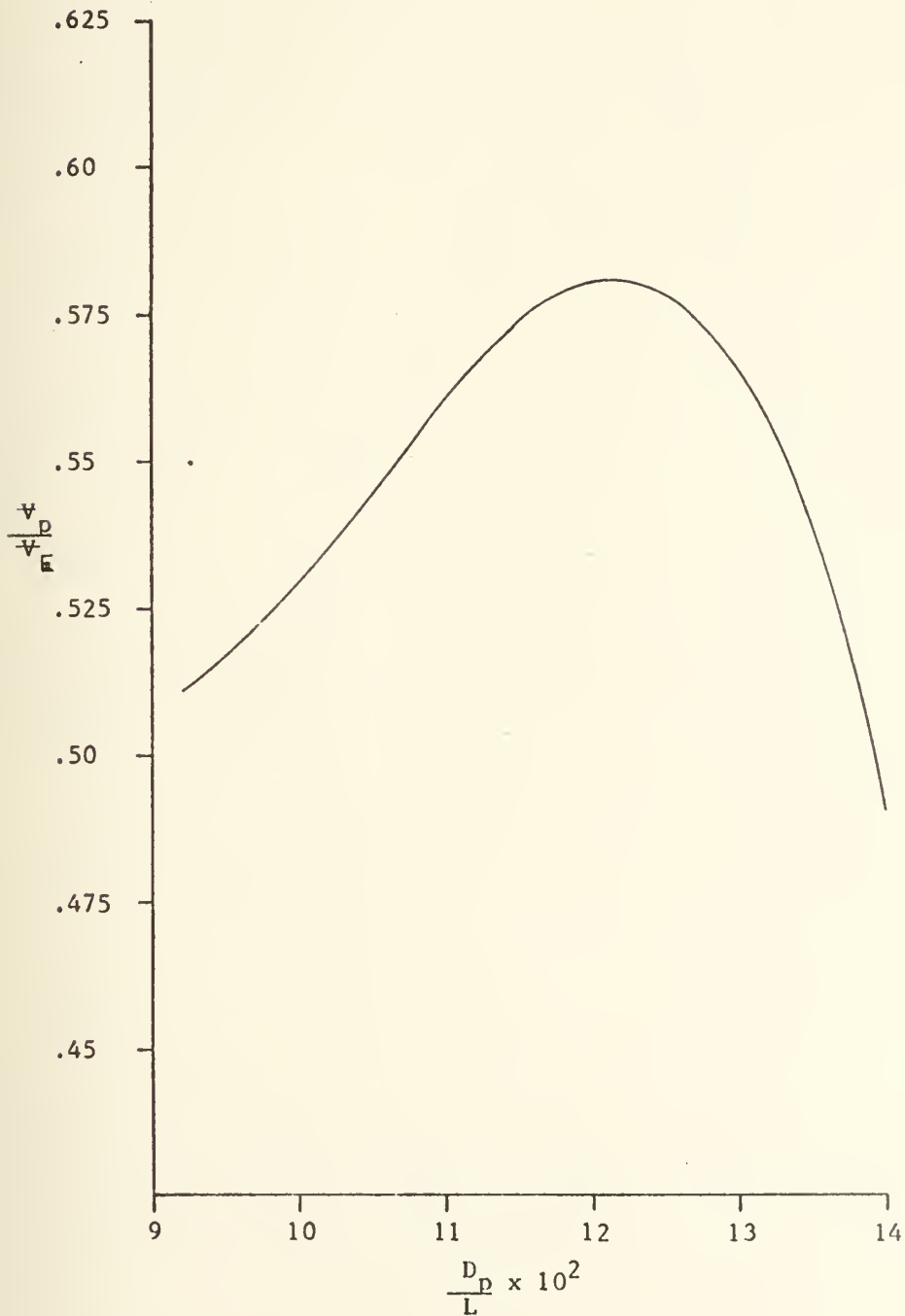
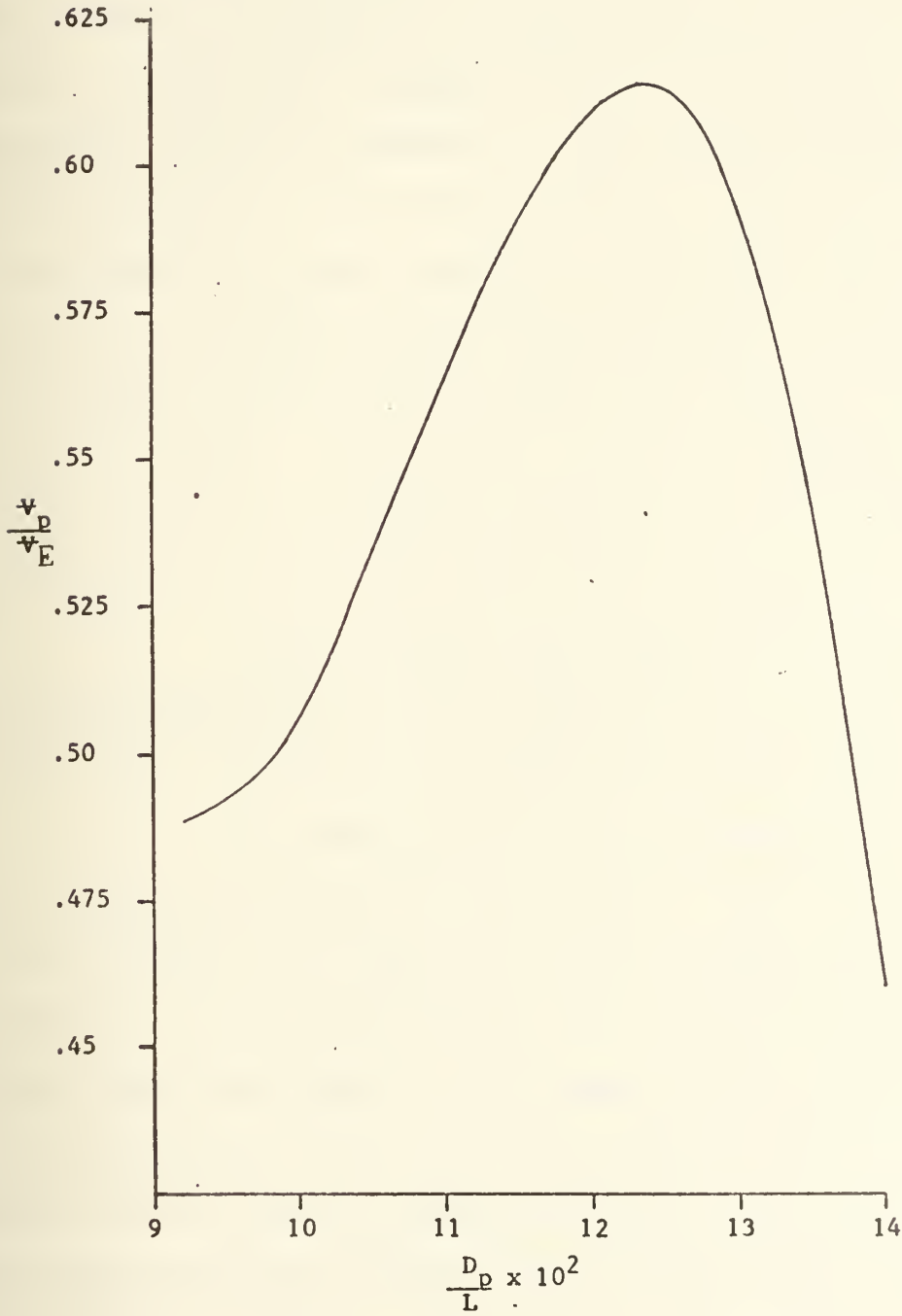
FIGURE A2-5  $v_p/v_E$  versus  $D_p/L$  FOR SERIES 58 FORM 4173



FIGURE A2-6  $v_p/v_E$  versus  $D_p/L$  FOR SERIES 58 FORM 4166



volumes of  $5 \text{ ft}^3$ ,  $7.65 \text{ ft}^3$ , and  $10 \text{ ft}^3$  and for pressure hull volumes of  $3 \text{ ft}^3$ ,  $5 \text{ ft}^3$ , and  $7 \text{ ft}^3$ , at 3, 5 and 7 knots. The results are presented in Tables A 2 - 6 and 7. On the basis of equivalent envelope volume the Form 4165 is considerably better, as expected. When measured versus constant optimum pressure hull volume, however, the three form's resistances are nearly identical. Also the outside pressure hull diameters are all nearly equal and, therefore, no envelope form has an advantage over another for its ability to hold a large object inside the pressure hull. In the case of a sub optimum pressure hull size, the Form 4165 still is better than the other two options.

This analysis concludes that the best hull form from the Series 58 for the robot will be the Form 4165. But, how does this compare with the torpedo shape?

For the purpose of this comparison, the concept of the equivalent form was developed. This is a configuration of another hull form which has the same enclosed volume or cylindrical pressure hull volume as that of the first generation robot. Since these exact volumes of the first generation robot were not tabulated, they were estimated from the robot's characteristics and dimensions. The estimated envelope volume is  $7.65 \text{ ft}^3$  and the volume of a cylindrical pressure which could be accommodated is  $5 \text{ ft}^3$ . A comparison of the two forms on this basis yields the results plotted in Figure A 2 - 7.





TABLE A2-6

Resistance Comparison for Series 58 Forms 4165,  
4173, and 4166 on the Basis of Envelope Volume

For  $\forall_E = 5 \text{ ft}^3$

Model	L	S	D <sub>p</sub>	$\forall_p$	R <sub>T</sub> @ 3	R <sub>T</sub> @ 5	R <sub>T</sub> @ 7
4165	8.05	21.43	0.93	2.8	2.37	6.11	11.42
4173	7.83	21.36	0.94	2.9	2.41	6.20	11.60
4166	7.64	21.20	0.96	3.05	2.48	6.41	12.00

For  $\forall_E = 7.65 \text{ ft}^3$

Model	L	S	D <sub>p</sub>	$\forall_p$	R <sub>T</sub> @ 3	R <sub>T</sub> @ 5	R <sub>T</sub> @ 7
4165	9.27	28.45	1.08	4.28	3.08	7.95	14.87
4173	9.03	28.36	1.08	4.44	3.13	8.08	15.11
4166	8.81	28.17	1.11	4.67	3.23	8.36	15.63

For  $\forall_E = 10 \text{ ft}^3$

Model	L	S	D <sub>p</sub>	$\forall_p$	R <sub>T</sub> @ 3	R <sub>T</sub> @ 5	R <sub>T</sub> @ 7
4165	10.13	34.01	1.18	5.60	3.64	9.39	17.56
4173	9.87	33.9	1.18	5.80	3.69	9.53	17.85
4166	9.63	33.66	1.21	6.10	3.80	9.86	18.49

Velocities in Knots

Dimensions in Ft.

Bare Hull Resistance in Pounds



TABLE A2-7

Resistance Comparison for Series 58 Forms 4165, 4173,  
and 4166 on the Basis of Pressure Hull Volume

For  $V_p = 3 \text{ ft}^3$

Model	L	S	D <sub>p</sub>	$V_E$	$R_T$ @ 3	$R_T$ @ 5	$R_T$ @ 7
4165	8.23	22.44	0.95	5.37	2.47	6.38	11.92
4173	7.95	21.97	0.95	5.22	2.47	6.37	11.92
4166	7.60	20.97	0.96	4.92	2.45	6.34	11.88

For  $V_p = 5 \text{ ft}^3$

Model	L	S	D <sub>p</sub>	$V_E$	$R_T$ @ 3	$R_T$ @ 5	$R_T$ @ 7
4165	9.76	31.54	1.13	8.93	3.39	8.75	16.37
4173	9.42	30.87	1.13	8.69	3.38	8.74	16.36
4166	9.01	29.47	1.135	8.20	3.36	8.71	16.33

For  $V_p = 7 \text{ ft}^3$

Model	L	S	D <sub>p</sub>	$V_E$	$R_T$ @ 3	$R_T$ @ 5	$R_T$ @ 7
4165	10.92	39.47	1.27	12.50	4.17	10.78	20.18
4173	10.54	38.65	1.26	12.17	4.17	10.77	20.18
4166	10.08	36.89	1.27	11.48	4.14	10.74	20.14

Velocities in Knots

Dimensions in Ft.

Bare Hull Resistance in Pounds



In Figure A 2 - 7, Curve 1 represents the estimated actual drag for the first generation robot. Point A is the estimated actual operating point for the original robot at a velocity of 2.2 knots or 3.71 feet per second. Curve two represents the predicted drag curve for the robot according to [14] where point B corresponds to the predicted operating point. Curves 3 and 4 refer to a Form 4165 of lengths 9.85 feet and 9.3 feet respectively. Appendage sizes with 7.5 per cent of the envelope surface area are assumed present in calculating these curves. This assumed appendage wetted surface is the same as that present in the tail controls of the original submarine. The form 4165 of length 9.3 feet corresponds to an envelope with the same enclosed volume as that of the original submarine. The Form 4165 of length 9.85 feet corresponds to the size Form 4165 which will carry the same volume cylindrical pressure hull as that which could be carried in the first generation submarine. The actual drag curve for the original submarine had to be estimated since only the actual operating speed of the submarine was available. The actual propeller RPM was not recorded.

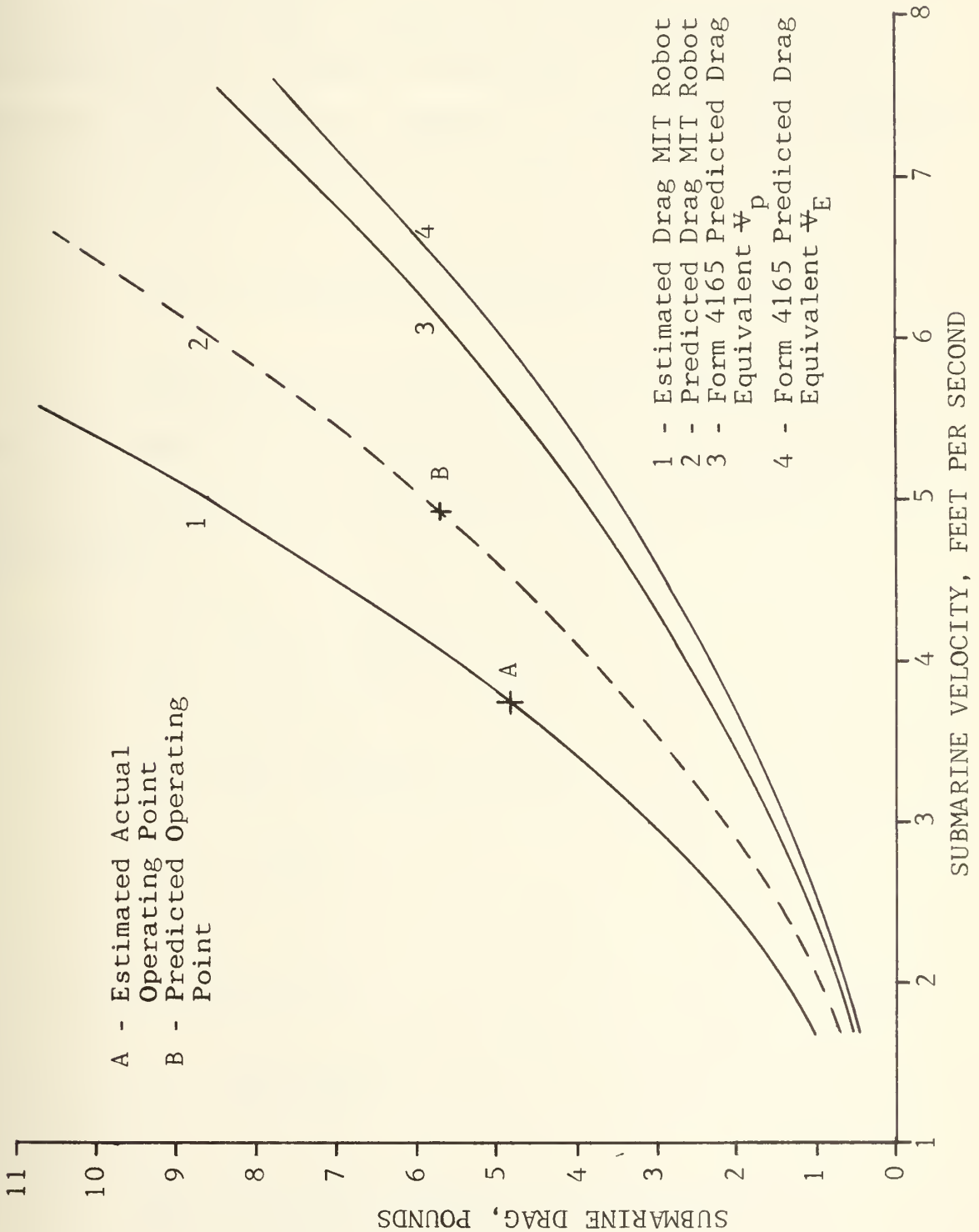
Figure A 2 - 7 shows a considerable drag reduction is predicted over the estimated actual operating curve for the original robot as well as over the predicted drag curve for the original robot.

The only remaining questionable asset of the



# RESISTANCE COMPARISON BETWEEN THE FIRST GENERATION ROBOT AND THE FORM 4165 EQUIVALENT FORMS

FIGURE A2-7







Form 4165 is its producibility. Should the Form 4165 in its pure form be employed, or should a 4165 form with a maximum diameter equal to  $D_p$  be used and the pressure hull surrounded with an easier to fabricate cylindrical shell? Reference [19] presents a formula to account for the addition to  $C_r$  due to this cylindrical section. This correction is

$$\Delta C_r \text{ due cylindrical midsection} = .002 (C_p - .6)$$

Using this correction, the resistance of a form with the same size cylindrical section as the original robot can be calculated, but with a Form 4165 nose and tail. For this body:

$$D_p = 14.75 \text{ inches} = 1.23 \text{ ft}$$

$$L_p = 50.5 \text{ inches} = 4.21 \text{ ft}$$

$$V_p = 5 \text{ ft}^3$$

$$L = 12.82 \text{ ft}$$

$$S = 40.8 \text{ ft}^2$$

$$V_E = 11.14 \text{ ft}^3 \quad V_p / V_E = .45$$



Without continuing further, it is evident that the envelope volume is poorly used. Fitting the same hull dimensions into a pure Form 4165 yields an envelope with dimensions as follows:

$$L = 11.4 \text{ ft}$$

$$D_x = 1.63 \text{ ft}$$

The resistance of this form will be obviously less than the previous form's resistance. Further, to enclose the same volume pressure hull, but with more optimum dimensions in the pure Form 4165 requires a length of only 9.85 feet with a pressure hull diameter of 1.14 ft.

The use of the pure Form 4165 is, therefore, chosen as the most suitable envelope.

#### A2.1 Conclusions

1. The Series 58 Form 4165 proves to be the best selection for the envelope form of those considered.
2. The laminar flow hull forms offer the possibility of considerable drag reductions; however, it is very questionable whether the laminar boundary layer can be sustained in an operational environment.
3. Choice of the Form 4165 envelope will show significant drag reduction over the first



Generation robot's resistance.



## APPENDIX III

## PROPULSION SYSTEM TRADE OFF STUDY

The propulsion system consists of the propulsor, transmission and the prime mover. Since this system places the greatest power demands on the energy storage system, the overall propulsion system efficiency is very important to extending the range and endurance of the submarine.

## A3.1 Propulsor.

For the propulsor selection three alternative configurations are considered.

1. Contra-rotating propellers
2. Ducted propeller
3. Conventional single screw propellers

The first alternative, the contra-rotating propellers, have advantages and are usually used in high power applications, especially where cavitation is a problem. A pair of contra-rotating propellers can be designed to be speed or torque balanced as discussed in [20]. In the torque balanced design the propellers may operate at different speeds, but will each operate with the same magnitude, but opposing torques. The pair are, therefore, torque balanced.

This attribute is important for small vehicles which might roll considerably to counter any unbalanced torque. In the operation of the first generation robot,





this roll was approximately three degrees. The ability of a set of contra-rotating propellers to put high power into the water with reduced cavitation and for the propulsion system to be torque balanced are the main reasons torpedoes use contra-rotating propeller propulsors almost exclusively.

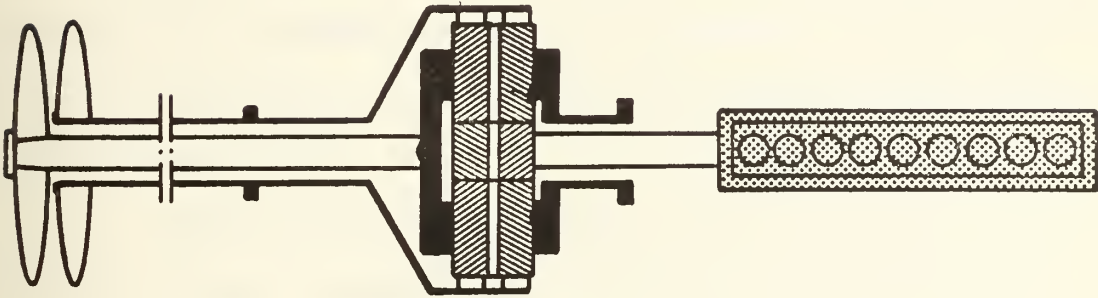
An additional advantage of the contra-rotating propeller set is the improvement this propulsor can make in the propulsive coefficient as shown in [21] and [22]. An improvement of up to fifteen per cent in the propulsive coefficient over that of a heavily loaded single screw propulsor was reported by the use of the contra-rotating propeller set. This was, however, a specific case and these improvements are certainly not the rule.

The contra-rotating configuration does have its faults as well as advantages, however. Perhaps the most significant is the added complexity of the drive train required to drive the two propellers in opposite directions about the same axis. This requires concentric shafts which have significant problems with shaft bearings and seals. The transmission for this set up can also be rather complex, but the use of an epicyclic gear train, as presented in [20] and [22] and depicted in Figure A3-1, driven by a single motor provides an efficient solution to the problem. The design of a pair of contra-rotating propellers presents another problem. Usually the two propellers differ in diameter, pitch, number of blades, as well as the obvious



FIGURE A3-1

Contra-rotating Propellers Driven by a Single  
Motor Through a Set of Epicyclic Reduction Gears



From Reference 20



direction of rotation. In part due to the complexities of flow associated with this propulsor and the variation of these conditions from application to application and the limited prior use of this propulsor, data for a standard series of contra-rotating propellers are not available. The design of a set of contra-rotating propellers for a specific application is usually, therefore, performed on a computer. Presently, however, in association with an effort to improve the propulsor efficiencies of merchant ships, some work is being done in this area. An additional drawback of the contra-rotating propeller set is the weight of the two propellers located far astern. This may possibly cause some trim problems.

These problems associated with the contra-rotating propulsor system outweigh the advantage which might amount to a five to ten percent improvement in propulsor efficiency. A significant technical risk would be accepted by selecting this alternative, however. This risk is felt to be especially pronounced in the area of the shaft seals. On these grounds the contra-rotating propeller set is therefore eliminated from further consideration.

The second alternative is the ducted propeller system, which has three forms:

1. Accelerating inflow or Kort nozzle
2. Decelerating inflow or pump jet design
3. Ring propeller



The third ducted configuration, the ring propeller, is discussed in [24] and is the least suitable for the intended application. The viscous drag on the ring increases the swirl left in the wake by the propeller, thus reducing its efficiency and its inertia adds to the torque required to spin the screw. The first two configurations may be more suitable, and a great deal of study has been conducted in the Netherlands as documented in [23], [25], [26], [27], [28], [29] and [30] on these configurations.

Reference [30] addresses the suitability of the ducted propeller design and concludes that these propulsors can improve propulsor efficiency for highly loaded screws with a value of:

$$K_T = \frac{T}{[1/2] \rho V_A^2 [\pi/4] D_{pr}^2} > 2.0$$

It is at this point that the gain in ideal efficiency exceeds the losses due to the increased drag of the nozzle. A direct comparison of the accelerating and decelerating designs indicates the accelerating flow has a higher ideal efficiency than the decelerating flow design. The decelerating flow is most useful where cavitation is a problem since the nozzle increases the static pressure at the propeller plane. The robot vehicle does not, however, have a cavitation problem and, therefore, only the accelerating





inflow configuration will be considered further.

Reference [31] lists some of the advantages of the accelerating inflow ducted propellor over conventional open screws as follows:

1. Improved efficiency for highly loaded propellers.
2. Smaller propeller sizes. (The ducted propeller is generally about fifteen per cent smaller than an optimum open screw.)
3. Improved propulsor flow control.
4. Better utilization of wake inflow.
5. Improved propeller blade loading.
6. Reduced propeller induced vibration.
7. Possibility exists to use a steerable duct to control the vehicle.

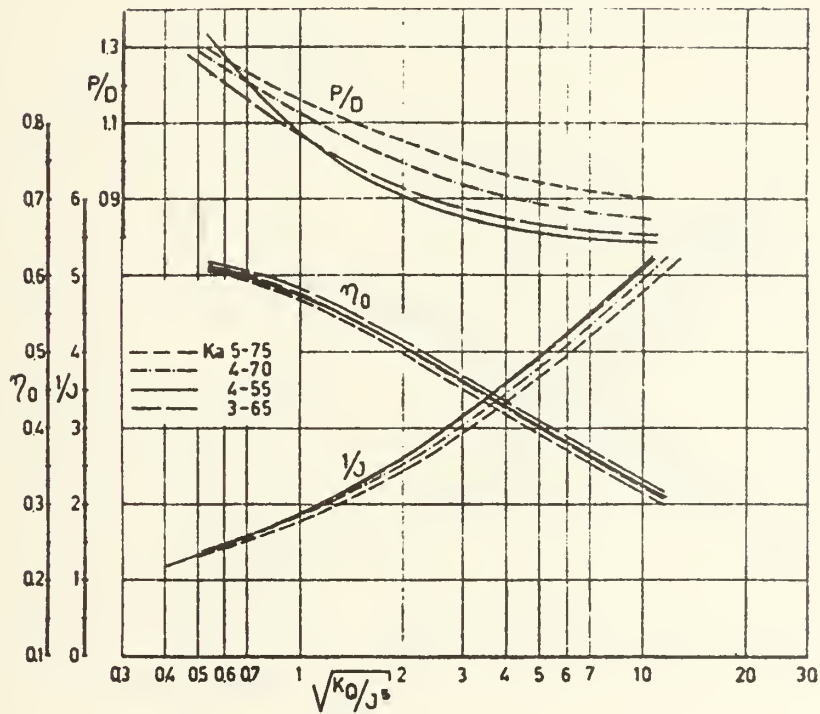
Reference [26] provides a series of propeller charts for the Kaplan screw series in a number 19A duct. These figures are reproduced in Figures A3-2 through 5. Figures A3-2 and A3-3 provide data for design of an optimum ducted propeller if the propeller RPM is specified and Figure A3-4 is employed if the propeller diameter is specified. Figure A3-5 is the conventional propeller chart presentation for a Kaplan 3-65 screw in a 19A duct.

The Kaplan series screws were designed specifically for use inside a duct. They have much larger tip areas than conventional propellers, and accordingly, can carry a greater



FIGURE A3-2

Optimum Kaplan Propeller Series in Duct 19A  
 Selection with Propeller RPM Specified  
 Using Propeller Torque



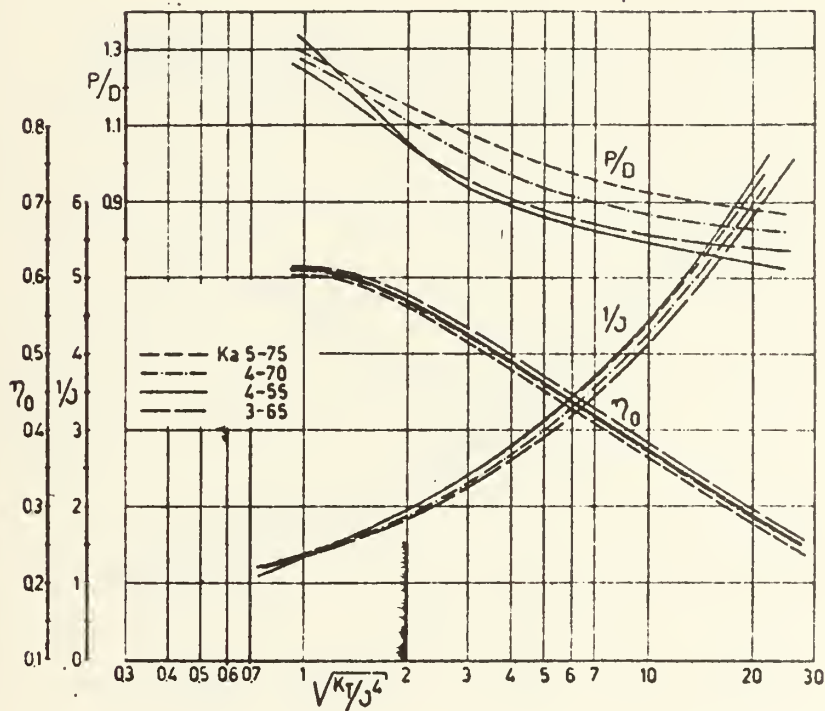
$$\frac{K_0}{J^5} = \frac{Q n^3}{\rho v^5 (1-w)^5} ; n = \frac{N}{60}$$

From Reference 26



FIGURE A3-3

Optimum Kaplan Propeller Series in Duct 19A  
 Selection with Propeller RPM Specified  
 Using Propeller Thrust



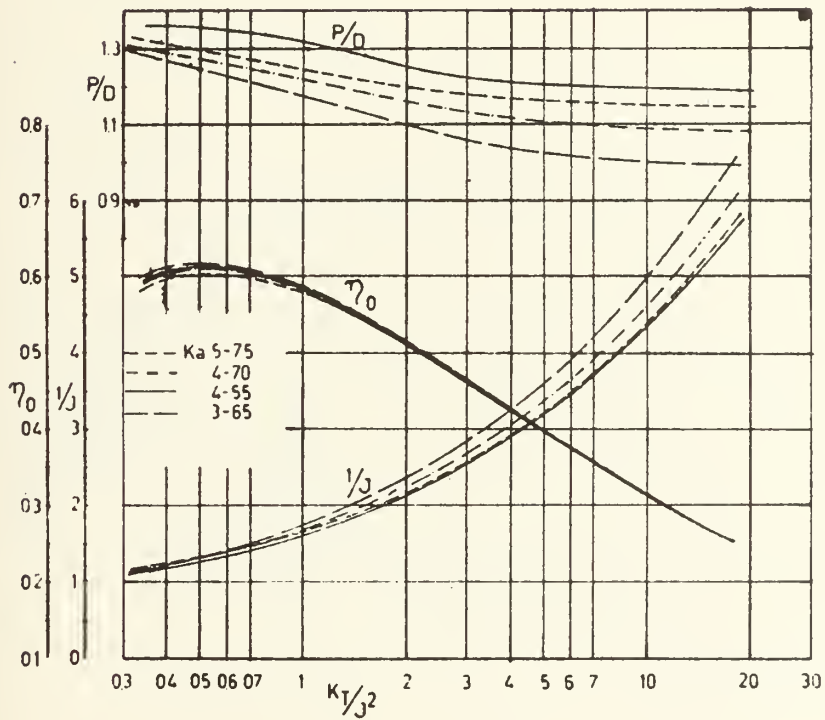
$$\frac{K_T}{J^4} = \frac{R_T n^2}{\rho v^4 (1-w)^4 (1-t)} ; \quad n = \frac{N}{60}$$

From Reference 26



FIGURE A3-4

Optimum Kaplan Propeller Series in Duct 19A  
Selection with Propeller Diameter Specified



$$\frac{K_T}{J^2} = \frac{R_T}{\rho v^2 (1-w)^2 D^2 (1-t)} ;$$

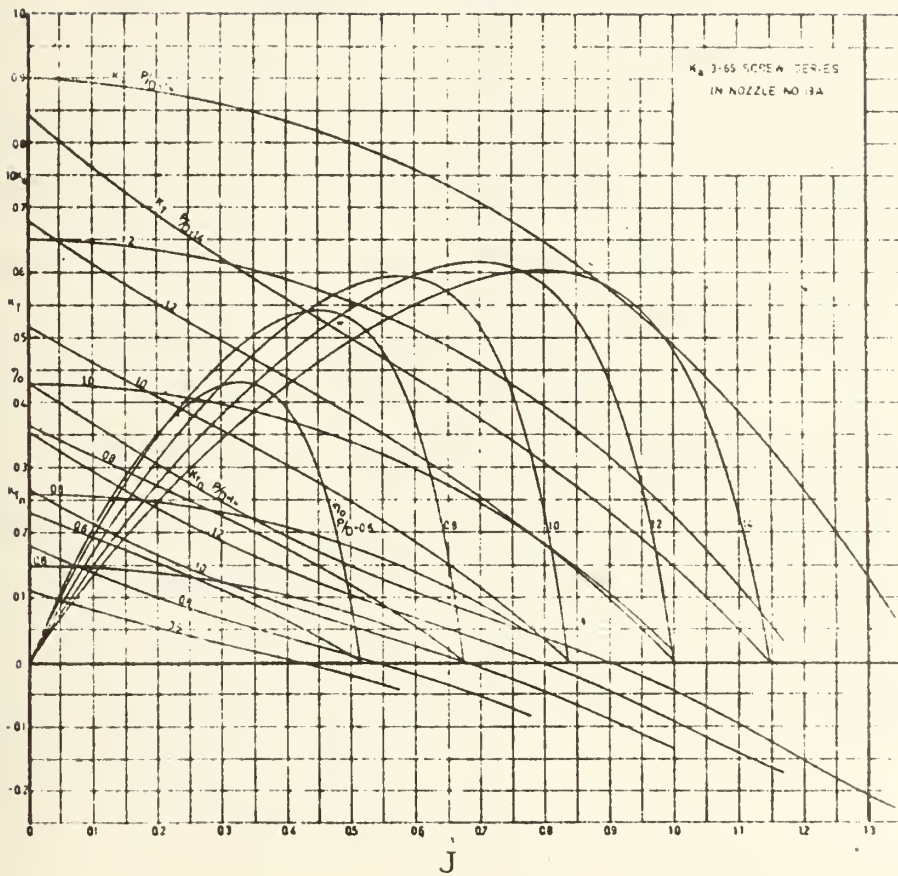
From Reference 26





FIGURE A3-5

Propeller Chart for Ka 3 - 65 Screw  
Series in Nozzle No. 19A



From Reference 26



load in their outer radii than a conventional screw. The particulars of the Kaplan 3-65 screw are presented in Figure A3-6 and Tables A3-1 and A3-2.

The 19A duct design was selected after a series of propeller tests as discussed in [26]. This design was determined to be the best of those tested. The profile of the 19-A duct, or nozzle, is shown in Figure A3-7.

After studying the data in Figures A3-2 through A3-5 and applying data from a variety of the different hull configurations, it is evident the best selection for this purpose is the B 3-65 screw. Perhaps more ideally suited would be a three bladed screw with a smaller expanded area ratio; but this data is not available.

Before using the previous figures to select a particular screw, first an estimate of the interaction between the propeller and the hull must be made. This propeller hull interaction is determined by the two factors, "t", the thrust deduction coefficient, and "w", the wake fraction as defined below:

$$R_{TA} = (1 - t) T$$

where:  $R_{TA}$  = Appended Hull Form Drag

$T$  = Propeller Thrust



Typical Propeller Blade of Ka 3-65 Series

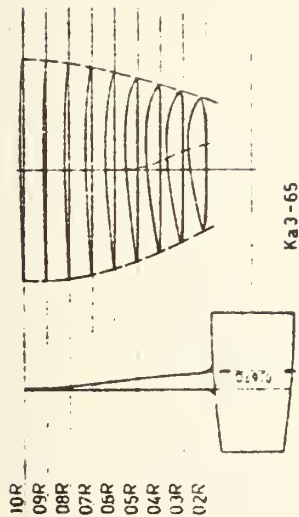


TABLE A3-1

Propeller Blade Data for Ka Series Propellers

	0.2	0.3	0.4	0.5	0.6	0.7	0.8	0.9	1.0	
$r/R$										
Length of the blade sections in percentages of the maximum length of the blade section at $0.6 R$	30.21	36.17	41.45	45.99	49.87	52.93	55.04	56.33	56.44	Length of blade section at $0.6 R$
	36.94	40.42	43.74	47.02	50.13	52.93	55.04	56.33	56.44	$1.969 \frac{r}{R}$
	67.15	76.59	85.19	93.01	100.00	105.86	110.08	112.66	122.88	$Z/A_0$
total length										
Max. blade thickness in percentages of the diam.	4.00	3.52	3.00	2.45	1.90	1.38	0.92	0.61	0.50	Maximum thickness at centre of shaft $\approx 0.049 D$
Distance of maximum thickness from leading edge in percentages of the length of the sections	34.98	39.76	46.02	49.13	49.98	—	—	—	—	

Reference (26)



TABLE A3-2

## Propeller Blade Offsets for Ka Series Propellers

$r/R$	Distance of the ordinates from the maximum thickness												
	From maximum thickness to trailing edge						From maximum thickness to leading edge						
	100%	80%	60%	40%	20%		20%	40%	60%	80%	90%	95%	100%
						Ordinates for the back							
0.2	—	38.23	63.65	82.40	95.00	97.92	90.83	77.19	55.00	38.75	27.40	—	—
0.3	—	39.05	66.63	84.14	95.86	97.63	90.06	75.62	53.02	37.87	27.57	—	—
0.4	—	40.56	66.94	85.69	96.25	97.22	88.89	73.61	50.00	34.72	25.83	—	—
0.5	—	41.77	68.59	86.42	96.60	96.77	87.10	70.46	45.84	30.22	22.24	—	—
0.6	—	43.58	68.26	85.89	96.47	96.47	85.89	68.26	43.58	28.59	20.44	—	—
0.7	—	45.31	69.24	86.33	96.58	96.58	86.33	69.24	45.31	30.79	22.88	—	—
0.8	—	48.16	70.84	87.04	96.76	96.76	87.04	70.84	48.16	34.39	26.90	—	—
0.9	—	51.75	72.94	88.09	97.17	97.17	88.09	72.94	51.75	38.87	31.87	—	—
1.0	—	52.00	73.00	88.00	97.00	97.00	88.00	73.00	52.00	39.25	32.31	—	—
						Ordinates for the face							
0.2	20.21	7.29	1.77	0.1	—	0.21	1.46	4.37	10.52	16.04	20.62	33.33	—
0.3	13.85	4.62	1.07	—	—	0.12	0.83	2.72	6.15	8.28	10.30	21.18	—
0.4	9.17	2.36	0.56	—	—	—	0.42	1.39	2.92	3.89	4.44	13.47	—
0.5	6.62	0.68	0.17	—	—	—	0.17	0.51	1.02	1.36	1.53	7.81	—

Note: The percentages of the ordinates relate to the maximum thickness of the corresponding section.

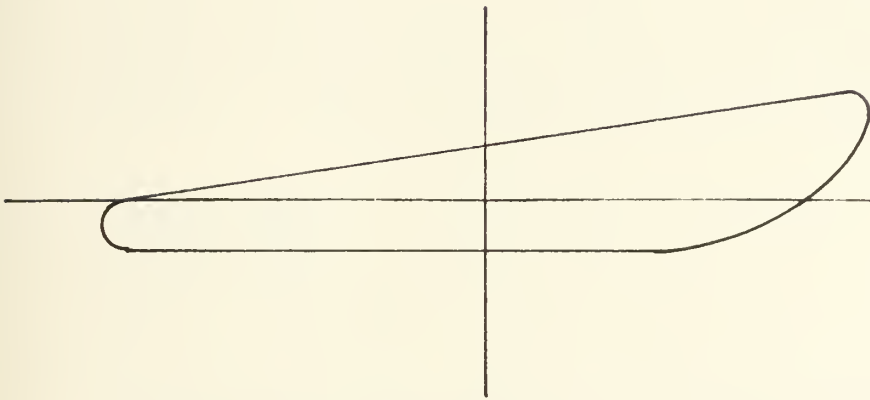
Reference (26)





FIGURE A3-7

Profile of Nozzle Number 19A



Reference (26)



$$V_A = (1-w)V$$

Where:  $V$  = Ship speed through the water

$$V_A = \text{Propeller speed of advance}$$

These values may be determined either by model tests or are more commonly determined from past designs. Reference [32] presents data for a hull form similar to that selected for the proposed robot, which uses a ducted propeller. The values of the coefficients from [32] are as follows:

$$(1-t) = .912$$

$$(1-w) = .823$$

These values are used for all further calculations with ducted propellers.

Using Figures A3-2 through A3-4 with the parameters for the particular envelope form and speed leads to selection of the best ducted propeller. In a configuration not limited by propeller diameter or speed, a maximum open water efficiency of 0.62 can be obtained. The parameter of interest is, however, the propulsive coefficient, PC.

$$\text{Where: } PC = \eta_H \times \eta_O \times \eta_{rr}$$



$$\text{and } \eta_H = \frac{1-t}{1-w}$$

$\eta_o$  = calculated propeller open water efficiency

$\eta_{rr}$  = relative rotative efficiency  
assumed = 1.0

Using this data a maximum PC of 0.69 may be achieved for the Ka 3-65 ducted propeller. During this calculation, however, the size or speed of the propeller may be considered a limitation in which case the appropriate optimum design curves or the more general Figure A3-5 must be used. These conditions may yield a propulsive coefficient less than the 0.69 value previously calculated.

The optimum propulsive coefficient calculated for the Ka 3-65 in the 19A duct of 0.69 does not compare favorably with the predicted propulsive coefficient for the first generation robot of 0.82 [14]. Data obtained from a series of optimum ducted propeller calculations on various sized bodies at different operating speeds indicates the value of  $K_T$  for these designs varies from 1.27 to 1.28, which is less than the recommended value of 2.0, above which the ducted propeller is more suitable than the open propeller. Since the robot's operating conditions do not meet this condition, an open screw might be expected to be superior to the ducted one.



The ducted propeller does have advantages over the open screw as listed previously, however. One of the most important could be the presence of the duct itself which protects the screw from becoming entangled on stray lines or sea weed. Entanglement could stop the screw and entrap the vehicle, thus resulting in the loss of the robot. Also, the duct reduces propeller induced vibrations which might otherwise affect the quality of certain data collected. The ducted configuration also has the capability of using the duct for steering as is done with Alvin [3]. A ducted propeller used in this configuration would eliminate the need for control surfaces and their resultant drag. This configuration might also improve the control characteristics of the robot. These possibilities are evaluated further in this Appendix and in Appendix VI.

The investigation proceeds, then, to consideration of standard open propellers. As pointed out in [14], open propellers with low area ratios and small numbers of blades yield the best performance in the robot vehicle's case.

The propeller used on the first generation robot was a two-bladed torpedo design. In military submarine design, however, only odd number bladed propellers are used so vibration will be reduced. When the propeller blade passes directly behind a control surface, the flow over the blade changes drastically, and so does the thrust, momentarily. Since the number of control surfaces is always even





usually 4), for hydrodynamic reasons, when an even number bladed propeller is used, these changes occur simultaneously on each blade. This effect can be reduced somewhat by using higher even numbered bladed propellers with larger area ratio. With an odd number bladed propeller, on the other hand, the blades do not pass behind the control surfaces simultaneously, and the effect is spread out and is, consequently, less noticeable. Since these vibrations might affect data collection, only three bladed screws will be considered.

Before selection of the best three bladed screw can be accomplished, the question of propeller hull interaction for the open screw by specifying "t" and "w" must be addressed. Jackson [19], presents a formula which relates these parameters to the wetted surface as follows:

$$1 - w = .371 + 3.04 \frac{\text{Diameter Propeller}}{\sqrt{\text{Wetted Surface}}}$$

$$1 - t = .632 + 2.44 \frac{\text{Diameter Propeller}}{\sqrt{\text{Wetted Surface}}}$$

For the selected hull form, these equations can be modified to make them functions of the propeller diameter, maximum diameter ratio as follows:

For 4165 envelope form with seven per cent additional wetted surface for appendages:



$$1-w = .371 + .73 \frac{D_{\text{propeller}}}{D_x}$$

$$1-t = .632 + .586 \frac{D_{\text{propeller}}}{D_x}$$

From other sources, information regarding these parameters which were recorded from actual submarine designs was obtained. These data consists of four points relating  $1-t$  and  $1-w$  to the propeller diameter, maximum diameter ratio. A computer least squares fit routine was used to fit a second order curve through these points and yielded the following equations:

$$1-w = 0.14 + 1.6 \frac{D_{\text{pr}}}{D_x} - \left(\frac{D_{\text{pr}}}{D_x}\right)^2$$

$$1-t = .4836 + 1.145 \left(\frac{D_{\text{pr}}}{D_x}\right) - .7496 \left(\frac{D_{\text{pr}}}{D_x}\right)^2$$

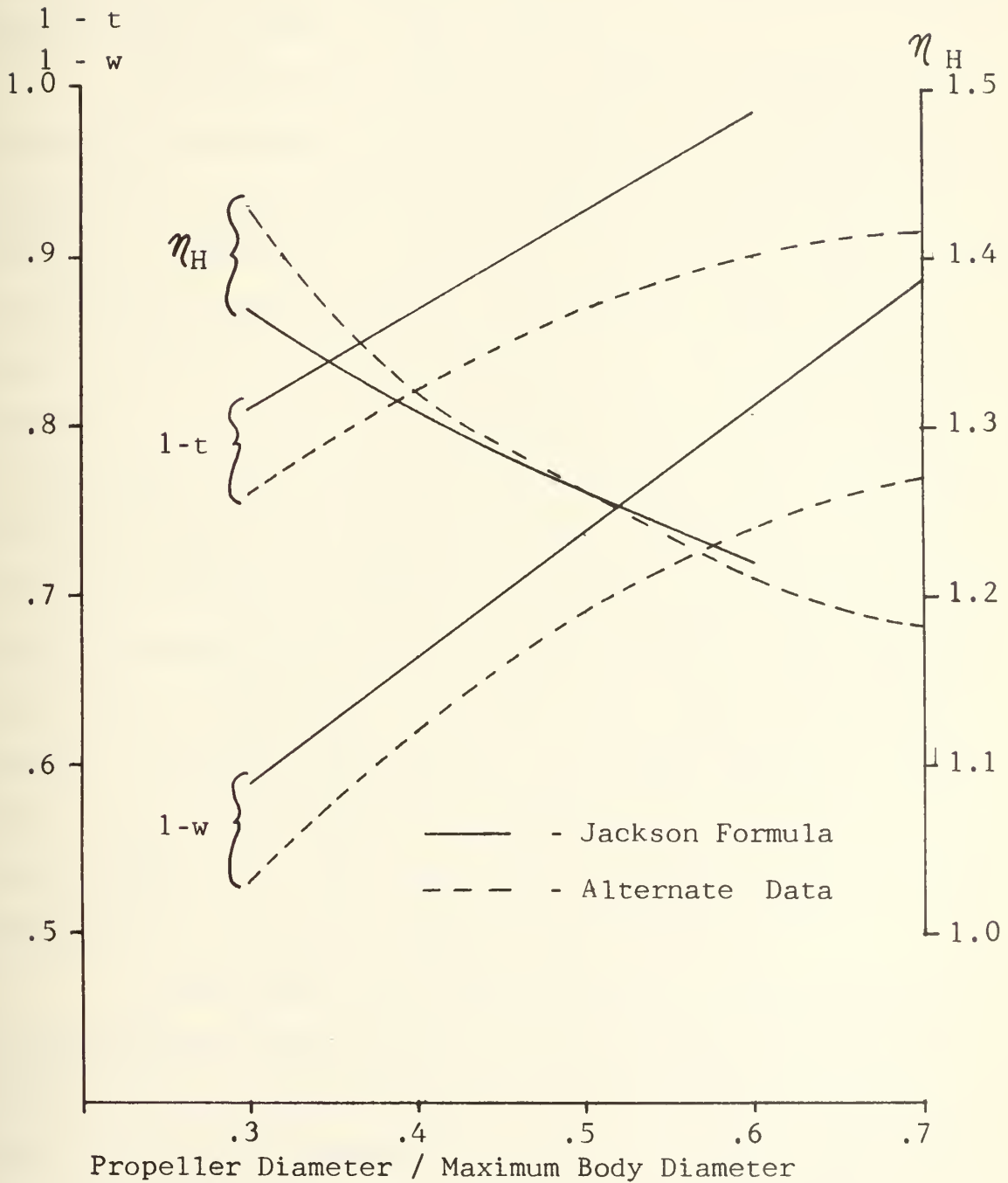
These equations are valid for  $.3 < \frac{D_{\text{pr}}}{D_x} < .6$ .

The results of both of these equations are presented in Figure A3-8, along with the resulting hull efficiencies. The values for  $1-t$  and  $1-w$  calculated by the two equations differ by as much as nine per cent, but the hull efficiencies differ by a maximum of only three per cent. Since the relation derived from the alternate data is



FIGURE A3-8

Comparison of  $1-t$ ,  $1-w$ , and  $\eta_H$  as Calculated by  
 Jackson's Formula and Formula Derived from  
 Alternate Data





obtained from operating submarines, whereas the Jackson formula is a linear relation, the formula based on the alternative data is used to define  $l-t$  and  $l-w$ . Additionally, looking at the plot of this curve, it is reasonable to extend the applicable region to  $\frac{D_{pr}}{D_x}$  less than 0.7.

Reference [33] outlines a method for determining the optimum propeller from the B series. This method is summarized in Table A3-3 and the curves for the B 3-45 propeller are presented in Figures A3-9 and A3-10. Additionally, the data from these curves is tabulated for Reynold's numbers  $2 \times 10^6$  and  $2 \times 10^7$  in Tables A3-4, A3-5, A3-6 and A3-7. Reference [14] presents an alternate three bladed propeller of the highly skewed destroyer variety which was considered for use on the first generation robot. Matching the drag curves of a series of different suitably sized vehicles with the performance of this second screw, an open water propeller efficiency of only about sixty-seven per cent is obtained; whereas, propeller selections for the same bodies from the data in [33] yields open water efficiencies of about 0.7, using a  $\frac{D_{pr}}{D_x} = 0.7$ . This open water propeller efficiency results in a PC of 0.805, assuming  $\eta_{rr} = 1.0$ .

Thus, the B 3.45 series screw will operate with a PC approximately equal to 0.8 and the KA 3-60 series in a 19A duct with an approximate PC = 0.69. These values may vary slightly for individual designs; but since they correspond to best values calculated for the same body at the same





TABLE A3-3

USE OF OPTIMUM B 3-45 SCREW SELECTION DATA

$$\frac{K_T}{J^2} = \frac{0.351 R_T}{V^2 (1-w)^2 D_{pr}^2 (1-t)}$$

$$\frac{K_T}{J^4} = \frac{.123 R_T n^2}{V^4 (1-w)^4 (1-t)}$$

$$Re = 0.273724 \times 10^6 \frac{V D_{pr} (1-w) A_e / A_o}{z} \frac{J^2 + (0.75)^2}{J}$$

$$J = \frac{V (1-w)}{N D_{pr}} \times 35.58$$

V - knots,  $D_{pr}$  - feet

## PROCEDURE

- I. If Propeller RPM is specified.
  - a. Compute  $\sqrt{K_T / J^4}$
  - b. Assume a Value for Re
  - c. Use Figure A3-8 or Tables A3-4 and A3-5 using linear interpolation for Re.
  - d. Determine J and  $D_{pr}$  from the data
  - e. Compute Re using the formula above
  - f. Determine J and  $D_{pr}$  from the Table with the new value of Re.
  - g. Continue this process until the solution converges.



123  
TABLE A3-3 contd.

II. If the Propeller Diameter is Specified.

- a. Compute  $\sqrt{K_T / J^2}$
- b. Assume a value of Re.
- c. Use Figure A3-9 or Tables A3-4 and A3-5  
with linear interpolation for Re.
- d. Determine J and RPM.
- e. Compute Re from the above Formula
- f. Use the figure or tables to obtain  
new values for J and RPM.
- g. Continue the process until the solution  
converges.



FIGURE A3-9 PROPELLER OPTIMIZATION CURVES FOR B 3-45 PROPELLER  
WITH PROPELLER RPM SPECIFIED

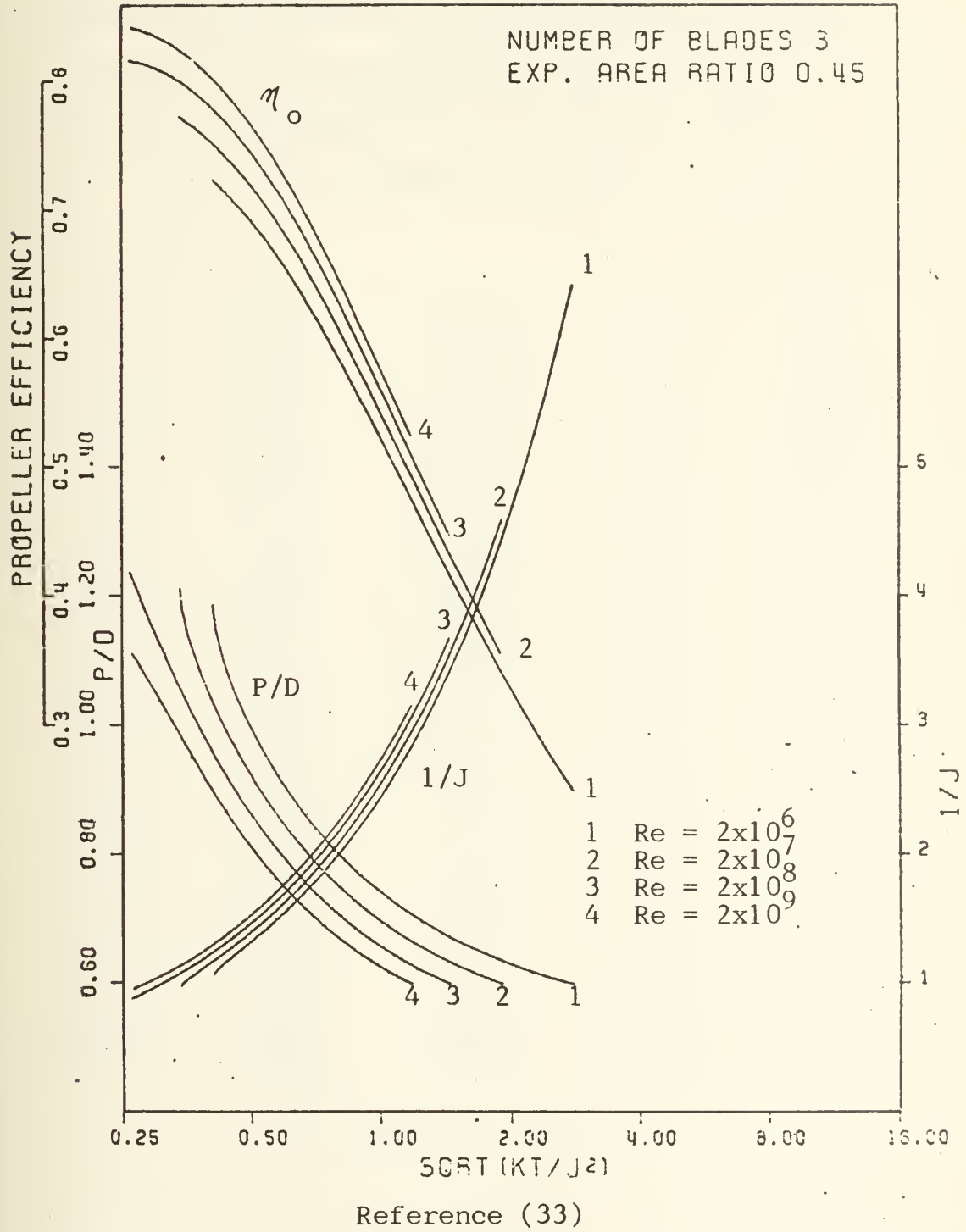




TABLE A3-4

TABULATED DATA OF P/D, J, AND PROPELLER EFFICIENCY  
 VERSUS  $K_T/J^4$ , OR  $K_Q/J^5$ , FOR OPTIMUM DIAMETER  
 OF B 3.45 SCREW SERIES AT A REYNOLD'S NUMBER  
 OF  $2 \times 10^6$  IF PROPELLER RPM IS SPECIFIED

$2\sqrt{K_T/J^4}$	P / D	1 / J	$\eta_o$	$4\sqrt{K_Q/J^5}$
3.0953	0.600	2.9316	0.4983	1.3227
2.5634	0.625	2.6727	0.5267	1.1871
2.1660	0.650	2.4608	0.5517	1.0786
1.8596	0.675	2.2836	0.5739	0.9896
1.6173	0.700	2.1328	0.5935	0.9151
1.4225	0.725	2.0030	0.6110	0.8521
1.2624	0.750	1.8894	0.6265	0.7977
1.1296	0.775	1.7895	0.6404	0.7504
1.0174	0.800	1.7006	0.6529	0.7088
0.9224	0.825	1.6211	0.6640	0.6720
0.8404	0.850	1.5493	0.6740	0.6391
0.7696	0.875	1.4843	0.6829	0.6095
0.7080	0.900	1.4252	0.6910	0.5829
0.6540	0.925	1.3711	0.6983	0.5588
0.6064	0.950	1.3216	0.7048	0.5368
0.5645	0.975	1.2760	0.7106	0.5168
0.5274	1.000	1.2341	0.7158	0.4987
0.4945	1.025	1.1953	0.7206	0.4821
0.4654	1.050	1.1596	0.7248	0.4670
0.4397	1.075	1.1266	0.7286	0.4533
0.4170	1.100	1.0962	0.7319	0.4410
0.3973	1.125	1.0683	0.7349	0.4300
0.3801	1.150	1.0428	0.7376	0.4202
0.3655	1.175	1.0195	0.7399	0.4117
0.3536	1.200	0.9987	0.7419	0.4047
0.3442	1.225	0.9801	0.7436	0.3990
0.3377	1.250	0.9643	0.7448	0.3951
0.3342	1.275	0.9512	0.7456	0.3929

Reference (33)





TABLE A3-5

TABULATED DATA OF P/D, J, AND PROPELLER EFFICIENCY  
 VERSUS  $K_T/J^4$ , OR  $K_Q/J^5$ , FOR OPTIMUM DIAMETER  
 OF B 3.45 SCREW SERIES AT A REYNOLD'S NUMBER  
 OF  $2 \times 10^7$  IF PROPELLER RPM IS SPECIFIED

$K_T/J^4$	P / D	1 / J	$\eta$	$K_Q/J^5$
2.4361	0.600	2.6634	0.5614	1.1389
2.0479	0.625	2.4480	0.5882	1.0321
1.7515	0.650	2.2691	0.6115	0.9453
1.5189	0.675	2.1175	0.6320	0.8731
1.3325	0.700	1.9872	0.6501	0.8120
1.1805	0.725	1.8739	0.6660	0.7596
1.0543	0.750	1.7742	0.6801	0.7142
0.9482	0.775	1.6855	0.6927	0.6742
0.8580	0.800	1.6061	0.7039	0.6387
0.7805	0.825	1.5345	0.7139	0.6071
0.7135	0.850	1.4697	0.7229	0.5786
0.6550	0.875	1.4105	0.7309	0.5529
0.6037	0.900	1.3563	0.7380	0.5295
0.5584	0.925	1.3066	0.7444	0.5081
0.5182	0.950	1.2607	0.7501	0.4886
0.4826	0.975	1.2183	0.7553	0.4707
0.4507	1.000	1.1790	0.7598	0.4542
0.4223	1.025	1.1425	0.7639	0.4390
0.3968	1.050	1.1086	0.7675	0.4251
0.3741	1.075	1.0771	0.7707	0.4123
0.3539	1.100	1.0478	0.7736	0.4007
0.3359	1.125	1.0205	0.7761	0.3900
0.3200	1.150	0.9954	0.7782	0.3804
0.3062	1.175	0.9722	0.7801	0.3719
0.2944	1.200	0.9509	0.7818	0.3645
0.2848	1.225	0.9317	0.7831	0.3583
0.2773	1.250	0.9147	0.7842	0.3534
0.2722	1.275	0.9000	0.7850	0.3501
0.2701	1.300	0.8881	0.7854	0.3487

Reference (33)



FIGURE A3-10 PROPELLER OPTIMIZATION CURVES FOR B 3-45 PROPELLER  
WITH PROPELLER DIAMETER SPECIFIED

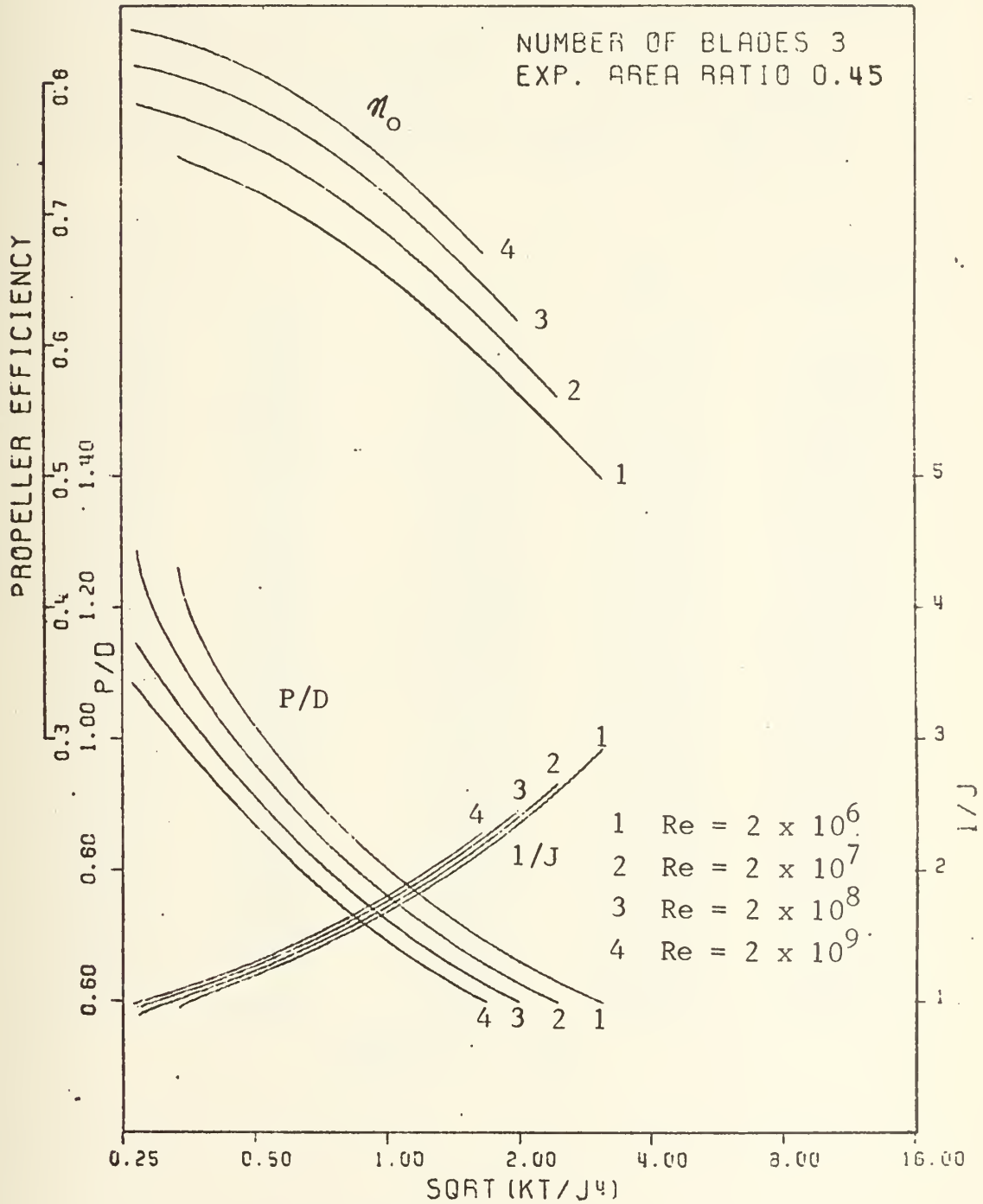




TABLE A3-6

TABULATED DATA OF P/D, J, AND PROPELLER EFFICIENCY  
 VERSUS  $K_T/J^2$ , OR  $K_Q/J^3$ , FOR OPTIMUM RPM  
 OF B 3.45 SCREW SERIES AT A REYNOLD'S NUMBER  
 OF  $2 \times 10^6$  IF PROPELLER DIAMETER IS SPECIFIED

$\sqrt[2]{K_T/J^2}$	P / D	1 / J	$\eta_o$	$\sqrt[4]{K_Q/J^3}$
2.7917	0.600	6.4241	0.2495	1.4932
2.1030	0.625	4.8922	0.3148	1.2228
1.6932	0.650	3.9828	0.3717	1.0526
1.4212	0.675	3.3804	0.4210	0.9348
1.2272	0.700	2.9514	0.4638	0.8479
1.0819	0.725	2.6303	0.5009	0.7809
0.9689	0.750	2.3807	0.5330	0.7276
0.8784	0.775	2.1807	0.5610	0.6840
0.8043	0.800	2.0167	0.5852	0.6476
0.7427	0.825	1.8798	0.6063	0.6169
0.6905	0.850	1.7635	0.6247	0.5904
0.6459	0.875	1.6636	0.6407	0.5674
0.6074	0.900	1.5767	0.6546	0.5473
0.5739	0.925	1.5005	0.6668	0.5295
0.5446	0.950	1.4331	0.6774	0.5138
0.5189	0.975	1.3733	0.6866	0.4998
0.4963	1.000	1.3198	0.6946	0.4874
0.4765	1.025	1.2718	0.7016	0.4764
0.4594	1.050	1.2288	0.7075	0.4668
0.4445	1.075	1.1903	0.7126	0.4583
0.4321	1.100	1.1558	0.7169	0.4512
0.4219	1.125	1.1252	0.7204	0.4453
0.4142	1.150	1.0985	0.7230	0.4408
0.4091	1.175	1.0756	0.7248	0.4378
0.4070	1.200	1.0568	0.7256	0.4366

Reference (33)



TABLE A3-7

TABULATED DATA OF P/D, J, AND PROPELLER EFFICIENCY  
 VERSUS  $K_T/J^2$ , OR  $K_Q/J^3$ , FOR OPTIMUM RPM  
 OF B 3.45 SCREW SERIES AT A REYNOLD'S NUMBER  
 OF  $2 \times 10^7$  IF PROPELLER DIAMETER IS SPECIFIED

$2\sqrt{K_T/J^2}$	P / D	1 / J	$\eta_o$	$4\sqrt{K_Q/J^3}$
1.8962	0.600	4.5958	0.3541	1.1275
1.5356	0.625	3.7719	0.4139	0.9758
1.2939	0.650	3.2208	0.4653	0.8699
1.1204	0.675	2.8257	0.5093	0.7914
0.9897	0.700	2.5280	0.5471	0.7306
0.8876	0.725	2.2954	0.5796	0.6820
0.8057	0.750	2.1083	0.6075	0.6422
0.7382	0.775	1.9541	0.6316	0.6087
0.6818	0.800	1.8247	0.6525	0.5803
0.6340	0.825	1.7145	0.6704	0.5558
0.5928	0.850	1.6191	0.6861	0.5343
0.5570	0.875	1.5358	0.6996	0.5154
0.5256	0.900	1.4622	0.7115	0.4986
0.4979	0.925	1.3969	0.7217	0.4836
0.4733	0.950	1.3384	0.7307	0.4700
0.4513	0.975	1.2855	0.7385	0.4577
0.4318	1.000	1.2378	0.7453	0.4467
0.4143	1.025	1.1944	0.7512	0.4367
0.3987	1.050	1.1549	0.7564	0.4276
0.3848	1.075	1.1188	0.7608	0.4195
0.3727	1.100	1.0860	0.7646	0.4124
0.3623	1.125	1.0563	0.7678	0.4061
0.3537	1.150	1.0294	0.7704	0.4009
0.3469	1.175	1.0055	0.7724	0.3968
0.3424	1.200	0.9848	0.7738	0.3941
0.3407	1.225	0.9677	0.7743	0.3930

Reference (33)





velocity, specifically the equivalent envelope volume form presented in Appendix II, they give a good comparison of the two alternative's performance.

Considering both of these configurations to drive the same body, the open propeller seems the obvious choice; but the ducted propeller may be used to control as well as propell the vehicle, and accordingly, no conventional control surfaces are needed. In the ducted steerable configuration, an appendage fraction of only four per cent is needed, versus the thirteen per cent of body wetted surface area for all the appendages as used on the first generation robot. The increase in drag factor for the steerable duct design due to appendages is 1.092 versus 1.309 for the open propeller design. Assuming a body with bare hull resistance, "R" is to be propelled by either of the propulsors, the following comparison is developed:

For the B 3-45 series screw:

$$R_{TA} = 1.173 R_T$$

$$SHP_B = \frac{1.309 R_T V}{550 PC} = \frac{1.636 R_T V}{550}$$

Where 1.309 is the increase in resistance due to appendage drag.

For the Ka 3-60 screw in a 19A Duct:



$$R_{TA} = 1.092 R_T$$

$$SHP_D = \frac{1.092 R_T V}{550 PC} = \frac{1.583 R_T V}{550}$$

Comparing the two calculations:

$$\frac{SHP_B}{SHP_D} = 1.03$$

In this situation, the ducted propeller requires three per cent less shaft horsepower than the B 3.45 screw powered model. By eliminating the forward diving planes on the B screw series driven vehicle, the appendages then constitute only 7.5 per cent of the bare hull wetted surface on the B screw series powered vehicle; and performing the same analysis as before, the B series propulsor requires eight per cent less power than the ducted propeller.

The previous analysis assumes the transmission efficiencies of the two configurations are the same which may not be exactly correct, since the ducted propeller requires a universal in the drive train which will reduce the drive train's efficiency. The interesting aspect of this analysis is the favorable power requirement comparison between the B 3-45 screw and the steerable ducted propeller.

The propulsor selection then comes down to two questions. First, can the front fins be eliminated in the



conventional control configuration, and secondly, is the concept of the steerable ducted propeller feasible in this situation? These questions are investigated in Appendix VI. The outcome of that analysis will determine the better propulsor.

### A3.2 Prime mover and transmission.

The transmission and drive train will be considered as one group, since they are so closely related. Two configurations will be investigated. The first is the pressure vessel contained motor and reduction gear of the type presented in [14] and used in the original robot. The second is the pressure compensated motor and attached reduction gear set of the type manufactured by the Hoover Electric Company.

The pressure compensated motor does not require a pressure hull, since the motor operates in a bath of isolating dielectric oil at the local pressure. The reduction gear is attached to the motor housing and the whole motor and transmission comes as one unit.

The pressure compensated motor has the following advantages and disadvantages:

#### Advantages of the Pressure Compensated Propulsion Motor:

1. The heavy pressure housing is not required.  
This becomes increasingly important as the operating depth increases.
2. The motor compartment cannot be flooded,  
which could result in sinking of the vehicle.



3. These motors are widely used in present submersibles.
4. If the design operating depth of the submersible changes in the future, very little modification of the propulsion motor housing is required.

Disadvantages of the Pressure Compensated Propulsion Motor.

1. These motors are available only as special order items. They are manufactured from stock and other components to specification. Accordingly, they are very costly in comparison to other motors.
2. Previous D. C. motor designs have operated at from 24 to 325 volts. This effectively requires the energy storage system to be at least a 24 volt system.

A typical efficiency curve for the pressure compensated motor is presented in Figure A3-11.

The pressure housed configuration, on the other hand, offers more flexibility in the selection of the motor and reduction gear, but requires a pressure housing which could partially flood if the shaft seal leaked. For this reason, the pressure housing should be kept as small as possible to reduce the volume which could become flooded.

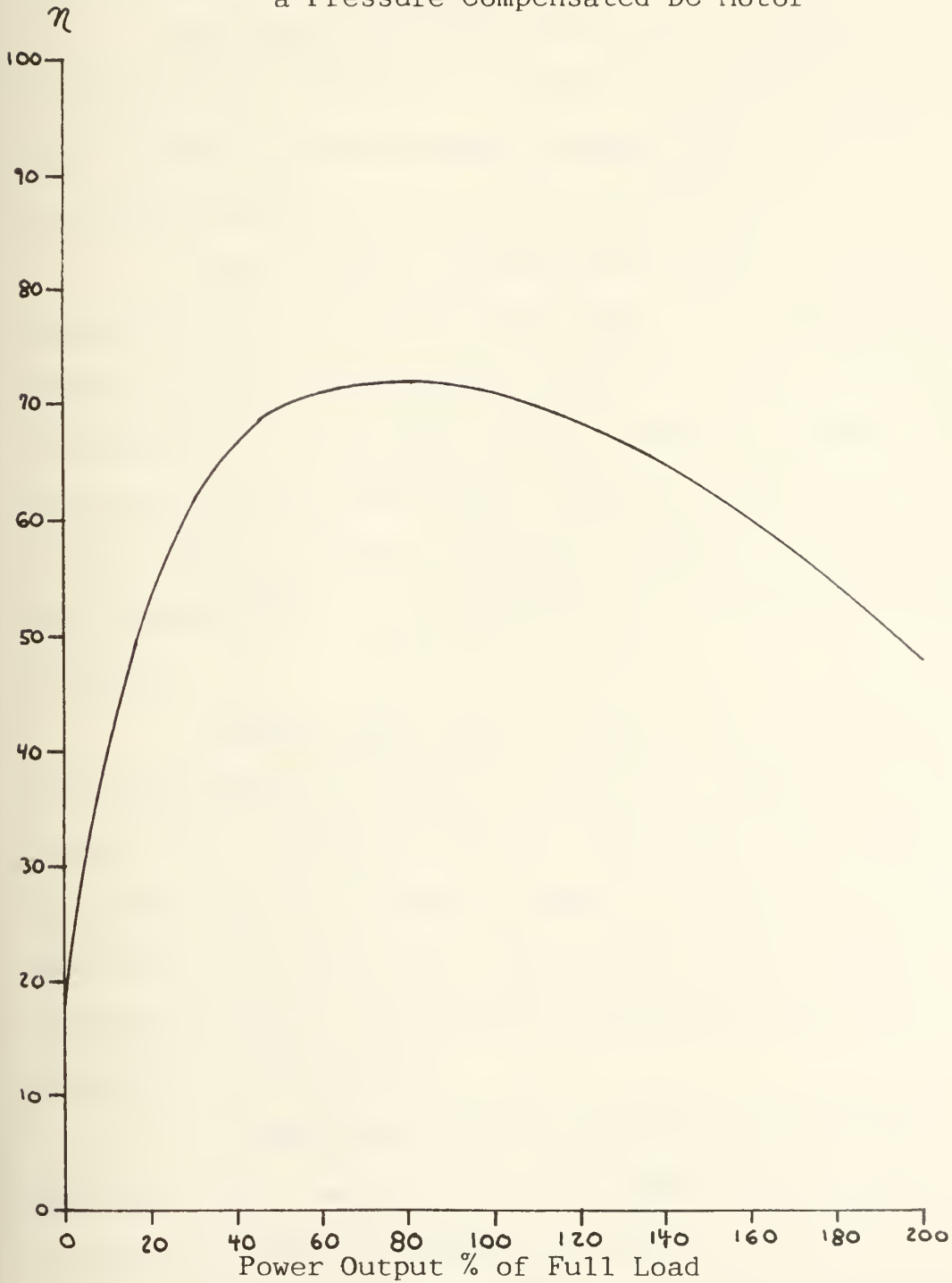
The reduction gear set for this alternative does





FIGURE A3-11

Typical Motor Efficiency for  
a Pressure Compensated DC Motor





not have to be an exotic epicyclic gear drive because the power is very low and, therefore, the weight and size of the gears is not very significant.

The motor efficiency curve from [14] is presented in Figure A3-12. Comparing Figures A3-11 and A3-12 performance curves shows the pressure compensated motor to be substantially better than the MIT robot's motor.

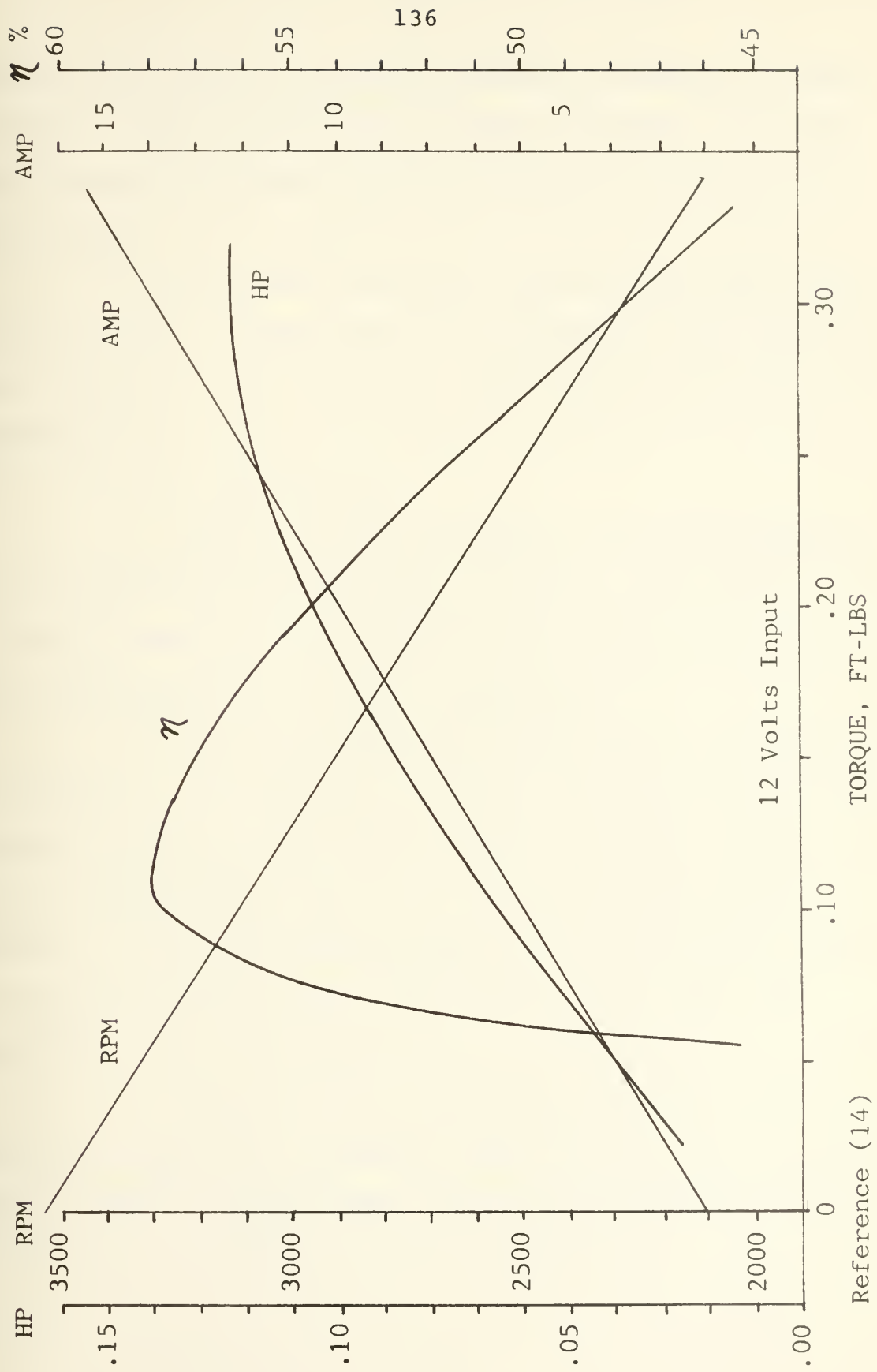
From a purely engineering viewpoint, the pressure compensated motor and reduction gear is the obvious selection; however, if the availability and cost of this alternative are considered, its selection becomes somewhat tenuous. The acquisition of this motor might, however, prove cost effective in the long run, since it would be usable in variations of the vehicles with little modification as operating depths increase.

Another more obvious choice for the prime mover and transmission is the prime mover and reduction gears used on the first generation robot, since the power output is in the right range, the unit is usable on a 12 volt system, and the unit is available and performance known. These last factors eliminate the need for acquisition, building, and testing of a new system.

As mentioned earlier though, the performance of the MIT robot's motor is not too good, but the motor was the only motor readily available designed to operate on 12 volts. Motors designed to operate at higher voltages generally are



FIGURE A3-12 PERFORMANCE CURVES FOR FIRST GENERATION ROBOT PROPULSION MOTOR





smaller and lighter than those designed to operate at lower voltages, which is certainly a weight advantage; but this also places a constraint on the voltage of the energy storage system.

A selection of the motor must be made after studying the energy storage system and determining the trade off there between voltage and size. This study is undertaken in Appendix IV.

### A3.3 Conclusions

1. Contra-rotating propellers offer the possibility of improving the propulsive coefficient and operation as a torque balanced pair, but drive train complexities render it a risky selection for this intended use.

2. A Ka 3-65 propeller operating in a 19A nozzle, if used in a steerable duct configuration with no additional control surfaces, will operate with lower power output than the B 3.45 open screw with tail and nose diving planes. However, if the nose diving planes can be eliminated, the B 3.45 screw operates with lower power output than the steerable duct configuration.

3. From a purely engineering consideration, a pressure compensated propulsion motor is the superior choice over a pressure housed model, but cost considerations and its limited availability act to its detriment.





## APPENDIX IV

## ENERGY STORAGE SYSTEM TRADE OFF STUDY

The energy storage system consists of the energy storage units and the power distribution system. The primary energy storage unit in the original MIT robot consists of an automobile storage battery designed to operate immersed in water. The distribution system is made up of a series of voltage regulators which provide the required voltages for the various installed equipments.

Of all the systems onboard the robot, the energy storage system has the greatest impact on size and weight. In a vehicle of the type considered, the energy storage unit is often the single largest and heaviest piece of equipment onboard. In the first generation robot, the battery accounted for about twenty-five per cent of the total vehicle weight. Accordingly, the energy storage system can dictate the envelope diameter and, in turn, the overall vehicle size.

The primary energy storage unit should have the following attributes:

1. High energy density, both in terms of energy per unit volume and per unit weight.
2. Size of the unit should be compatible with, but not dictate, vehicle size, if possible.
3. The output characteristics of the device must be compatible with the characteristics of the propulsion system.



For example, if the propulsion motor is a 24 volt design, the primary voltage supply should be at least 24 volts.

4. The unit must be capable of operating in the required environment, either enclosed in a pressure housing or immersed in water.
5. The unit must provide sufficient power to meet endurance requirements.

The energy storage unit must be able to supply energy in the form of electrical power to the onboard electronics. For main propulsion, however, the prime mover need not be an electric motor; it could be any one of a variety of thermodynamic cycles designed to power underwater vehicles as described in [34]. For the robot, though, electrical propulsion is the only satisfactory solution, mainly because of the vehicle's size and operating characteristics, which place unrealistic constraints on the size of any thermodynamic system. Additionally, the thermodynamic systems involve discharge of mass into the water, which places a compensation requirement on the vehicle to make up for the lost weight of the exhaust to remain near neutral buoyancy.

Many electrical power sources are available, such as radioactive isotope decay heat power supplies and fuel cells as proposed for robot use in [10]. The most readily available and best suited power source for this application, however, is the electrochemical storage battery.



Batteries are available as primary or secondary types. A primary battery is a design which is used only once and can not be recharged. A variation of the primary battery is the reserve battery, which can be reused after the electrolyte is replenished. The secondary battery, on the other hand, can be discharged and recharged repeatedly, depending on the operating requirements and battery design.

The primary battery can offer a weight advantage, since it can be nearly completely discharged during a mission, thus obtaining nearly the maximum capability out of the unit. This practice would damage a secondary battery, which is rarely designed to be fully discharged repeatedly. After the mission, however, the primary battery must be replaced, since it cannot be recharged.

The secondary battery can be repeatedly charged and discharged, the exact number of times is dependent on the depth of discharge, type of battery, and battery design. The depth of discharge is limited, since repeated full discharging will quickly destroy the battery's ability to hold a charge. Usually, the limit of discharge is thirty to fifty per cent of rated capacity remaining. The batteries must be specifically designed to be repeatedly discharged. Accordingly, the common automobile battery, which is designed to provide a short high burst of power for starting the motor, is not suited for continual deep discharge.

Table A4-1 provides characteristics of candidate



TABLE A4-1 CHARACTERISTICS OF CANDIDATE BATTERIES

TYPE	TYPICAL OPERATING VOLTAGE (V)	THEORETICAL ENERGY DENSITY (Wh/lb)	ACTUAL ENERGY DENSITY (Wh/lb)(Wh/in <sup>3</sup> )	OPERATING LIFE (Cycles)
Zinc-Air (Oxygen)	1.36	435	40-100 2-6	Primary
Lithium-Chloride	2.7-3.2	1000	250 NA	Still Under Development
Silver-Zinc	1.3-1.6	205	30-80+ 1.8-5.6	80-100
Silver-Cadmium	1.0-1.3	120	16-33 1.4-3.0	150-300
Nickel-Cadmium	1.0-1.3	105	12-15 0.7-1.0	1000-2000
Lead Acid	1.7-2.1	80-115	5-20 0.4-1.2	250-1500

141





battery systems for comparison. The wide discrepancy between the theoretical energy density and the actual energy density is due to inefficiencies in the actual designs such as weight of the case, voids in the reactant materials, etc. Presently, the state of the art of the design of the conventional storage batteries is far enough advanced that improvements in present designs will not yield more than a 30 per cent improvement in energy densities [34].

Of the battery types listed in Table A4-1, the lithium chloride battery has the most attractive features. The U. S. Navy is currently sponsoring work being conducted with this battery for use as an underwater vehicle power source [35]. The results to date seem very encouraging, however, the battery is still under development and is not yet commercially available in the size required for the robot.

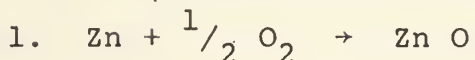
The Zinc-Air (Oxygen) battery is also very attractive, though the figures shown will be reduced substantially if the weight of the required oxygen tankage is added to the weight of the basic cell. This cell generally has a high energy density, but the power densities are limited. Power densities can be improved by forcing the flow of air, or oxygen, through the battery. The amount of oxygen used by this cell is estimated at five to nine cubic feet at STP per kilowatt hour.

The reactions involved in the Zinc-Air cell are

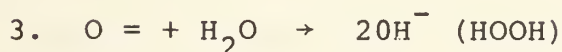
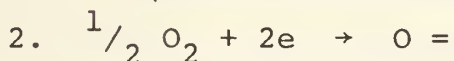


as follows [36]:

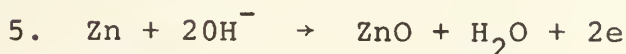
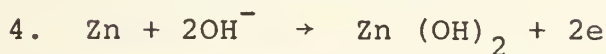
(Oxidation Reaction)



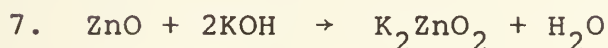
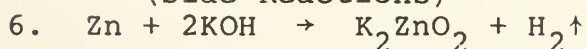
(Cathode Reactions)



(Anode Reactions)



(Side Reactions)



Equation six is a potential problem, since the evolution of hydrogen could prevent oxygen, in the closed system, from entering the cell to react. This side reaction is, however, easily suppressed by choice of plate material. The cell may then be run in a closed environment on oxygen or air with an oxygen supply to replace oxygen used in the reaction.

Several configurations of this cell have been proposed, including an encapsulated pressurized system where the battery is contained in a pressure shell with oxygen at



1000 psi [37]. As the cell is discharged, the oxygen is used up and the pressure in the shell drops. After discharge, the battery can be recharged and the oxygen pressure restored. This cell was predicted to have an energy density of 60 Whr/lb. The development of this cell, however, is not complete.

Several configurations of Zinc-Air batteries, such as those presented in [38] were studied, but a design could not be located which met the vehicle's requirements.

The oxygen supply for this battery also posed a considerable problem, since the weight of the tankage required is considerable, even for a small battery. In this respect, much like the fuel cell, the advantage of the Zinc-Air cell cannot be realized until the endurance is sufficiently long that the support equipment weight becomes less significant when compared with the fuel.

Due to the lack of a presently available Zinc-Air battery to meet the needs of the robot and the oxygen supply problems, the Zinc-Air (oxygen) battery is considered an unsuitable choice for the vehicle and is eliminated from further consideration.

Of the remaining alternatives listed in Table A4-1, the silver-zinc and lead-acid batteries have seen the most use in submersible ocean vehicles. The efficiency of the silver-zinc cell reactions are inherently greater than that of the lead-acid cell. Accordingly, silver-zinc cells



have been built with energy densities four times as high as those of lead-acid designs. Both of these cells can be modified to operate either in the pressure compensated configuration, where the electrolyte is exposed to the local external pressure, or enclosed in a pressure vessel. As pointed out in [39], the compensated configuration is advantageous at great operating depths, but for the shallow operation intended for this design, the pressure housed design is a lighter weight alternative. This becomes especially true when the weight of the compensation equipment and battery support structure is added in. In the second generation robot design, only pressure housed batteries will be considered.

The silver-zinc cells have been used in many submerged ocean vehicles as listed in [40]. They are used especially in small vehicles such as torpedoes, the UARS [8] and the OSR [9], where the battery weight and size has such an important impact on the vehicle size. Table A4-2 lists the characteristics of several silver-zinc cells, modules, and batteries which are available commercially. As the list shows, the designer has a great deal of flexibility in his choice of configurations for the energy storage unit using these cells.

The silver-zinc cells do have some drawbacks, however. The first is their tendency to generate hydrogen on charge and discharge. This is more pronounced on charging





TABLE A4-2 CHARACTERISTICS OF VARIOUS PRODUCTION SILVER-ZINC BATTERIES

MODEL	VAVG	CAPACITY AH.	WIDTH in	DEPTH in	HEIGHT in	WEIGHT lbs.
LR3/3	4.5	3.0	1.87	1.47	2.88	.36
LR3/5	4.5	5.0	1.87	1.47	4.00	.575
LR2/10	3.0	10.0	1.69	1.31	4.00	.625
LR3/10	4.5	10.0	5.61	0.80	3.90	1.16
LR4/22	6.0	22.0	2.80	3.04	4.33	2.60
LR4/80	6.0	80.0	3.32	5.35	7.12	9.50
LR60	1.52	60.0	2.73	2.36	4.50	1.81
LR90	1.52	90.0	3.26	2.16	7.06	3.57
LR100	1.51	100.0	3.44	2.78	4.81	2.75
LR130	1.52	130.0	3.275	2.50	6.55	3.93
LR200	1.50	200.0	4.19	1.79	10.94	.656
8xLR100	12.0	99.0	11.1	6.90	4.80	22.0
16xLR200	24.0	254.0	14.3	8.40	11.0	110.0

Yardney Electric Corp. All Cells are High Impact, Leakproof, and Spillproof



and the hydrogen produced on discharge can be contained in an enclosure to prevent its spread. Another problem is also associated with battery charging. The charging of each cell is done with a constant current until the prescribed voltage is achieved. This current must be controlled for each cell so they all end with the same charge. This process is controlled in large cells by circuits built into the battery. Also during the charging process, the cell voltage changes sharply as the chemical reactions change. The first voltage rise occurs at about twenty per cent of full charge, and the second occurs at full charge when the voltage rises rapidly to 2.0 volts. This second voltage rise is useful in signaling completion of charging to an automatic charging device.

Another drawback is the cost of silver-zinc batteries, which is at least three times that of lead-acid batteries. The silver-zinc cell is also only good for 80 - 100 charge - discharge cycles, versus the lead-acid, which is good for about 300 cycles for the deep discharge designs being considered.

Another cell which is considered is the silver-cadmium cell, which has many of the characteristics of the silver-zinc, but does not have as high an energy density. They will, however, last for more cycles than the silver-zinc batteries. Physical characteristics of suitable production silver-cadmium cells are given in Table A4-3.

The nickel-cadmium cell is also considered. It,



TABLE A4-3 CHARACTERISTICS OF VARIOUS SILVER-CADMIUM BATTERIES

MODEL	VAVG	CAPACITY A.H.	WIDTH in.	DEPTH in.	HEIGHT in.	WEIGHT lbs.
BD-3/3	3.2	3.0	1.87	1.47	2.88	0.35
BD-3/5	3.25	5.0	1.87	1.47	4.0	0.65
BD-8/5.5	8.4	5.5	3.12	3.17	3.94	2.6
BD-3/10	3.2	10.0	5.61	0.80	3.90	1.2
YS-20	1.08	20.0	1.73	2.05	4.28	0.94
YS-40	1.10	40.0	3.25	3.25	7.05	1.64
YS-60	1.10	60.0	2.73	2.36	4.5	2.66
YS-70	1.10	70.0	3.64	1.41	6.25	2.63
YS-85	1.08	85.0	2.81	1.81	9.44	3.81
YS-100	1.08	100.0	2.78	3.44	4.81	3.3
YS-150	1.06	150.0	4.19	1.78	10.72	6.81
YS-300	1.07	300.0	4.19	1.78	17.50	11.4

Yardney Electric Corp. All Cells are High Impact, Leakproof, and Spillproof



however, does not offer a significant improvement in energy density over the lead-acid cell and is considerably more expensive. These cells can be completely sealed and, therefore, evolve no gasses. Generally, the nickel-cadmium cell designs are small and intended for portable equipment; as such, they may prove to be a perfect back up emergency battery. Details of some commercially available nickel cadmium cells are presented in Table A4-4.

The last type of battery considered is also the one which has seen the widest usage, the lead-acid battery. The most familiar form of lead-acid cell is the standard car battery. However, if this cell is deep discharged, it will only last about 25 cycles; whereas, a battery designed for deep discharge can last up to 1,000 cycles. Until rather recently, though, the majority of deep discharge cells available were heavy duty models designed as batteries for electric driven vehicles or for energy storage systems. These batteries are exactly as the description indicates: heavy, due mainly to the battery case. Recently, several deep discharge batteries have been developed for use with electric trolling motors and on pleasure boats without generator plants. Available configurations of these cells are listed in Table A4-5. These types use the new lightweight cases so common in automobile batteries. They also produce hydrogen on charge and discharge, however, and are designed to operate in an upright position.





TABLE A4-4 CHARACTERISTICS OF VARIOUS PRODUCTION NICKEL-CADMIUM BATTERIES

MODEL	VAVG	CAPACITY A.H.	LENGTH in.	DEPTH in.	HEIGHT in.	WEIGHT lbs.
VO3-HS	1.25	3.0	2.12	0.81	2.83	0.39
VO9-HS	1.25	9.0	2.98	0.89	3.70	0.91
VO12-HS	1.25	12.0	2.98	0.89	4.39	1.28
VO15-HS	1.25	15.0	2.98	0.89	4.82	1.41
VO20-HS	1.25	20.0	2.98	0.89	6.89	2.10
VO50-HS	1.25	50.0	4.93	1.34	6.15	4.30
VO100-HS	1.25	100.0	7.29	1.43	8.17	8.60

Gulton Industries Inc. Cases are Sealed Stainless Steel.



TABLE A4-5 CHARACTERISTICS OF VARIOUS PRODUCTION DEEP DISCHARGE LEAD-ACID BATTERIES

MODEL	VAVG	CAPACITY A.H.	WIDTH in.	DEPTH in.	HEIGHT in.	WEIGHT lbs.
Gould Action Pack	12.0	34.0	—	—	—	20.0
Die-Hard Marine	12.0	80.0	10.25	7.0	8.0	47.0
Gould Action Pack	12.0	105.0	—	—	—	55.0

Data From Various Manufacturers

All Batteries are Designed For Deep Discharge



Another type lead-acid battery has been developed by the Gates Energy Systems Corporation, which is sealed so it is completely maintenance free, and designed to be completely discharged without damage. These cells are available only in small sizes intended for use in portable equipment and are not competitive in energy density with the non sealed deep discharge cells mentioned previously. For example, sufficient cells to match the 81 AH deep discharge battery which weighs about 50 lbs would weigh 80 lbs. and occupy twice the volume of the deep discharge model. The sealed lead-acid cell is, however, an excellent candidate for an emergency battery. Available configurations are listed in Table A 4-6.

Of the batteries considered, the silver-zinc designs are clearly the most attractive because of their high energy density. They are also available in leakproof spillproof containers which can operate in almost any attitude except completely inverted. These cells are also available in sizes which give the designer considerable flexibility in choosing system voltage and overall configuration.

The lead-acid deep discharge batteries, on the other hand, are available only in six or twelve volts models. The larger sizes of these batteries give the highest energy densities, but also require larger pressure hull diameters.

These batteries also are designed to be operated



TABLE A4-6 CHARACTERISTICS OF VARIOUS PRODUCTION SEALED LEAD-ACID BATTERIES

MODEL	VAVG	CAPACITY A.H.	LENGTH in.	DEPTH in.	HEIGHT in.	WEIGHT lbs.
0802-0001	4.0	10.0	5.4	3.6	3.1	3.7
0802-0002	6.0	10.0	5.4	3.6	3.1	5.3
0810-0007	10.0	2.7	4.2	2.8	2.7	2.1
0810-0018	10.0	2.7	6.9	1.5	2.7	2.1
0800-0007	10.0	5.0	5.4	3.6	3.1	4.5
0800-0018	10.0	5.0	8.9	1.9	3.1	4.5
0810-0008	12.0	2.5	4.2	2.8	2.7	2.5
0810-0016	12.0	2.5	8.2	1.5	2.7	2.5
0800-0008	12.0	5.0	5.4	3.6	3.1	5.3
0800-0016	12.0	5.0	10.6	1.9	3.1	5.3

Gates Energy Products, Inc. All Cells are Sealed





in an upright position which limits the pitch angle the submarine can assume during its transits to and from the bottom.

To get a feel for the effect of the battery on the overall vehicle, two battery configurations were investigated using the techniques described in Appendix X. A pressure hull volume of 2000 in<sup>3</sup> was assumed required to carry all the electronics and the required battery volume was added to this value. The 81 AH 12 volt deep discharge battery was compared with a combination of silver-zinc cells with a 96 AH rating. The characteristics of the deep discharge battery equipped vehicle were as follows:

I.D. shell	=	12.0 inches
$L_{BAT}$	=	12.0 inches
$L_p$	=	30.0 inches
$L$	=	9.0 feet
$D_x$	=	15.43 inches

The silver-zinc equipped vehicle has the following characteristics:

I.D. shell	=	8.071 inches
$L_{BAT}$	=	8.0 inches
$L_p$	=	30.0 inches
$L$	=	7.5 feet
$D_x$	=	12.86 inches

If the two configurations are compared at speeds through the water of three knots with no auxilliary load,



the lead-acid configuration will have an endurance of 6.8 hours versus the 12 hour endurance of the silver-zinc configuration, and both have the same dry payload capability.

This analysis shows the impact of the lead-acid battery on the vehicle. Choice of a lead-acid battery forces the vehicle's size and the result is a vehicle which basically carries around a large battery.

The silver-zinc battery offers the designer considerably more flexibility, and the battery becomes another part of the design, rather than the controlling element. In a larger vehicle designed to carry more payload this advantage might not be so pronounced, depending on the configuration; but in a small weight limited vehicle, as considered here, the choice of the higher energy density battery offers a tremendous savings in space and weight devoted to the energy storage unit.

#### A4.1 Conclusions.

1. The energy storage unit has the biggest impact on the overall design of any of the submarine's systems.
2. The high energy density and compact size of silver-zinc cells make them very attractive for use in a vehicle the size of the robot submarine. These advantages overwhelm the disadvantages.
3. Deep discharge lead-acid batteries are too big and have too low energy densities for this design. They consequently impact the overall design tremendously.



4. The ideal battery for the robot submarine is not yet available. The battery plays, perhaps, the biggest role of any system, outside the computer, in the design. Research is continuing in this area which could yield a much more suitable battery. The Lithium-chloride battery [35] has probably the greatest potential of any system under study today. When and if these cells become commercially available in the required size, they could provide a means to vastly improve the robot's capability with very little, if any, additional impact.



## APPENDIX V

## PRESSURE HULLS CONFIGURATION TRADE OFF STUDY

## A5.0

The pressure hulls are considered those enclosures within the envelope which house equipment operating at normal atmospheric pressure. These pressure hulls must have the following characteristics:

1. Be able to operate at a maximum depth of 1000 feet in sea water.
2. The hull shall be able to withstand collapse to 1500 feet.
3. Pressure hulls should be manufactured of a non-magnetic material to reduce magnetic compass interference.
4. Mechanical linkage penetrations through large pressure hulls should be eliminated to reduce chances of flooding.
5. Access must be provided to facilitate maintenance on the enclosed equipment.

The most efficient shape for a pressure hull is spherical since a sphere encloses the most volume with the least surface area. This surface area, in turn, translates into hull weight. The sphere also is perfectly symmetrical which helps the hull withstand a very large external pressure. For these reasons, spherical pressure hulls are used almost exclusively for very deep submergence vehicles where pressure





hull weight is very critical, and external pressures are enormous. The sphere with a length to diameter ratio of one is not very compatible with an envelope form which has a length to diameter ratio of seven, however. A single spherical pressure hull obviously will not very effectively fill an envelope of this sort and a great deal of wasted volume will result between if multiple spherical hulls are used. The alternative is the cylindrical pressure hull forms used in most military submarines today. With this configuration, the pressure hull also forms the primary structural member of the vehicle.

The 1st generation robot employed a series of unstiffened cylindrical pressure hulls constructed of PVC tubing. This was an excellent solution to that design problem since the material was readily available and easy to work with. However, a volume is more efficiently enclosed by a single pressure volume with a larger diameter. PVC pipe will not, however, be able to withstand the stresses present in a larger diameter hull at the 1000 foot operating depth. An alternative material is, therefore, required for this application.

The best material choice seems to be aluminum which is light weight, corrosion resistant, easy to work, and available. [41] lists the characteristics of the types of aluminum used in the marine industry today. One type is 6061-T6 which the Aluminum Company of America uses to manufacture seamless extruded pipe up to twelve inches in diameter. A summary of the available sizes of this pipe and their characteristics is con-



tained in table A5-1. These products are well suited to form the shell of the pressure hull.

The collapse pressures listed in table A5-1 indicate the larger diameters of these pipes will not withstand the required 1500 foot crush depth pressure. At that depth, in the cylinder diameters under consideration, the unstiffened cylinder is an excessively heavy design. A lighter solution is the frame stiffened cylinder. A cylindrical ring frame added to the cylindrical shell at intervals greatly increases the external pressure the cylinder can withstand. The stiffening frames can be added internally or externally to the cylinder. Internal frames are, however, difficult to attach to a ten or twelve inch pipe and greatly reduce the available inside diameter. When the frames are attached internally, though, the outside of the pressure hull shell can be used as part of the envelope. Conversely, when the frames are attached externally another shell must be placed around the pressure hull for streamlining. The externally framed arrangement does allow the frame to be more easily affixed to the cylinder and allows the internal volume to be used more effectively. Additionally, with the externally framed arrangement, the space between the pressure hull and envelope can be used for flotation tanks, sonar arrays, or other uses. This arrangement also allows an envelope form without a cylindrical mid section to be used.

For the stiffened cylindrical pressure hull, the required shell thickness can be determined from the following



TABLE A5-1

## CHARACTERISTICS OF AVAILABLE 6160-T6 ALUMINUM ALLOY PIPE

Outside Diameter in.	Inside Diameter in.	Wall Thickness in.	Moment of Inertia in <sup>4</sup>	Collapse Pressure psi
2.375	2.067	0.154	0.6657	4020
2.875	2.469	0.203	1.530	4480
3.500	3.068	0.216	3.017	3760
4.000	3.548	0.226	4.788	3290
4.500	4.026	0.237	7.232	2930
5.563	5.047	0.258	15.16	2200
6.625	6.065	0.280	28.14	1660
8.625	7.981	0.322	72.49	1140
10.750	10.192	0.279	125.9	385
10.750	10.136	0.307	137.4	515
10.750	10.020	0.365	160.7	860
12.750	12.090	0.330	248.5	-
12.750	12.000	0.375	279.3	560
12.750	11.750	0.500	361.5	-

Aluminum Company of America

$$E = 10.0 \times 10^6 \text{ psi} \quad \mu = .33$$

$$\sigma_y = 35000 \text{ psi}$$



formula [19]:

$$t_{\text{shell}} = \frac{PD}{2\sigma_y}$$

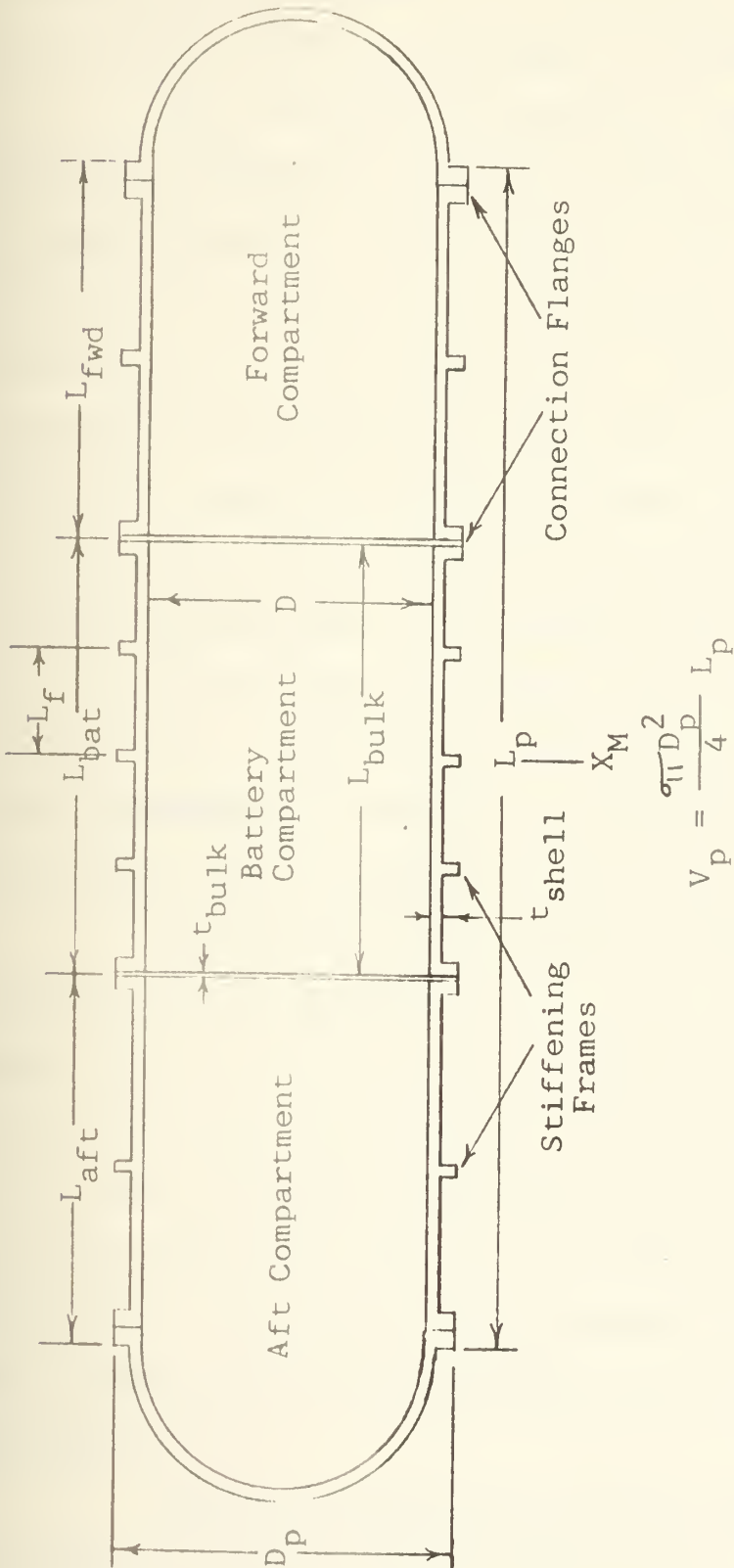
Applying this formula to the piping in table A5-1, it is apparent that even the thinnest walled piping is too thick for the intended application. The result is a shell which requires fewer stiffening frames. This is not the best solution, but since the correct wall thickness tubes are not available and reducing the wall thickness of the available piping is a dubious procedure with doubtful significant gain, it seems the best solution.

The stiffened cylindrical pressure hull constructed of 6061-T6 aluminum pipe is, therefore, a viable pressure hull configuration, but the envelope form under consideration is not a cylinder and the available diameter for a pressure hull gets smaller near the ends of the envelope. One solution is to step the cylindrical pressure hull diameter at various points so it can better fill the volume. The step, though, is a discontinuity which adds considerable complexity to the pressure hull's construction. This additional complexity is considered unnecessary for this design. The pressure hull will, therefore, be a straight cylindrical hull of the configuration shown in figure A5-1.

The main pressure hull as shown in figure A5-1 is divided into three compartments so the battery compartment can







Above configuration shows hemispherical end closures, but elliptical end closures with a semi-axis ratio equal 2 are an alternative.

FIGURE A5-1 TYPICAL PRESSURE HULL CONFIGURATION AND NOMENCLATURE



be sealed from the other two. The battery is located amidships so it will be close to the center of buoyancy of the vehicle.

The calculations required to check the ability of a particular stiffened cylinder to withstand external pressure are quite involved. The procedure, [19] and [42], involves calculating the external pressures which will cause failure of various parts of the pressure hull. The computation is very lengthy and the designer can only use a rule-of-thumb to determine the necessary stiffening frame size. The scantlings of this frame are then used in the calculation to determine if they are satisfactory. This process can be very time consuming. The calculations, therefore, lend themselves to the use of a computer. A FORTRAN computer program was written for use on the Interdata M70 computer to perform this task, using the calculation method described in [19] and [42].

The input to the computer consists of the material specifications, hull diameter and configuration, operating depth, factor of safety, and stiffening frame scantlings. The program determines the maximum allowable spacing for the frames in the three different compartments and finally calculates the enclosed volume and weight of the pressure hull. A detailed description of the use of this program, the program listing, and a sample output are provided in the sections at the end of this appendix.

The main pressure hull is not the only pressure vessel onboard, several other components such as fin servos and



solenoid valves will have to be contained.

The pressure housing for these components will be much smaller in diameter than the main pressure hull. A cylindrical unstiffened piece of aluminum pipe can, therefore, be used for these housings as long as the external crush pressure listed in table A5-1 is greater than the actual external crush pressure.

Since the cylindrical pressure hull forms the main structural member of the submarine in the midships area, no additional structure is required in this region. The nose and tail sections will, however, have to have suitable structure to support any wet equipment contained therein. The structure in this area should be sufficient to support the equipments contained therein. It should be lightweight to help reduce the overall vehicle weight. No specific structural framing method for these areas will be presented since this will be a function of the specific equipment to be supported.

#### A5.1 Procedure for use of the pressure hull

##### Computer Program

This computer program reads in five or six data cards which specify the program. The first data card read in is the number of pressure hulls to be investigated. This is written in I Format in the first five columns of that card.

The second data card reads in the hull material specifications as follows:



Columns 1-10	Yield stress psi; E Format
11-20	Modulus of elasticity, psi; E Format
21-30	Possion's ratio; F Format
31-40	Density, lbs/in <sup>3</sup> ; F Format

The third data card reads in the operating depth and factor of safety as follows:

Columns 1-10	Operating depth, feet; F Format
11-20	Factor of Safety; F Format

The fourth data card reads in the inside hull diameter and thickness of the shell as follows:

Columns 1-10	Shell inside diameter, inches; F Format
11-20	Shell wall thickness, inches; F Format.

The shell wall thickness may be specified as zero here in which case the program will calculate the required wall thickness and then choose the closest larger size which is commercially available.

The fifth data card reads in the pressure hull compartment lengths and frame type as follows:

Columns 1-10	Length of Forward Compartment, inches; F Format
11-20	Length of Battery Compartment, inches; F Format
21-30	Length of Aft Compartment, inches; F Format. If this is specified as zero, then only a two compartment pressure hull is assumed.





31-35        This is a code 1 or 2 which  
              specifies the framing to be used;  
              I Format

If the code in columns 31-35 is a 1 then the program will try two frame configurations internal to the program. The first has the following dimensions:

Web Thickness = 0.25 inches

Web Height     = 0.50 inches

The flange dimensions are both zero.

The second frame's dimensions are as follows:

Web Thickness = 0.50 inches

Web Height     = 0.75 inches

The flange dimensions are both zero.

These dimensions were chosen as reasonable assumptions for the required frame sizes. They are rectangular rather than the normal T shape since it is felt the fabrication of a rectangular frame is much easier than a T frame and the weight saved by T frames is negligible in these dimensions. If the frame code is 2 then the program will read in an optional sixth card with frame dimensions of the designer's choice, and will ignore the previous canned frame sizes.

For the sixth data card the frame dimensions are specified as follows:

Columns 1-10	Flange Thickness; F Format
11-20	Flange Width; F Format
21-30	Web Thickness; F Format
31-40	Web Height; F Format



Definitions of these dimensions are provided in figure A5-2. The flange dimensions may be specified as zero but the web dimensions may not.

Using the previous input data the program will calculate the maximum frame spacing which satisfies the required pressure criteria for each compartment individually. The program then calculates the weight of the entire pressure hull with either elliptical or hemispherical end closures.

A listing of the program with descriptive comments included for clarity is presented in table A5-2.

#### A5.2 Description of Sample Computer Output

The sample output presented in table A5-3 was run with the following input data:

##### Hull Material Specifications

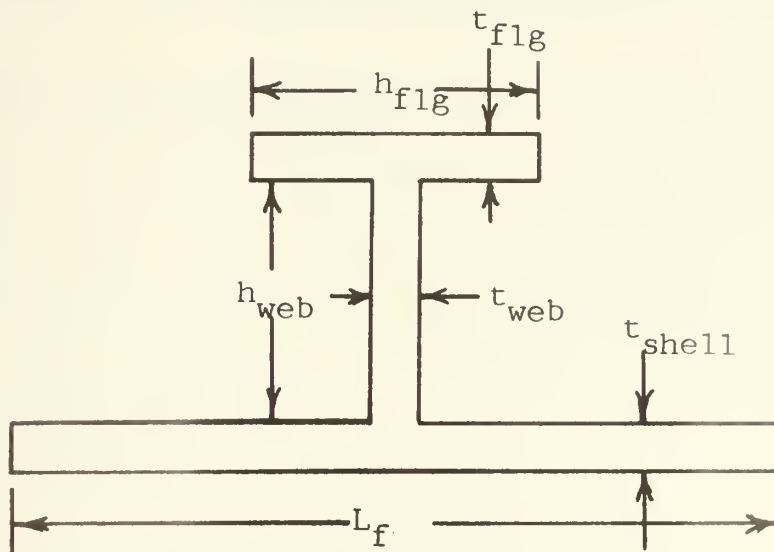
Yield Stress	= $3.5 \times 10^4$
Modulus of Elasticity	= $10.0 \times 10^6$
Poisson's Ratio	= 0.33
Density	= 0.098

##### Hull Parameters

Operating Depth	= 1000 Feet
Factor of Safety	= 1.5
Hull Inside Diameter	= 12.092 inches
Hull Thickness	= 0.33 inches
Length Forward Compartment	= 9.0 inches



FIGURE A5-2 TYPICAL STIFFENING FRAME NOMENCLATURE



If a rectangular frame is to be specified rather than a "T" frame as shown, then  $t_{flg}$  and  $h_{flg}$  should be set equal to zero and the appropriate dimensions given to  $t_{web}$  and  $h_{web}$

#### APPROXIMATE OPTIMUM FRAMING DIMENSIONS

$$\begin{aligned}
 t_{shell} &= \frac{P D}{2 \sigma_y} & t_{flg} &= t_{shell} \\
 L_f &= \frac{D}{10} & t_{web} &= .8 t_{shell} \\
 h_{flg} &= \frac{L_{frm}}{4} & h_{web} &= 7 t_{shell}
 \end{aligned}$$



Length Battery Compartment = 12.0 inches

Length Aft Compartment = 9.0 inches

The canned frame sizes mentioned previously were used in the calculation.

The first six pages of output print the results of the calculations for the two frame sizes considered for the three compartments. The program prints out the critical external pressures for failure in the various modes and calculates the volume and weight of the stiffening frames for the particular compartment. The critical pressures are coded as follows:

- PCSB - External pressure for shell buckling
- PCYF - External pressure for shell yielding at the frame
- PCYMD - External pressure for shell yielding between frames
- PCFMY - External pressure for frame yielding
- PCGS - External pressure for general instability
- PCFIS - External pressure for frame instability
- SIGMA - Maximum frame stress
- N - Number of lobes for failure in general instability

A factor of safety of 2.25 is applied to satisfy the criteria for PCSB. Also a factor of safety of 3.75 is applied to satisfy the criteria for PCGS. These additional factors are applied due to uncertainty in the accuracy of the calculations for these two modes of failure [19].





The last page of output gives data on the weight and displacement of the entire pressure hull less stiffening frames. To determine the total pressure hull weight and volume a satisfactory stiffening framing must be chosen from the previous output and the appropriate weight and volume listed added to the totals. Generally these additions will be small compared with the weights and volumes of the shell, end closures, and connecting flanges.

#### A5.3 Conclusions

1. An externally frame stiffened cylindrical pressure hull is the best selection for the robot's primary pressure hull.
2. Aluminum piping commercially available is well suited for use as a pressure hull shell.
3. Smaller pressure housings can be readily constructed of unstiffened aluminum pipe.
4. The computer programs provides a useful tool to develop a stiffened cylindrical shell pressure hull.



TABLE A5-2 STIFFENED CYLINDRICAL PRESSURE HULL PROGRAM LISTING

```

USER=BUNCE      265 15422      JOINT COMPUTER FACILITY, MIT
C
C THIS IS A COMPUTER PROGRAM WHICH PERFORMS STIFFENED CYLINDRICAL
C PRESSURE HULL CALCULATIONS FOR THE ROBOT SUBMARINE PRESSURE HULL.
C
      REAL WOMI, LOD, LERM, LBULK, LAFT, LFWD, LEAT
      DATA KI/8/, KO/5/
C IKIL IS AN INDEX WHICH KEEPS TRACK OF THE NUMBER OF HULLS UNDER
C CONSIDERATION.
      IKIL = 0
C NIKF IS AN INDEX WHICH ACCOUNTS FOR KING FRAMES IN THE SHELL
C WEIGHT CALCULATION, WHICH MUST BE PLACED BETWEEN BULKHEADS FOR
C STABILITY IN LONG COMPARTMENTS.
      NIKF = 0
C
C NJOBS IS THE NUMBER OF JOBS TO BE PERFORMED. IF THREE
C HULLS ARE TO BE INVESTIGATED THEN NJOBS = 3.
      READ (KI, 999) NJOBS
      999 FORMAT(I5)
      998 CONTINUE
      IKIL = IKIL + 1
C READ IN MATERIAL SPECS
C
C SIGMAY IS THE YIELD STRENGTH OF THE HULL MATERIAL IN PSI.
C EMOD IS THE MODULUS OF ELASTICITY OF THE HULL MATERIAL.
C POSR IS POISSON'S RATIO FOR THE HULL MATERIAL.
C DENS IS THE DENSITY IN POUNDS PER CUBIC INCH OF THE HULL MATERIAL.
C
      READ (KI, 1) SIGMAY, EMOD, POSR, DENS
      1 FORMAT (2E10.4, F10.5, F10.5)
C
C READ IN DESIGN OPERATING DEPTH AND FACTOR OF SAFETY
C DEPTH IS THE DESIGN MAXIMUM OPERATING DEPTH OF THE HULL.
C FSFAT IS THE FACTOR OF SAFETY FOR THE PRESSURE HULL. IT DETERMINES

```



TABLE A5-2 contd.

```

USER=BUNCE      265 15422      JOINT COMPUTER FACILITY, MIT
C THE CRUSH DEPTH OF THE PRESSURE HULL.
C
      READ (KI,2) DEPTH, FSAFE
      2 FORMAT (2F10.5)
C CRPRESS IS THE PRESSURE AT THE CRUSH DEPTH = FSAFE *DEPTH.
      CRPRES = .44474 * FSAFE * DEPTH
C READ SHELL IN INCHES
C
C DSHELL IS HE ID OF THE PRESSURE CYLINDER.
C TSHEL IS THE THICKNESS OF THE SHELL. IF ZERO IS ENTERED
C THEN THE PROGRAM WILL CALCULATE THE THICKNESS REQUIRED.
C
      READ (KI,3) DSHEL, TSHEL
      3 FORMAT (2F10.5)
C THIS SECTION CALCULATES THE REQUIRED SHELL THICKNESS TO P43
C NEAREST MANUFACTURABLE THICKNESS.
C IF TSHEL IS SPECIFIED AS NONZERO THEN THE FOLLOWING SECTION IS
C SKIPPED.
      IF (TSHEL.GT..0001) GO TO 50
      TSHEL = (CRPRES * DSHEL)/(2.*SIGMA)
      IF (TSHEL.LE..25) GO TO 49
C TINC IS A VALUE OF THE MINIMUM DIFFERENCE IN THICKNESS WHICH
C ARE AVAILABLE.
      TINC = .0525
C TEST IS THE MINIMUM THICKNESS SHFL AVAILABLE.
      TEST = .279
      DO 45 K = 1,10
      IF (TSHEL-TEST) 42,42,41
      41 TEST = TEST + TINC
      45 CONTINUE
      42 TSHEL = TEST
      GO TO 50
      49 TSHEL = .25

```



```

USER=BUNCE      255 15422      JOINT COMPUTER FACILITY, *IT
50 CONTINUE
C READ IN FRAMING DATA
C
C LFWD IS THE LENGTH OF THE FORWARD COMPARTMENT.
C LBAT IS THE LENGTH OF THE BATTERY COMPARTMENT.
C LAFT IS THE LENGTH OF THE AFT COMPARTMENT.
C IFRAME ISA CODE TO DETERMINE THE STIFFENING FRAME TYPE.
C IFRAME = 1 WILL USE THE CANNED FRAME SIZES.
C IFRAME = 2 READS DATA IN TO BE USED FROM THE FRAME SIZES.
C
      READ (KI,4) LFWD, LBAT, LAFT, IFRAME
      4 FORMAT (3F10.5, I5)
C
      IF (IFRAME.EQ.1) GO TO 10
C
C TFLG IS THE THICKNESS OF THE FLANGE OF THE SPECIFIED FRAME,
C HFLG IS THE WIDTH OF THE FLANGE OF THE SPECIFIED FRAME.
C TWEB IS THE THICKNESS OF THE WEB OF THE SPECIFIED FRAME.
C HWEB IS THE HEIGHT OF THE WEB OF THE SPECIFIED FRAME.
C
      READ (KI,6) TFLG, HFLG, TWEB, HWEB
      6 FORMAT (4F10.5)
      10 CONTINUE
C
C NCOMPT IS A NUMBER TO BE DETERMINE THE NUMBER OF COMPARTMENTS.
C NCOMPT CAN BE 2 OR 3.
C IF LAFT IS READ AS ZERO THEN NCOMPT IS 2 AUTOMATICALLY.
C IS LAFT IS .GT. ZERO THEN NCOMPT = 3.
C
      IF (LAFT.LE..1) NCOMPT = 2
      IF ( LAFT.GE..1) NCOMPT = 3
      DO 300 N = 1, NCOMPT
C UNDER CONSIDERATION.

```





TABLE A5-2 contd.

```

USER=BUNCE      265 15422      JOINT COMPUTFF FACILITY, 4IT

C LBULK IS THE DISTANCE BETWEEN BULKHEADS OF THE COMPARTMENT
  IF(N.EQ.1) LBULK = LFWD
  IF(N.EQ.2) LBULK = LBAT
  IF (N.EQ.3) LBULK = LAFT
C BULKMAX IS THE MAXIMUM DISTANCE WHICH CAN BE PRESENT BETWEEN
C BULKHEADS WITHOUT A KING FRAME IN BETWEEN
  BULKMX = 2. * DSHEL
C IF LBULK IS GREATER THAN BULKMAX THEN A KING FRAME IS INSTALLED AT
C MIDCOMPARTMENT AND HALF THE ACTUAL COMPARTMENT LENGTH IS USED FOR
C THE COMPARTMENT LENGTH IN THE CALCULATION.
C EACH HALF OF THE COMPARTMENT WILL THEN BE FRAMED IDENTICALLY.
  IF (LBULK.LE.BULKMX) GO TO 55
  NIKF = NIKF + 1
  WRITE (KO,215)
  LBULK = LBULK/2.
  55 CONTINUE

C
C IWER IS AN INDEX WHICH DETERMINES WHICH OF THE TWO ALTERNATIVE
C FRAME SIZES TO USE IN THE CALCULATION.
  IWER = 0
  IF (IFRAME.EQ.2) GO TO 20
  58 CONTINUE
C IF IWEB = 1 THEN THE FRAMING DIMENSIONS ARE AS FOLLOWS.
C HWEB = .5, TWEB = .25, TFLANGE = HFLANGE = 0..
  IWEB = IWEB + 1
  IF (IWEB.EQ.2) GO TO 56
  HWEB = .5
  TWEB = .25
  GO TO 57
  56 CONTINUE
C IF IWEB = 2 THEN THE FRAMING DIMENSIONS ARE AS FOLLOWS.
C HWEB = .75, IWEB = .5, TFLANGE = HFLANGE = 0..
  HWEB = .75

```



TABLE A5-2 contd.

```

USER=BUNCE      265 15422      JOINT COMPUTER FACILITY, MIT

      TWER = .5
57 CONTINUE
      TFLG = 0.
      HFLG = 0.
20 CONTINUE
C THESE STATEMENTS WRITE THE APPROPRIATE HEADING FOR THE SOLUTION.
      WRITE (KO,643) DEPTH , FSAFE
      IF (N.EQ.1) WRITE (KO,200) LEWD
      IF (N.EQ.2) WRITE (KO,205) LBAT
      IF (N.EQ.3) WRITE (KO,210) LAET
C THE FOLLOWING LOOP USES THE FRAME DIMENSIONS PREVIOUSLY
C DETERMINED AND FIGURES THE MAXIMUM SEPARATION BETWEEN FRAMES
C WHICH WILL STILL SATISFY ALL THE STRENGTH CRITERIA.
      DO 59 NF = 1,15
      LERM = LBULK/FLOAT(NF)
C
C SCANCK IS A SUBROUTINE WHICH PERFORMS THE STRENGTH CALCULATIONS.
C AND WRITE THE RESULTS.
C
      CALL SCANCK (DSHEL,SIGWAY,FWDD,FOSR,CRPRES,LFRM,LBULK,HWER,TWER,
1 HFLG,TFLG,TSHEL,ICK,DENS)
      IF (ICK.EQ.7) GO TO 66
      IF (NF.EQ.15) WRITE (KO,220)
59 CONTINUE
56 CONTINUE
      IF (IWER.EQ.2) GO TO 300
      IF (IWER.GT.0) GO TO 58
300 CONTINUE
C
C END CAP VOLUME AND TOTAL WEIGHT CALCULATIONS
C
C RSHEL IS THE SHELL RADIUS.
      RSHEL = DSHEL/2.

```



TABLE A5-2 contd.

```

USER=BUNCE      266 15422      JOINT COMPUTER FACILITY, MIT

C VOLIM IS THE VOLUME INSIDE THE PRESSURE CYLINDER.
  VOLIM = ((3.14159*(DSHEL**2.))/4.)*(TEND+LAFI+LBAT)
C VENDH IS THE VOLUME INSIDE THE HEMISPHERICAL END CAPS.
  VENDH = 4.189 *(RSHEL**3.)
C VENDE IS THE VOLUME INSIDE THE ELIPTICAL END CAPS.
  VENDE = 2.09 * (RSHEL**3.)
C TEND-1 REFERS TO THE THICKNESS OF THE END CAP.
C ACCORDING TO THE FIRST CRITERIA.
C H REFERS TO THE HEMISPHERICAL END CAPS.
C E REFERS TO THE ELIPTICAL END CAPS.
  TENDH1 = (CPPRES*RSHEL)/(2.*SIGMAY)
C TEND-2 REFERS TO THE THICKNESS OF THE END CAP ACCORDING
C TO THE SECOND CRITERIA.
  TENDH2 = SQRT((CPPRES*(RSHEL**2.))/.3*EMOD))
C VIOTH IS THE TOTAL ENCLOSED VOLUME WITH HEMISPHERICAL END CAPS.
  VIOTH = VOLIM + VENDH
C VIOTE IS THE TOTAL ENCLOSED VOLUME WITH ELIPTICAL END CAPS.
  VIOTE = VOLIM + VENDE
C R IS THE RADIUS OF CURVATURE OF THE ELIPTIC END CAP ON THE CENTER
  R = ((RSHEL**2.)*2.)/RSHEL
C LINE AXIS.
  TENDE1 = (CPPRES* R)/(2.*SIGMAY)
  TENDE2 = SQRT((CPPRES*RSHEL**2.))/.3*EMOD))
C THE FOLLOWING STATEMENTS DETERMINE WHICH VALUE OF THE END CAP
C THICKNESSES ARE GREATER AND ARE REQUIRED.
  IF (TENDH1.GT.TENDH2) TENDH = TENDH1
  IF (TENDH2.GT.TENDH1) TENDH = TENDH2
  IF (TENDE1.GT.TENDE2) TENDE = TENDE1
  IF (TENDE2.GT.TENDE1) TENDE = TENDE2
C THE FOLLOWING STATEMENT MAKE THE END CAP THICKNESS THE SAME AS
C THE SHELL THICKNESS IF THE END CAP IS NOT REQUIRED TO BE AT
C LEAST THAT THICK.
  IF (TENDE.LT.TSHEL) TENDE = TSHEL

```



TABLE A5-2 contd.

```

USER=BUNCE      266 15422      JOINT COMPUTER FACILITY, MIT

      IF (TENDH.LT.TSHEL) TENDH = TSHEL
C RSH IS THE MID SHELL RADIUS OF THE HEMISPHERICAL END CAP.
      RSH = RSHEL + TENDH/2.
C RSE IS THE MID SHELL RADIUS OF THE ELLIPTICAL END CAP.
      RSE = RSHEL + TENDE/2.
C VHEM IS THE VOLUME OF THE MATERIAL IN THE HEMISPHERICAL END CAP.
      VHEM = 12.57*(RSH**2.)*TENDH
C VEP IS THE VOLUME OF MATERIAL IN THE ELLIPTICAL END CAP.
      VEP =(6.293 * (RSE**2.) + 3.6276*((RSP/2.)*2.)*2.5339)*TENDE
C DMAX IS THE OUTSIDE DIAMETER OF THE CYLINDRICAL HULL AND FRAMES.
      DMAX = DSHEL + 1.5 + 2. * TSHEL
C DOD IS THE OUTSIDE DIAMETER OF THE CYLINDER.
      DOD = DSHEL + 2. * TSHEL
C AKF IS THE CROSS SECTIONAL AREA OF THE CONNECTING FLANGES.
      AKF = .7854 * (DMAX**2. - DOD **2.)
C VKF IS THE VOLUME OF ALL THE CONNECTING FLANGES.
      VKF = FLOAT (NCOMPT + 1 + NIKF) * AKF * 1.25
C VBULK IS THE VOLUME OF THE MATERIAL IN THE BULKHEADS.
      VBULK = FLOAT (NCOMPT-1) * .1963*DSHEL **2.
C VSHEL IS THE VOLUME OF MATERIAL IN THE CYLINDRICAL SHELL.
      VSHEL = 3.14159*(DSHEL*TSHEL)*TSHEL*(LFWD+LBAT+LAFT)
C VOAHH IS THE DISPLACED VOLUME OF THE PRESSURE HULL WITH HEMISPHERICAL
C END CAPS.
      VOAHH = VTOTH + VKF + VHEM+VSHEL
C VOAEL IS THE DISPLACED VOLUME OF THE PRESSURE HULL WITH ELLIPTICAL
C END CAPS.
      VOAEL = VTOTE + VKF + VEP + VSHEL
C WTSHLH IS THE WEIGHT OF THE PRESSURE HULL WITH HEMISPHERICAL END
C CAPS.
      WTSHLH = (VKF+VHEM+VSHEL+VBULK) * DENS
C WTSHLE IS THE WEIGHT OF THE PRESSURE HULL WITH ELLIPTICAL END CAPS.
      WTSHLE = (VKF+VEP+VSHEL+VBULK)*DENS
C

```





TABLE A5-2 contd.

178

```

USER=BUNCE      266 15422      JOINT COMPUTER FACILITY, 4IT

C DISP-S IS THE DISPLACEMENT OF THE PRESSURE HULL IN SALT WATER.
C DISP-F IS THE DISPLACEMENT OF THE PRESSURE HULL IN FRESH WATER.
C H REFERS TO HEMISPHERICAL END CAPS.
C E REFERS TO ELIPTICAL END CAPS.
C
      DISPHS = (VOAH/1728.) * 64.043
      DISPEF = (VOAE/1728.) * 64.043
      DISPHF = (VOAH/1728.) * 52.365
      DISPEF = (VOAE/1728.) * 52.365
      WRITE(KO,701) LFWD,LEAF,LAFT,DMAX
      WRITE(KO,800) TENDH,VOLIM,VENDH,VTOH,VOAH,DISPHS,DISPHE,WTSHLH
      WRITE(KO,801) TENDE,VOLIM,VENDE,VTOE,VOAE,DISPEF,WTSHLE
C THE FOLLOWING STATEMENTS ARE THE FORMAT STATEMENTS.
900 FORMAT(10X,'THIS DATA IS GOOD IF HEMISPHERICAL END CAPS ARE USED',
2 //,10X,'THICKNESS END CAP =',F8.3,12X,'VOLUME IN CYLINDER =',
3F8.1,/,10X,'VOLUME IN END CAPS =',F8.1,12X,
4'TOTAL INSIDE VOLUME =',F8.1,/,
410X,'DISPLACED VOLUME =',F8.1,12X,'DISP SALT WATER =',
5 F8.1,/,10X,'DISP FRESH WATER =',F8.1,12X,
6'WEIGHT SHELL & FRAMES =',F6.2,/)
801 FORMAT(10X,'THIS DATA IS GOOD IF ELIPTICAL END CAPS ARE USED',
2 //,10X,'THICKNESS END CAP =',F8.3,12X,'VOLUME IN CYLINDER =',
3F8.1,/,10X,'VOLUME IN END CAPS =',F8.1,12X,
4'TOTAL INSIDE VOLUME =',F8.1,/,
410X,'DISPLACED VOLUME =',F8.1,12X,'DISP SALT WATER =',
5 F8.1,/,10X,'DISP FRESH WATER =',F8.1,12X,
6'WEIGHT SHELL & FRAMES =',F6.2,/)
215 FORMAT(10X,'BULKHEAD SEPARATION IS GREATER THAN 1.5 D SIFLL',
1 'THEREFORE THE COMPARTMENT',/,10X,'WILL HAVE TO BE SPLIT',
2 'AND A KING FRAME INSTALLED AT MID COMPARTMENT',/)
643 FORMAT('1,/,/,/,/,/,10X,'THE DESIGN OPERATING DEPTH =',
177.0,5X,'DESIGN FACTOR OF SAFETY =',F6.2,/)
200 FORMAT(10X,'THE FOLLOWING SCANTLINGS ARE FOR THE FORWARD',

```



TABLE A5-2 contd.

```

USER=BUNCE      266 15422      JOINT COMPUTER FACILITY, YIT

1'COMPARTMENT',/,10X,'WHICH HAS A LENGTH OF ',F8.2,2X,'INCHES',///)
205 FORMAT(10X,'THE FOLLOWING SCANTLINGS ARE FOR THE BATTERY .
1'COMPARTMENT',/,10X,'WHICH HAS A LENGTH OF ',F8.2,2X,'INCHES',///)
210 FORMAT(10X,'THE FOLLOWING SCANTLINGS ARE FOR THE AFT .
1'COMPARTMENT',/,10X,'WHICH HAS A LENGTH OF ',F8.2,2X,'INCHES',///)
220 FORMAT(10X,'WE HAVE FRAME SEPARATIONS UP TO 1/15 COMPARTMENT',
1 'LENGTH AND FRAMES HAVE FAILED TO SATISFY REQUIRED CRITERIA',///)
701 FORMAT('1',////////,10X,'THE FOLLOWING DATA IS FOR A PRESSURE HULL',
2,' WITH THE FOLLOWING CONFIGURATION',///,
310X,'COMPARTMENT LENGTHS.',/,10X,'FORWARD  = ',F8.2,2X,
3'BATTERY  = ',F8.2,2X,'AFT    = ',F8.2,///,
410X,'MAXIMUM DIAMETER = ',F8.3,///)
IF (IKIL.LI.NJ2BS) GO TO 399
WRITE (K0,685)
635 FORMAT ('1')
STOP
END
PROGRAM *MAIN* HAS      NO ERRORS

```



TABLE A5-2 contd.

```

USER=BUNCE      266 15422      JOINT COMPUTER FACILITY, 4IT

      SUBROUTINE SCANCK (DSHELI,SIGMAY,EMOD,POSR,CRRPES,LFRM,LBULK,
1 HWEB,IWEB,HFLG,TFLG,TSHEL,ICK,DENS)

C SUBROUTINE SCANCK IS THE SUBROUTINE WHICH PERFORMS THE CALCULATIONS
C FOR THE EXTERNALLY FRAMED STIFFENED CYLINDRICAL PRESSURE HULL.
C ALL VARIABLES ARE AS PREVIOUSLY DEFINED. THE PROCEDURE IS
C OUTLINED IN TABLE A5-2.
C DSHELI IS THE INSIDE DIAMETER OF E CYLINDRICAL SHELL.
C
      REAL LFRM,LBULK,LCD,MOMI
      DATA KI/3/,KO/5/
C ICK IS A SCORE WHICH DETERMINES IF A FRAME SIZE AND SPACING HAS
C PASSED ALL THE CRITERIA, A SCORE OF SEVEN IS REQUIRED TO PASS ALL THE
C CRITERIA. ONE POINT IS GIVEN FOR EVERY CRITERIA PASSED.
      ICK = 0
C HERE DSHEL IS RESPECIFIED AS THE MIDSHELL DIAMETER.
      DSHEL = DSHELI + TSHEL
      LOD = LFRM/DSHEL
      TOD = TSHEL/DSHEL
      AWEB = TWEB * HWEB
      AFLG = TFLG * HFLG
      AFRM = AWEB + AFLG
      BT = IWEB * TSHEL
      B = BT / (AFRM + BT)
      THETA = (18.2 * LOD) / SQRT (100.*TOD)
      THETA2 = THETA / 2.
      FNKD = SINH(THETA) + SIN(THETA)
      FN = (COSH(THETA) - COS(THETA)) / FNKD
      FK = (SINH(THETA) - SIN(THETA)) / FNKD
      PSQR = POSR **2.
      OMMS = 1. - PSQR
      BETA = ((2.*FN)/(AFRM+BT))*((1./(3.*OMMS)) ** .25) *
1SQRT ((DSHEL * .5) * TSHEL **3.)

```



TABLE A5-2 contd.

```

USER=BUNCE      266 15422      JOINT COMPUTER FACILITY, MIT

      FUNMU = SQRT((3.*PSOR)/(OWMS))
      H = (-2./FNKD) * ((1.+ FUNMU) * SIN(THETA2)*COS(THETA2) +
      1 (1.- FUNMU) * COSH(THETA2) * SIN(THETA2))
      C PCSB IS THE CRITICAL PRESSURE FOR SHELL BUCKLING.
      PCSB =(2.42 * EMOB * (TOD ** 2.5))/(OWMS ** .75)*(LDD- .45 * SPT
      1(TOD))
      TPC =(2. * SIGMA*TSHEL)/ DSHEL
      BPC = (.85 -B)/(1.+BETA)
      C PCYF IS THE CRITICAL EXTERNAL PRESSURE FOR SHELL YIELD AT THE FRAM,
      PCYF = TPC /(.5 + 1.815*FK*BPC)
      C PCYMD IS THE CRITICAL PRESSURE FOR SHELL YIELD AT MIDFRAM,
      PCYMD = TPC /(1. + H * BPC)
      APLT = TSHEL * LFRM
      AMPLT = TSHEL/ 2.
      AMWEB = TSHEL + HWEB /2.
      AMFLG = TSHEL + HWEB + TELG/2.
      T1 = APLT + AFLG + AWEB
      T2 = APLT * AMPLT + AWEB * AMWEB + AFLG * AMFLG
      T3 = APLT * (AMPLT**2.) + AWEB*(AMWEB**2.) + AFLG*(AMFLG**2.)
      T4 = (TWB * (HWEB**3.))/12.
      CG = T2/T1
      T5 = T2*CG
      CG1 = T2/(AWEB+AFLG)
      C MOMI IS THE MOMENT OF INERTIA OF ONE FRAME AND A FRAME SPACE OF SHELL.
      MOMI = T3 + T4 - T5
      DFRM = DSHEL + 2. * CG1
      Q = TWB *((1.-PSR/2.)*(BETA/B))/(1.+BETA)
      C PCFMY IS THE CRITICAL EXTERNAL PRESSURE FOR FRAME YIELDING.
      PCFMY = (SIGMA * (AFRM + BT))/(Q *(DFRM/2.))
      SIGC = (Q*(DSHEL/2.)*CRPRES)/(AFRM + BT)
      MD = IFIX(((1.571*DSHEL)/LBULK)+.5)
      FM = FLOAT(MD)
      FM2 = FM ** 2.

```





TABLE A5-2 contd.  
 USER=BUNCE 266 15422 JOINT COMPUTER FACILITY, MIT

```

FM4 = FM2 ** 2.
C CALCULATE PRESS FOR GENERAL INSTABILITY
GIS1N = (2.*EMOD*TSHEL*FM4)/DSHEL
GIS2 = (EMOD*WOMI)/((DSHEL/2.)*((DEPM/2.)**2.)*(LFRM-TWEL) )
PCGS2 = 10.*F+26
SN = 2.
DO 50 I = 1,10
DEN1 = ((SN**2.)-1.+(FM2/2.))*((CN**2.)+FM2)**2.)
TOP2 = (SN**2.)-1.
PCGS1 = GIS1N/DEN1 + TOP2 * GIS2
IF(PCGS2.LE.PCGS1) GO TO 70
PCGS2 = PCGS1
I = I + 1
SN = SN + 1.
50 CONTINUE
C PCGS IS THE CRITICAL EXTERNAL PRESSURE FOR GENERAL INSTABILITY.
70 PCGS = PCGS2
SN = SN - 1.
C PCFIS IS THE CRITICAL EXTERNAL PRESSURE FOR FRAME INSTABILITY.
PCFIS = (25.*EMOD*MOMI)/((DEPM**3.)*LFRM)
E = TSHEL / 2.
C = TSHEL + HWEB + TPLG - CG
SIGB = (4.*EMOD*C*E*(SN**2.)-1.)*CPPRES)/((DEPM**2.)*(PCGS-C.LFRM
1))
C SIGTOT IS THE MAXIMUM STRESS IN THE FRAMES.
SIGTOT = SIGB + SIGC
IF (PCSB.GT.1.5*CPRES) ICK = 1
IF (PCYF.GT.CRPRES) ICK = ICK + 1
IF (PCYMD.GT.CRPRES) ICK = ICK + 1
IF (PCFMY.GT.CRPRES) ICK = ICK + 1
IF (PCGS.GT.2.5*CPRES) ICK = ICK + 1
IF (PCFIS.GT.CRPRES) ICK = ICK + 1
IF (SIGTOT.LE.SIGMAY) ICK = ICK + 1

```



TABLE A5-2 contd.

```

USER=BUNCE      266 15422      JOINT COMPUTER FACILITY, VIT

C IS ICK IS 7 THEN THE CONFIGURATION IS OK AND THE RESULTS
C WILL BE PRINTED. IF NOT IT GOES BACK TO THE MAIN PROGRAM AND SETS UP
C A NEW CONFIGURATION.
  IF (ICK.LI.7) GO TO 10
  RSHEL = DSHEL/2.
  PKFGI = ((EMOD*TSHEL*FM4)/(RSHEL*(SN**2.))-1.+FM2/2.)
  1 *(((SN**2.)+FM2)**2.)) + ((EMOD*WCVI*(SN**2.))-1.))
  2 /((PSHEL**3.)*LBULK))
  VERMS = 3.14159 * DFRM * (AWER+AELS) * ((LBULK/LFRM)-1.)
  WFRMS = VERMS * DENS
  WRITE (K0,102) DSHEL,TSHEL,TELG,WELG,TWER,HWER,LFRM
  WRITE (K0,103) PCSB,PCYF,PCYMD,PCFMY,PCGS,PCEIS,SIGMA,SIGTOL,SN
102 FORMAT(10X,'THE SHELL AND STIFFENING MEMBER SIZES ARE AS FOLLOWS.',
1//,10X,'O SHELL =',F8.3,2X,'I SHELL =',F8.3,2X,'I FLANGE =',
2F8.3,2X,'H FLANGE =',F8.3,2X,'T WEB =',F8.3,2X,'Q WEB =',
3F8.3,2X,'FRM SEP =',F8.3,2X,/)
  WRITE (K0,666) PKFGI
666 FORMAT(10X,'THE PRESSURE FOR GENERAL INSTABILITY BETWEEN ',
1 'BULKHEADS =',F10.0,/)
103 FORMAT(10X,'THE FOLLOWING FIGURES ARE THE CRITICAL EXTERNAL ',
1 'PRESSURES IN PSI.',/,10X,'FOR FAILURE IN THE APPROPRIATE MODE.',
2//,10X,'PCSB =',F9.0,2X,'PCYF =',F9.0,2X,'PCYMD =',F9.0,2X,
3 'PCFMY =',F9.0,/,
4 10X,'PCGS =',F9.0,2X,'PCEIS =',F9.0,2X,'SIGMA =',F9.0,2X,
5 'N =',F8.0,/)
  WRITE (K0,104) WFRMS,WFRMS
104 FORMAT(10X,'THE VOLUME OF THE STIFFENING FRAMES =',F10.5,/,10X,
1 'THE WEIGHT OF THE STIFFENING FRAMES =',F10.5,/)
10 CONTINUE
  RETURN
  END
PROGRAM SCANCK HAS      NO ERRORS

```



TABLE A5-3 SAMPLE OUTPUT FROM CYLINDRICAL PRESSURE HULL PROGRAM

THE DESIGN OPERATING DEPTH = 1000.      DESIGN FACTOR OF SAFETY = 1.50

THE FOLLOWING SCANTLINGS ARE FOR THE FORWARD COMPARTMENT  
WHICH HAS A LENGTH OF 9.00 INCHES

THE SHELL AND STIFFENING MEMBER SIZES ARE AS FOLLOWS.

D SHELL = 12.420 T SHELL = 0.330 T FLANGE = 0.000 H FLANGE = 0.000

T WEB = 0.250 H WEB = 0.500 FRM SEP = 1.500

THE FOLLOWING FIGURES ARE THE CRITICAL EXTERNAL PRESSURES IN PSI  
FOR FAILURE IN THE APPROPRIATE MODE.

PCSB = 64029. PCYF = 3249. PCYMD = 2109. PCFVY = 2646.

PCGS = 8153. PCFIS = 1000. SIGMA = 30502. N = 4.

THE PRESSURE FOR GENERAL INSTABILITY BETWEEN BULKHEADS = 2628.

THE VOLUME OF THE STIFFENING FRAMES = 29.23013

THE WEIGHT OF THE STIFFENING FRAMES = 2.86455



TABLE A5-3 contd.

THE DESIGN OPERATING DEPTH = 1000. DESIGN FACTOR OF SAFETY = 1.50

THE FOLLOWING SCANTLINGS ARE FOR THE FORWARD COMPARTMENT WHICH HAS A LENGTH OF 9.00 INCHES

THE SHELL AND STIFFENING MEMBER SIZES ARE AS FOLLOWS.

D SHELL = 12.420	T SHELL = 0.330	T FLANGE = 0.00	H FLANGE = 0.000
T WEB = 0.500	H WEB = 0.750	FRM SEP = 4.500	

THE FOLLOWING FIGURES ARE THE CRITICAL EXTERNAL PRESSURES IN PSI FOR FAILURE IN THE APPROPRIATE MODE.

PCSB = 10508.	PCYF = 2004.	PCYMD = 1824.	PCFMY = 3098.
PCGS = 10928.	PCFIS = 1680.	SIGMA = 18261.	N = 3.

THE PRESSURE FOR GENERAL INSTABILITY BETWEEN BULKHEADS = 8424.

THE VOLUME OF THE STIFFENING FRAMES = 17.33260
THE WEIGHT OF THE STIFFENING FRAMES = 1.74759





TABLE A5-3 contd.

THE DESIGN OPERATING DEPTH = 1000. DESIGN FACTOR OF SAFETY = 1.50

THE FOLLOWING SCANTLINGS ARE FOR THE BATTERY COMPARTMENT WHICH HAS A LENGTH OF 12.00 INCHES

THE SHELL AND STIFFENING MEMBER SIZES ARE AS FOLLOWS.

D SHELL = 12.420 T SHELL = 0.330 T FLANGE = 0.000 H FLANGE = 0.000  
 T WEB = 0.250 H WEB = 0.500 FPV SEP = 1.714

THE FOLLOWING FIGURES ARE THE CRITICAL EXTERNAL PRESSURES IN PSI FOR FAILURE IN THE APPROPRIATE MODE.

PCSB = 46948. PCYF = 3177. PCYMD = 2072. PCFVY = 2525.  
 PCSS = 7127. PCFIS = 862. SIGMA = 34163. N = 4.

THE PRESSURE FOR GENERAL INSTABILITY BETWEEN BULKHEADS = 2307.

THE VOLUME OF THE STIFFENING FRAMES = 35.51602  
 THE WEIGHT OF THE STIFFENING FRAMES = 3.48057



TABLE A5-3 contd.

THE DESIGN OPERATING DEPTH = 1000. DESIGN FACTOR OF SAFETY = 1.50

THE FOLLOWING SCAVILLINGS ARE FOR THE BATTERY COMPARTMENT WHICH HAS A LENGTH OF 12.00 INCHES

THE SHELL AND STIFFENING MEMBER SIZES ARE AS FOLLOWS.

D SHELL = 12.420 T SHELL = 0.330 T FLANGE = 0.000 H FLANGE = 0.000  
 T WEB = 0.500 H WEB = 0.750 FRM SEP = 6.000

THE FOLLOWING FIGURES ARE THE CRITICAL EXTERNAL PRESSURES IN PSI FOR FAILURE IN THE APPROPRIATE MODE.

PCSB = 7410. PCYF = 2015. PCYMD = 1789. PCFMY = 3072.  
 PCGS = 9184. PCFIS = 1208. SIGMA = 32570. N = 4.

THE PRESSURE FOR GENERAL INSTABILITY BETWEEN BULKHEADS = 5067.

THE VOLUME OF THE STIFFENING FRAMES = 18.3457<sup>8</sup>  
 THE WEIGHT OF THE STIFFENING FRAMES = 1.79789



TABLE A5-3 contd.

THE DESIGN OPERATING DEPTH = 1000. DESIGN FACTOR OF SAFETY = 1.50

THE FOLLOWING SCANTLINGS ARE FOR THE AFT COMPARTMENT WHICH HAS A LENGTH OF 9.00 INCHES

THE SHELL AND STIFFENING MEMBER SIZES ARE AS FOLLOWS.

D SHELL = 12.420 T SHELL = 0.330 T FLANGE = 0.000 H FLANGE = 0.000  
T WEB = 0.250 H WEB = 0.500 FRM SEP = 1.500

THE FOLLOWING FIGURES ARE THE CRITICAL EXTERNAL PRESSURES IN PSI FOR FAILURE IN THE APPROPRIATE MODE.

PCSB = 64029. PCYF = 3249. PCYMD = 2109. PCFVY = 2646.  
PCGS = 8153. PCFIS = 1000. SIGMA = 30502. N = 4.

THE PRESSURE FOR GENERAL INSTABILITY BETWEEN BULKHEADS = 2629.

THE VOLUME OF THE STIFFENING FRAMES = 29.23013  
THE WEIGHT OF THE STIFFENING FRAMES = 2.86455



TABLE A5-3 contd.

THE DESIGN OPERATING DEPTH = 1000. DESIGN FACTOR OF SAFETY = 1.50

THE FOLLOWING SCANTLINGS ARE FOR THE AFT COMPARTMENT WHICH HAS A LENGTH OF 9.00 INCHES

THE SHELL AND STIFFENING MEMBER SIZES ARE AS FOLLOWS.

D SHELL = 12.420 T SHELL = 0.330 T FLANGE = 0.000 H FLANGE = 0.000  
T WEB = 0.500 H WEB = 0.750 FRY SEP = 4.500

THE FOLLOWING FIGURES ARE THE CRITICAL EXTERNAL PRESSURES IN PSI FOR FAILURE IN THE APPROPRIATE MODE.

PCSB = 10508. PCYF = 2004. PCYMD = 1824. PCFY = 3094.  
PCGS = 10928. PCFIS = 1680. SIGMA = 18261. N = 3.

THE PRESSURE FOR GENERAL INSTABILITY BETWEEN BULKHEADS = 8424.

THE VOLUME OF THE STIFFENING FRAMES = 17.83260  
THE WEIGHT OF THE STIFFENING FRAMES = 1.74759





TABLE A5-3 contd.

THE FOLLOWING DATA IS FOR A PRESSURE HULL WITH THE FOLLOWING CONFIGURATION

COMPARTMENT LENGTHS.

FORWARD = 3.00 BATTERY = 12.00 AFT = 3.00

MAXIMUM DIAMETER = 14.250

THIS DATA IS GOOD IF HEMISPHERICAL END CAPS ARE USED

THICKNESS END CAP =	0.330	VOLUME IN CYLINDER =	3444.0
VOLUME IN END CAPS =	925.3	TOTAL INSIDE VOLUME =	4369.3
DISPLACED VOLUME =	5074.6	DISP SALT WATER =	188.1
DISP FRESH WATER =	183.1	WEIGHT SHELL & FRAMES =	74.74

THIS DATA IS GOOD IF ELIPTICAL END CAPS ARE USED

THICKNESS END CAP =	0.330	VOLUME IN CYLINDER =	3444.0
VOLUME IN END CAPS =	461.7	TOTAL INSIDE VOLUME =	3905.7
DISPLACED VOLUME =	4561.3	DISP SALT WATER =	159.1
DISP FRESH WATER =	164.6	WEIGHT SHELL & FRAMES =	69.88



## APPENDIX VI

## CONTROL SYSTEM STUDY

The control system consists of the control surfaces and actuators. The autopilot which controls the actuators is considered a primary payload electronics item and is addressed in Appendix VII.

Two alternative control surface configurations will be investigated. First, the steerable ducted propeller presented originally in Appendix III, and, secondly, variations of the control surface configuration used in the original robot.

## A6.1 The Steerable Ducted Propeller

In order to use a steerable ducted propeller as presented in Appendix III, the duct will have to be able to pivot simultaneously about two axes. This will allow the duct to control both the yaw and pitch of the vehicle at once. Previous applications on Alvin [3], Aluminaut [4], and the Navy's DSRV [2] have used steerable ducted propellers for yaw control only. To prove the feasibility of a steerable ducted propeller used to control both the yaw and pitch involves developing a workable concept for this arrangement.

Several steerable ducted propeller configurations were investigated, but the arrangement presented in Figures A6-1 and A6-2 proved conceptually to be the most workable. In this arrangement a universal joint is installed in the



FIGURE A6-1 INBOARD DETAIL OF PROPOSED STEERABLE DUCTED PROPELLER

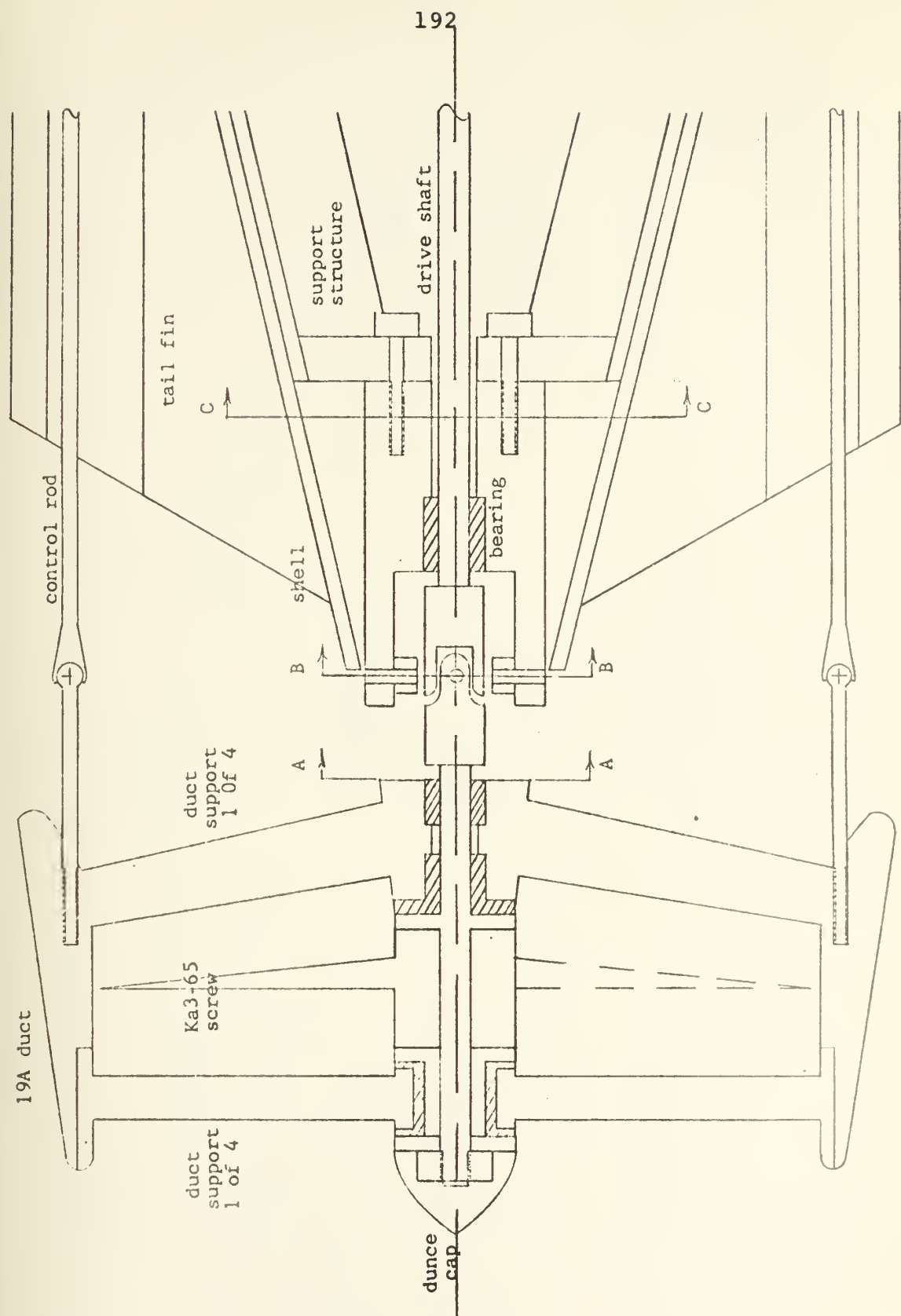
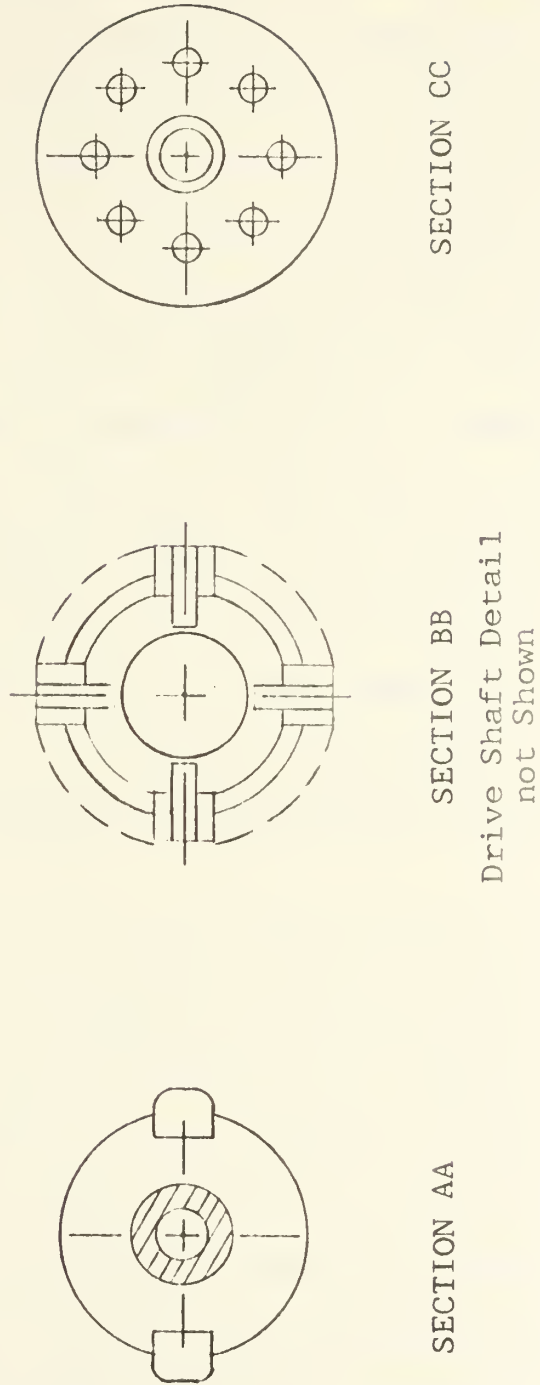




FIGURE A6-2 CROSECTION VIEWS OF PROPOSED STEERABLE DUCTED PROPELLER







drive shaft to allow power to be supplied to the propeller while the duct is deflected. The universal, however, limits the duct's deflection to a maximum of 30 degrees. The duct is supported and prevented from rotating itself by another universal, which surrounds the drive train universal.

The duct is the major structural member of the proposed configuration with the two four spur star supports providing support between the propeller tail shaft and the duct. The rear star is removable to allow removal of the propeller from inside the duct. The propeller thrust bearing is located directly in front of the propeller hub.

Rotation of the duct is accomplished by four control rods which lead forward to servo actuators. The slew rate of the duct must be carefully controlled to reduce unwanted gyroscopic effects and overreaction of the control system.

The ducted propeller configuration utilizes the deflected thrust of the propulsor in conjunction with the lift of the rotated duct to provide the steering forces. Previous experience with larger versions of this configuration have shown this system works very well in low speed maneuvering, as is the case with the deep submersibles previously mentioned. This is not, however, necessarily an advantage for the robot which will operate at constant speed.

Several problems with this arrangement may be



expected, which could cause serious problems. The most serious is the control linkage, which not only moves fore and aft, but pivots sideways about the duct pivot. This sideways rotation occurs when simultaneous commands to yaw and pitch are executed, causing the control rods to deflect sideways into the fins. Flexible control rods reduce this problem, but also introduce some cross coupling between the yaw and pitch control. This means that, if a yaw deflection is first actuated, a subsequent pitch deflection will remove some of the yaw deflection. This effect is small for small rotations, but becomes increasingly serious as the deflections increase. Under normal running, small rotations may be all that is necessary, but this is difficult to predict.

Some additional problems involve the determination of the hydrodynamic coefficients for the ducted propeller. For a normal lifting surface these are well known, but for the ducted propeller they would have to be determined to establish the required gains in the autopilot. The effect on the thrust due to the variable inflow direction to the propeller would have to be evaluated, as well.

There are also problems with the drive train. The universal operating in water could be a problem. Also, the propellers operate at 500 to 600 RPM, which could cause a problem with the tail shaft support. A model would have to be tested to adequately evaluate these problems.

Though the steerable ducted propeller proposed



offers advantages in reduced propeller induced vibrations and better propeller protection, some serious questions arise concerning its operation. The answers to these problems require more study of the proposed configuration. Until these questions can be satisfactorily answered, the use of this proposed steerable ducted propeller configuration is considered to involve a considerable risk.

#### A6.2 Conventional Control Surface Configuration.

The control surfaces used on the first generation robot consists of a set of vertical and horizontal fins located at the tail and a pair of diving fins located at the forward end of the cylindrical midsection. These forward fins would interfere with the pressure hull configuration proposed for the second generation submarine, as well as increase the drag. The question that ensues, then, is what effect does removing the forward diving surfaces have?

An analysis of the effect of longitudinal position of control surfaces on directional stability is presented in [43]. The analysis concludes that lifting surfaces located near the stern improve directional stability more than those located near the bow. By removing the forward fins, the robot would then be more inherently stable in its depth control, provided no large positive or negative buoyant forces are present. The robot would not be able to turn up or down as quickly without the forward diving planes, due to this



improved stability, but this is actually a desirable characteristic.

The forward diving planes also assist the robot in going from partly to fully submerged at the surface. To evaluate this effect requires an understanding of the mechanism which causes the vehicle to go below the surface.

Lift, or perhaps more correctly, negative lift, is developed by the body as the fluid inflow velocity rotates from being parallel with the body's axis of symmetry. This body lift can be very large. Tail mounted control surfaces produce a sideward force when deflected, which rotates the body in the flow and, thus, lift is developed on the body itself. This causes the body to turn or dive, as the case may be. The lift developed by the forward fins do not create this turning moment on the body, but rather act like a pair of airplane wings. This effect is useful at the surface where the amount of body rotation can be limited. The robot, however, only operates with an inch of freeboard at the surface and, therefore, it does not have far to go to be submerged. In this case, it is felt the stern horizontal planes will easily be able to cause the robot to dive from the surface if they are properly applied. Once the submarine is below the surface, the submarine's depth is easily controlled by the stern planes alone.

Elimination of the forward diving planes not only erases the conflict with the primary pressure hull, but also





reduces the appendage drag. Additionally, one of the control functions of the autopilot is eliminated, thus reducing the complexity of that piece of equipment.

One adverse effect might also be created, however. The diving planes provide a great deal of roll damping, which is eliminated by their removal. It is questionable if the stern planes would provide satisfactory roll damping by themselves. A form of bilge keel may have to be added to the body to improve the roll damping, but this will be dependent on other factors, such as the vertical location of the center of gravity, and are not investigated further here.

The location of the tail mounted control surfaces was also studied. Locating the control surfaces behind the propeller increases their effectiveness, due to the increased water velocity in the wake, and would allow them to be smaller. Also, this location improves the propulsive efficiency by as much as three per cent [31]. This location was investigated during development of the first generation robot submarine and found to be too complex to be practical. This alternative will, therefore, not be considered further.

### A6.3 Conclusions.

1. The steerable ducted propeller is a complex system with several drawbacks in addition to its advantages. Lack of information concerning the control aspects of this alternative and its overall complexity make it a risky



selection.

2. The forward diving planes can be eliminated, which will probably lead to an improvement in the depth stability of the vehicle.

3. With the forward fins eliminated, the results of Appendix III show the B series propeller with tail control surfaces requires lower propulsion power than the steerable ducted propeller design.



## APPENDIX VII

## Primary Control Payload Equipment Study.

The primary control payload equipment consists of those pieces of electronic equipment which perform the various control functions for the robot. The primary pieces of equipment in this group are the onboard computer and the autopilot.

The onboard computer is the brain of the robot, storing and processing all the mission instructions and data which is collected.

The autopilot receives commands from the computer and controls the course and depth at the ordered values. Depth, heading, and pitch sensors provide the input to the autopilot. The autopilot's output goes through a power amplifier to the servo motors, which actuate the control surfaces.

Several basic points were observed during the course of this investigation. First, the robot's equipment is very specialized for this application. The electronics must be small, lightweight, and have low power consumption. Second, the arrangement of the electronics is at the whim of the designer. Most computers use flat rectangular boards, whereas the first generation robot's computer was built on circular boards designed to fit into the circular pressure housing. Additionally, the density of electronics equipment is very low. Accordingly, the volume is more critical than



the weight. When packaged in pressure housings, electronic equipment will require some ballast to become neutrally buoyant.

The intent of this study is not to develop new designs for the electronics required of the robot, but to investigate what is available and develop a volume and power consumption estimate for the electronics package. This data will be input to the design to help size the robot.

#### A7.1 The Computer.

Computers using CMOS circuitry are the lowest power consumption units available. Only a few manufacturers produce this type of equipment, however. The COSMAC series produced by the Radio Corporation of America was one sample investigated. These products are usually provided to original equipment manufacturers. Accordingly, the only complete units available are in kit form to be assembled according to the user's requirements. This route would require development of a new computer entirely.

The computer onboard the first generation robot was designed expressly for that function, using the CMOS circuitry. It is then a more logical solution to improve its capability than to design a new model.

To improve the present computer, a larger memory is required to meet the requirements of the mission. Two basic kinds of memory are available: the random access





memory (RAM), and data stored on tape cassette recorders. Both of these kinds of memory will be required. The RAM's will be used to store mission instructions where rapid access is required, and the onboard tape drive will be used to store recorded data which requires large storage capacity, but has no requirement for access except at the completion of the mission when the data is retrieved.

A digital data mini cassette recorder, manufactured by the Raymond Corporation, is the perfect answer for the tape drive. The characteristics of this unit are as follows:

Transport size:	3.0" x 3.0" x 1.8"
Electronics:	3.5" x 5.75 " x 1.0"
Power:	Less than 1.5 watts max. @ 5.0 VDC; Less than 1/4 watt max standby.
Weight:	1 lb.
Capacity:	64k bytes/side unformatted
Data Transfer Rate:	2400 bits per second
Rewind:	20" per second
Packing Density:	800 bits per inch

With the addition of 8k more RAM and the data tape recorder, the computer requirements are estimated as follows:

Estimate Volume for Computer and power supplies:	700 in. <sup>3</sup>
Volume for data tape recorder:	36.5 in. <sup>3</sup>



Estimated Total Volume Allocation Required:	850 in. <sup>3</sup>
Estimate Total Power Consumption:	9.2 Watts

#### A7.2 Autopilot and sensors.

The autopilot must be compatible with the computer and the hydrodynamic characteristics of the vehicle. For the second generation robot, the autopilot will have to be redesigned, due to the change in the envelope form and the removal of the forward diving planes. The D→A and A→D interfaces with the computer will, however, still be compatible with the new design.

The heading sensor is the only other piece of equipment associated with the autopilot which requires further investigation. The unit used in the present robot is a magnetic compass with an optically scanned compass card.

As pointed out in [44], a vehicle which operates with the velocities and accelerations of the robot can be adequately controlled using a magnetic compass, rather than the much more expensive and complex gyroscopic variety. The present magnetic compass has, however, caused some problems with the robot's operation, due mainly to dynamic effects. To counter this problem, a Hall effect compass is presently under development. This compass has no moving parts and, thus, eliminates the dynamic problems.



The Hall effect compass uses two Hall effect crystals oriented orthogorally in a plane parallel to the earth's surface. The angular orientation of this pair in relation to the earth's magnetic field produces the heading signal. This signal is unaffected by dynamic effects. The signal is, however, affected by deviation from the horizontal plane, though. Accordingly, when the submarine goes into a straight dive, the compass signal will change, even though the submarine's actual heading has not. This effect is not too serious with the first generation robot's operation, because the submarine does not go very deep and its pitch is limited. For the proposed second generation robot's operation, though, the robot will dive at angles of 30 degrees for extended periods; and thus, the heading while diving is totally unsatisfactory. The heading deviation during a dive can be compensated for by including a pitch indication to the compass or by using three orthogonal Hall crystals: but this solution will require further development.

The Hall effect compass is very attractive because it is small, light weight, and requires only about 250 mw of power. The lack of a tested design, however, makes this a risky selection for the primary compass.

To account for space and volume of the compass, a Digicourse magnetic compass very similar in operation to the present robot's compass was selected. This magnetic compass can pitch up or down to 40 degrees, which should be compatible



with the submarine's diving angle. When the Hall compass is developed, it will easily occupy the space vacated by the magnetic compass.

An estimate of the space and power required by the autopilot, sensors and interfaces with the computer is as follows:

Volume Allocation for Autopilot and Sensors:	400 in. <sup>3</sup>
Estimated power requirements, including fin servo control motors:	10 watts continuous

#### A7.3 Acoustic Pinger.

The acoustic pinger provides a 4 ms burst of 10 KHZ signal every second for tracking and navigation. Part of the pinger, the transducer, is located in the wet part of the hull; the remainder is located in the pressure housing. The dry volume and power allocation for this system is as follows:

Volume:	15 in. <sup>3</sup>
Power:	1 watt

#### A7.4 Additional Payload Electronics.

Several other pieces of electronics equipment were investigated or specified for the robot. Among these was a dopplar navigation sonar which proved to be too large and required too much power.





A command data link was also specified in the design requirements; but, due to lack of information and time constraints, a suitable model was not located. This method of information transfer is used in other applications; but the vehicles are much larger, so space is not such a problem.

A collision avoidance sonar was under development for the original robot, but it had problems with surface return. This equipment is, as yet, still under development, but it should prove no problem for the second generation robot to accommodate.

An altitude sonar was also considered in the design requirements as a necessary sensor to improve data collection with side scan sonar or by photographic equipment. However, these two payload packages both proved to be infeasible for the robot at this point, due to recording problems and the size of a camera suitable for this application was just too big to fit in a vehicle like this without specialization to just that mission, which was not desired.

#### A7.5 Summary.

The equipment estimates determined are intended to assist in determining the size required for the vehicle. The data should represent a conservative estimate, since the figures derived from various sources was increased by 15 per cent to account for enclosure and other inaccuracies.



## APPENDIX VIII

## DATA COLLECTION PAYLOAD STUDY

The operational mission of the robot submarine is to collect data. To perform this function requires various sensors be installed onboard. These can vary from motion picture cameras to temperature recorders. The potential list is extensive, but is limited to water data sensors or survey equipment, since the robot is ill suited for collecting bottom samples.

The second generation robot is intended to be flexible enough that various sensors can be fitted and exchanged at will within the limits of buoyancy and volume constraints. To bring this study down to a manageable size, two very desirable high impact systems were investigated, a side scan sonar and an underwater camera.

## A8.1 Side Scan Sonar.

A side scan sonar developed by Klein Associates was investigated. The transducers could easily be fabricated into the envelope occupying the gap between the envelope and the main pressure hull. Other considerations concerning the feasibility of incorporating the sonar to the submarine are not quite so straightforward.

The biggest problem with this concept is the recording and storage of the data onboard the robot. This problem is currently being studied, and a system is under



development for incorporation into the present robot. If this is successful, the system will certainly be adaptable to the second generation design. Until this is accomplished, however, the system is considered infeasible.

#### A8.2 Photographic Equipment.

Only still cameras were considered because movie and television cameras require constant lighting which creates unrealistic demands on the energy storage system. Still camera shots can, however, be taken with a high intensity flash.

Cameras and flash equipment manufactured by Benthos Inc. for deep sea application were considered representative examples of this type equipment. The characteristics of two available models are presented in Table A8-1. These cameras come in their own pressure housings and can be triggered electrically, which is totally compatible with computer operation. The larger model has an option which will record the time the picture was taken on the film.

Reviewing the data in Table A8-1, these systems are obviously high impact systems. The smaller model is more realistic than the larger model, but its capability is seriously limited. The impact of these systems can be reduced by enclosing the flash electronics in the main pressure hull and eliminating the battery, instead powering the flash and camera from the robot's own energy storage unit. Only the



TABLE A8-1 SIZE AND WEIGHT OF VARIOUS MODELS EDGERTON DEEP SEA  
35MM PHOTOGRAPHIC SYSTEMS

MODEL	UNIT	CAPABILITY	PRESSURE HOUSING O.D.	HOUSING LENGTH	DRY WEIGHT	WET WEIGHT
371	Camera	to 80 exp.	5 in	14 in	22.11bs	14.51bs
381	Flash	500 flash	7 in	17 in	20.11bs	14.01bs
372	Camera	to 1600 exp	5 in	24 in	29.11bs	16.81bs
382	Flash	3200 flash	5 in	36 in	40.21bs	31.61bs

All data is for shallow (4000 ft.) water stainless steel pressure housings.  
Flash units have their own battery.

Data courtesy Benthos Inc.





flash tube and reflector need be installed in the nose of the vehicle then. This is the only realistic means of incorporating the unit onboard the robot.



## APPENDIX IX

## TRIM AND BUOYANCY AUGMENTATION SYSTEM STUDY

The first generation robot is operated with positive buoyancy so it will automatically come to the surface in the case of a motor failure. The amount of positive buoyancy and the trim is controlled by careful ballasting before the mission. The robot is kept below the surface by the thrust of the propulsion system and the lift of the control surfaces and the body itself to overcome the buoyancy. The vehicle was not equipped with any other buoyancy control system.

For the second generation robot, it is felt an easier method of trimming the vehicle is desirable. Such a system would eliminate the process of hand ballasting before the mission, which requires the operators to be right down next to the vehicle. An automatic system would also allow the robot to be operated in fresh and salt water alternately without changing onboard ballast weights.

The second generation robot is also designed to operate at depths down to 1,000 ft. From that depth the time for the vehicle to rise to the surface with five or ten pounds positive buoyancy and with no propulsion power, as in the case of an emergency surfacing, would be considerable. Additionally, a submarine with ten pounds of positive buoyancy on the surface could be neutrally buoyant, or even negatively buoyant, at 1,000 feet. In that condition, failure of a servo housing seal and subsequent flooding could spell doom for the



vehicle. For these reasons, it is felt necessary to provide a means to add additional buoyancy to the vehicle, even at depth. This additional buoyancy would also enable the robot to float higher out of the water on the surface so it is more visible for pickup.

The trim and buoyancy systems both operate similarly, since they change the balance between the weight and buoyancy of the vehicle. This balance can be altered in two ways: first by changing the buoyancy; and, second, by changing the vehicle's weight. Changing the buoyancy involves changing the displaced volume of the vehicle while keeping the weight constant. Changing the weight usually involves flooding or evacuating a compartment with water. The latter method is the most often employed.

Methods are available to alter the volume by using moving pistons in cylinders, but these structures are heavy and mechanically complicated, due to the movable piston which must be able to withstand the operating depth pressure. Another displacement altering system was employed by Alvin [3]. In this system, oil is carried in collapsible bladders located outside the pressure housing which can be transferred back and forth to special pressure housings. Transferring the oil changes the volume of the bladders and, thus, the buoyancy, while the weight of the submarine remains constant. Both of these methods are considered too complex for use in the robot.



Alternately, a tank flooding system involves filling two tanks, one forward and one aft, so the pitch can be controlled, with water until the desired draft and trim are achieved. The tanks are then sealed for the mission. These tanks must be able to withstand full operating pressure, since part of their volume will still be filled with air. A system such as this could use large tanks which at the end of a mission were evacuated to provide additional buoyancy. The evacuation, however, would have to be carefully controlled fore and aft so the robot would not be thrown too far out of trim during ascent.

For the robot, the system should be simple and involve as little weight and energy as possible. Several alternatives were considered, some combining the trim and buoyancy systems and others leaving them separate. The systems selected are presented schematically in Figures A9-1 and A9-2.

Separate trim and buoyancy systems are employed. This allows the heavier hard tanks required for the trim system to be as small as possible. For the buoyancy augmentation system, a bubble of gas would be trapped in a light weight enclosure surrounding the battery compartment. The position of the enclosure allows only one buoyancy tank to be used, which does not seriously affect the trim of the vehicle.

The trim system will consist of two tanks, one





FIGURE A9-1 SCHEMATIC DIAGRAM OF PROPOSED AUTOMATIC TRIM SYSTEM

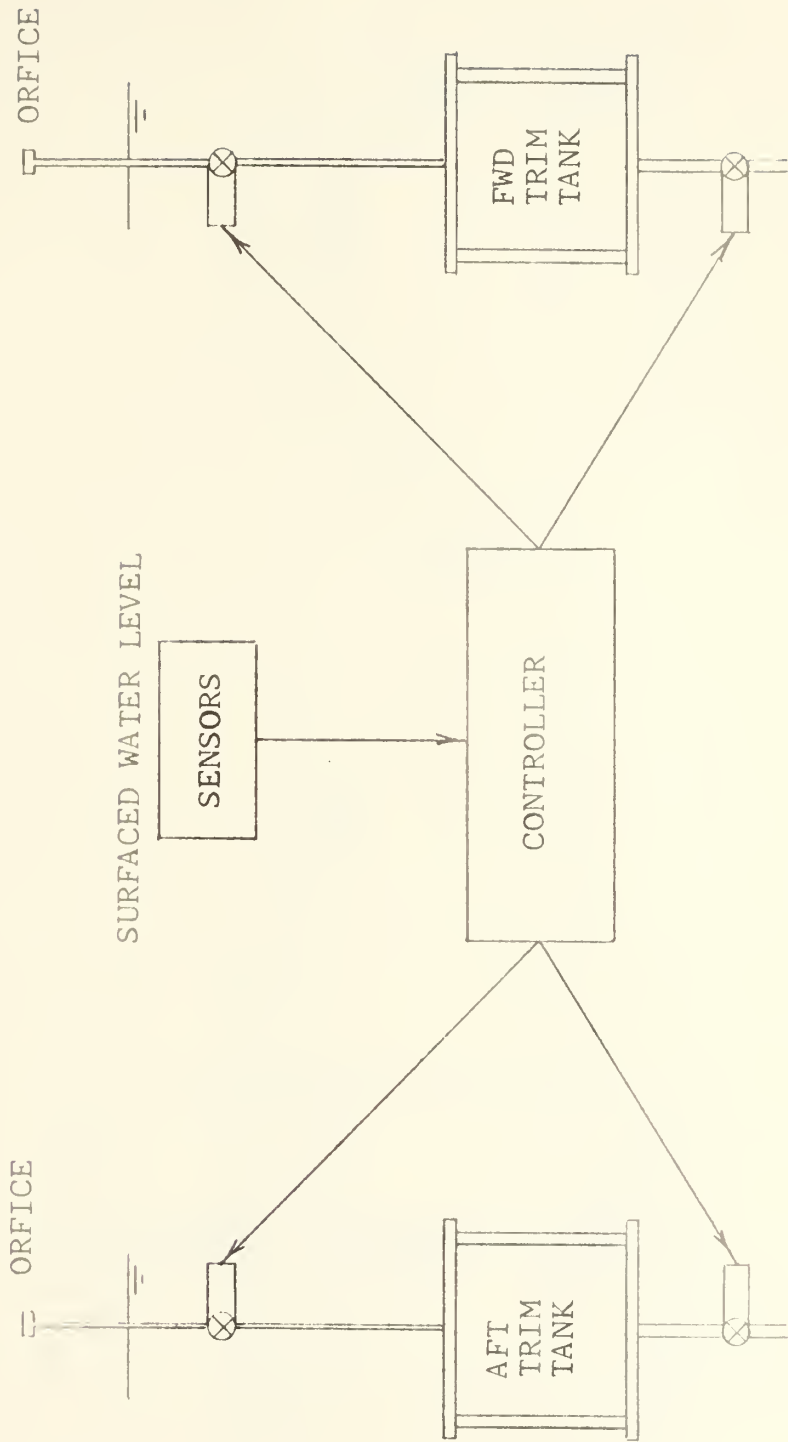
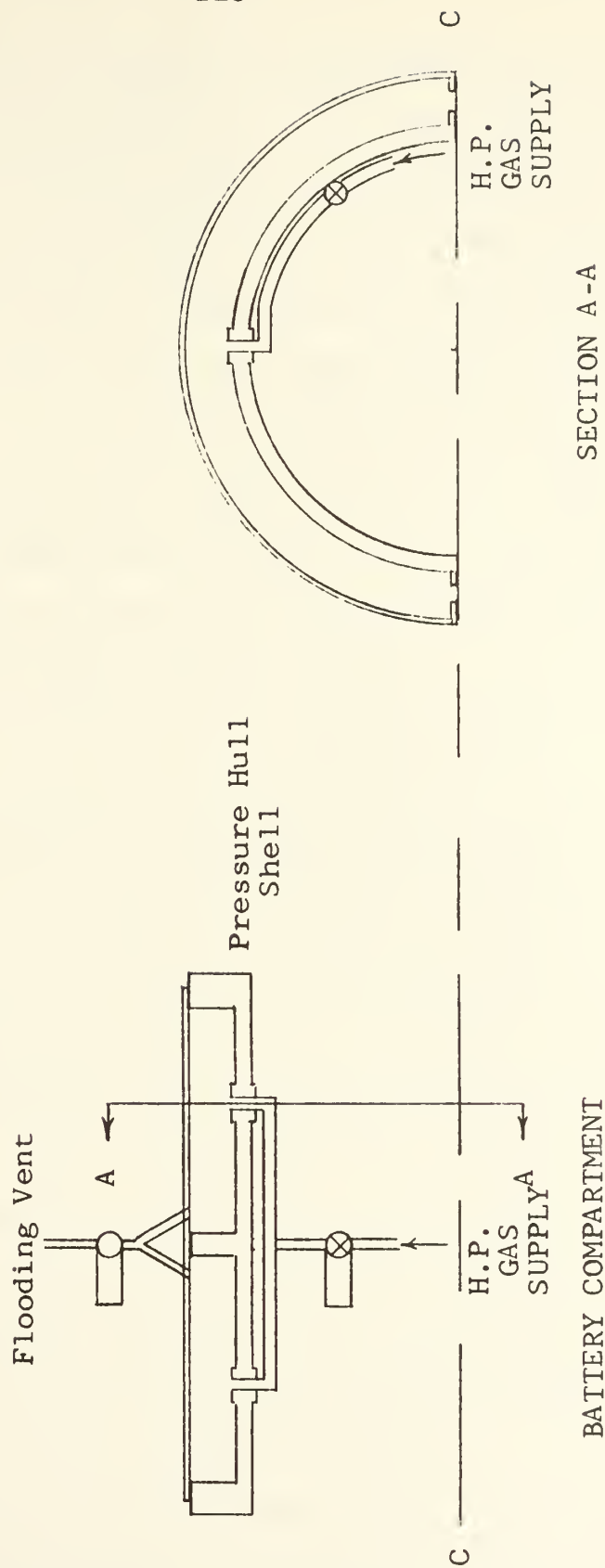




FIGURE A9-2 SCHEMATIC DIAGRAM OF PROPOSED BUOYANCY AUGMENTATION SYSTEM





forward and one aft. A pair of tubes lead to each tank, a bottom fill line and a top vent line. Both lines have solenoid activated, normally closed, two position, high pressure valves which control the flow. The vent line is additionally equipped with an orifice to restrict air flow and, thus, control the tank filling rate. The tanks are located low in the hull so they will be under water when the robot is placed in the water and to lower the center-of-gravity. They can be filled then, by merely opening the fill and vent valves. When the tanks are filled to the proper level, the valves are closed and the tanks remain sealed.

To coordinate the filling operation requires a controller, a pitch sensor, and a draft sensor. The draft sensor will be located inside the envelope where surface wave action will not disturb its reading. The controller will then sense the draft and trim and open and close the trim tank valves alternately until the desired draft, which corresponds to buoyancy, is achieved with zero pitch. At that point, the system will be secured. Provision is only made in this system for flooding. To drain the tanks, the submarine must be removed from the water and the valves opened. As a safety precaution, the valves will be designed to be held closed as the external pressure increases so they can not be inadvertently opened at depth.

This proposed trim system involves a minimum of moving parts and equipment to perform its task. The trim



tanks would be constructed of unstiffened aluminum pipe with flat end caps and would be sized to allow effective ballasting and trimming between fresh and salt water operations. Spherical glass tanks were also considered, but the smallest size available is too big for this application. These tanks need not be sized to compensate for changes in onboard equipment.

This proposed trim system is considered feasible, but is, at this stage, only conceptual. Development of an operational version will require testing to determine the proper fill rate as controlled by the vent line orifice, and development and testing of the sensors and controller. The concept is presented so an estimate of space and weight for such a system can be accounted for in the final design.

The proposed buoyancy augmentation system uses a partly sealed half cylinder placed over the frames of the battery compartment, which is sealed at the top and open to the sea on the bottom. There is also a controllable vent at the top which is opened during the submergence process to allow trapped air to escape. The vent will remain open until the submarine has been below the surface for a while so that all the air trapped in the enclosure gets a chance to escape. Small, high pressure, gas bottles, air or CO<sub>2</sub>, carried in the battery compartment will be connected by tubing through the pressure hull where they can be vented into the enclosure and, thus, evacuate the water. Flow of





the gas is regulated by another control valve which opens on mission completion, or in an emergency.

The previously proposed system is only possible if a double hull is employed. The required amount of buoyancy augmentation will have to be determined for each instance, but it should be sufficient to allow flooding of one of the servo motor housings and still bring the robot to the surface.

The previously proposed trim and buoyancy augmentation systems are felt to be acceptable low impact solutions to the problems. The design detail is not intended to be sufficient to allow construction, but is presented to prove system feasibility.



APPENDIX X  
ROBOT SIZING ROUTINE

## A10.0

Perhaps the most difficult problem facing the robot designer is to determine the overall size of the vehicle. The envelope size is a function of all the internal parts, and, in turn, affects the drag, which affects the propulsion plant size, which affects the battery size, etc. A routine to estimate the size and help calculate the performance is, therefore, very useful in performing these iterations.

This appendix presents a method for systematically looking at the vehicle size and estimating the performance. This method is outlined in Table A10-3.

The first step in the process is to estimate the volume required in the pressure hull for electronics and all other functions except the battery. This can be accomplished by adding the blocked volumes of the components and then increasing this value by a suitable percentage, 15 to 20 per cent, to account for the inefficiency of the enclosure and the additional volume required for connectors, supports, cabling, etc. The estimate should include all electronics including the expected payload items.

The second step is to select the battery from Appendix IV which might be suitable to provide the power for the vehicle. A detail must then be made of the battery



TABLE A10-3

## SUMMARY OF ROBOT SIZING ROUTINE STEPS

1. Determine required total payload volume + 15%.
2. Select candidate battery from appendix IV.
3. Determine battery compartment diameter and length,  $D$  and  $L_{bat}$
4. Using  $D$  and  $L_{bat}$  and the required volume for payload, calculate the internal volume in the cylindrical section of the pressure hull and then  $L_p$ .
5. Determine  $D_p = D + 2t_{shell} + 1.5$
6. Use figure A10-1 to determine  $L$ . The other curves may be more useful if the diameter of the pressure hull is not controlled by a large object such as the battery.
7. Use the computer program to determine speed vs power curves and optimum speed data.
8. Use the weight estimating routine to estimate the total weight of the vehicle.
9. Iterate through any or all of the steps again until satisfied with the results.



arrangement to determine the minimum diameter of the pressure hull and length of the compartment necessary to accommodate the battery. The battery is used to establish the hull diameter because it is usually the single largest individual component onboard. Then a suitable diameter of cylindrical pipe and wall thickness is chosen from the data provided in Appendix V.

To determine the outside cylinder diameter, use the following formula:

$$D_p = D_{\text{shell}} + 2 \times \text{wall thickness} + 1.5$$

The factor of 1.5 in the above equation accounts for the depth of the connecting flanges which hold the sections together.

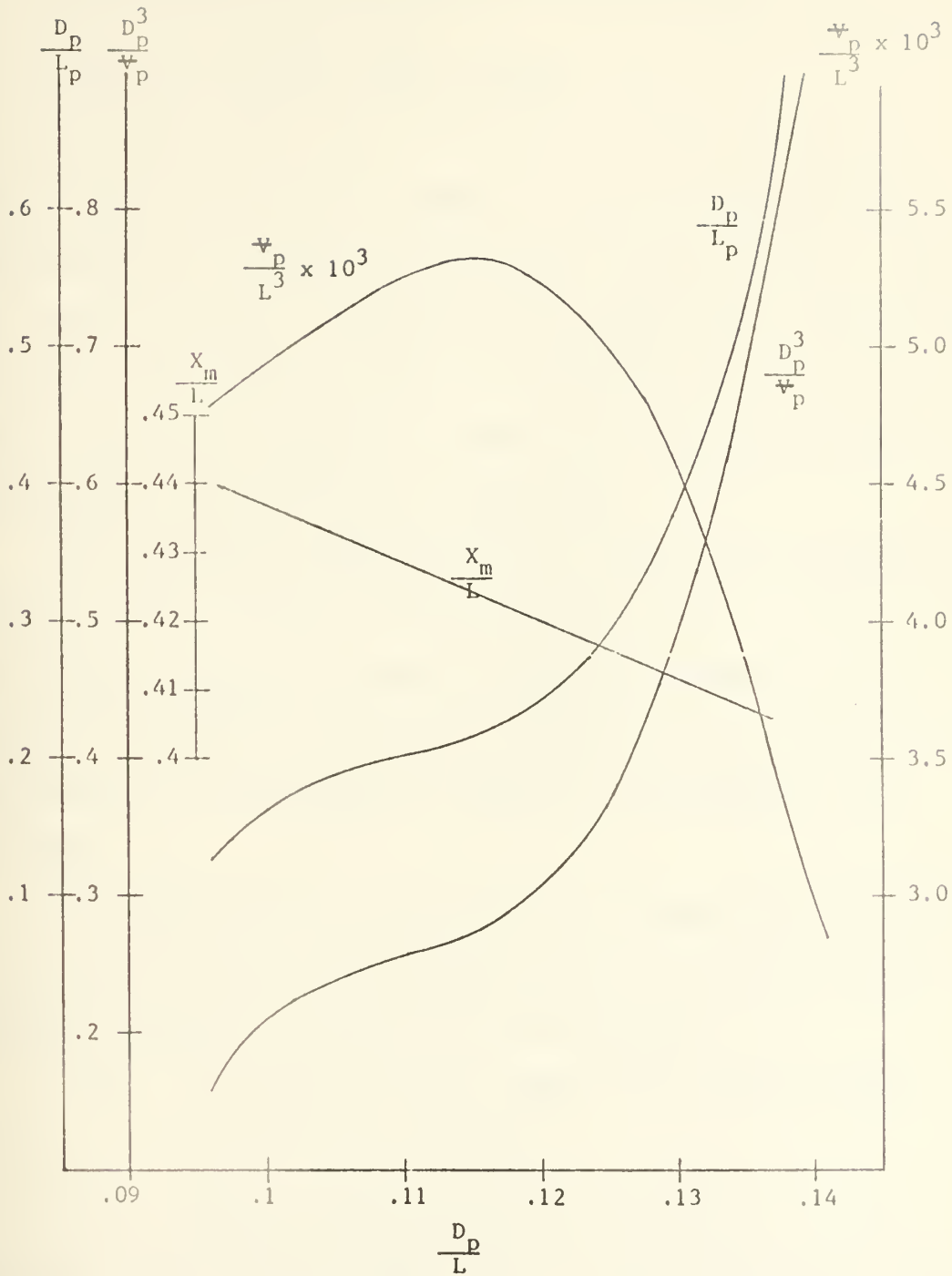
With the inside diameter of the pressure hull and the size of the battery compartment determined, this data can be used in conjunction with the volume required for electronics to calculate the total internal volume, less end closures, required for the pressure hull. The length of the pressure hull,  $L_p$ , can then be calculated.

With the values of  $D_p$  and  $L_p$  determined, and using the appropriate curve from Figure A10-1, the minimum length of the envelope can be determined. This length is the minimum length for the envelope and should be increased slightly for the actual design to allow clearance between the pressure hull and envelope. The estimated length from Figure A10-1 is, however, sufficiently accurate for comparison purposes.





FIGURE A10-1



RELATIONSHIPS BETWEEN CYLINDRICAL PRESSURE HULL PARAMETERS  
AND FORM 4165 ENVELOPE LENGTH



Figure A10-1 also shows curves relating

$$D_p^3/v_p, v_p/L^3 \times 10^3, \text{ to } D_p/L.$$

These other curves can be useful if other parameters are considered more suitable as an input than  $D_p$  and  $L_p$ . The  $x_M/L$  curve gives the location of the midpoint of the pressure hull from the envelope nose as a percentage of total envelope length. This information is useful for locating the fore and aft position of the battery compartment.

The previous routine does not take into account large objects located outside of the pressure hull. If this situation occurs, a detailed look at the arrangements in the wet volume of the envelope must be performed so the size of the envelope can be increased as needed to accommodate the equipment.

With the size of the vehicle estimated, an estimate of the vehicle's powering requirements can be made using a computer program developed for this purpose.

#### A10.1 Resistance versus Speed and Optimum Speed Calculation Program.

This computer program provides resistance versus speed data and optimum speed data for envelopes with various parameters.

The resistance calculations are computed using the method presented in [10]. This method involves writing an



expression for the total energy required for both propulsion and auxiliary or electronics load as a function of the speed over ground.

$$E_T = [P_O + K_D V_R^3] R/V_T$$

$P_O$  = Auxiliary electric load

$$K_D = 0.6779 \rho C_T S [1 + 2.3 \frac{S_t}{S}] / \eta_{OA}$$

$\eta_{OA} = \eta_{PC} \times \eta_{drive\ train} \times \eta_{motor} \times \eta_{battery\ conversion}$

0.6779 = A combination of constants and conversion factors to express the propulsion power in WATTS.

$V_T$  = Vehicle's speed over ground

$V_C$  = Current velocity (positive if in the same direction as  $V_T$ )

$V_R$  = Vehicle speed through water =  $V_T - V_C$

Setting the derivative of this equation with respect to  $V_T$  equal to zero yields a third order equation in  $V_T$  whose roots give values for  $V_T$  which are the best speeds to operate the robot at in a minimum energy sense. These solutions are as follows:

$V_T^*$  = optimum speed over ground

$V_T^* = A + B + (1/2)V_C$  one solution only

where  $V_C \leq V_{CO}$  and where:



$$A = \frac{V_{CO}}{2} \sqrt[3]{(2-X^3) + 2\sqrt{1-X^3}}$$

$$B = \frac{V_{CO}}{2} \sqrt[3]{(2-X^3) - 2\sqrt{1-X^3}}$$

$$V_{CO} = \sqrt[3]{[P_O/K_D]}$$

$$X = [V_C/V_{CO}]$$

$$V_T^* = \sqrt[3]{[P_O/2K_D]} \quad \text{if } V_C=0$$

when  $V_C > V_{CO}$  there are three real unequal solutions as follows:

$$V_T^* = A + B + (1/2)V_C$$

$$V_T^* = \frac{(A + B)}{2} + \frac{(A - B)}{2} j \sqrt{3} + (1/2)V_C$$

$$V_T^* = \frac{(A + B)}{2} - \frac{(A - B)}{2} j \sqrt{3} + (1/2)V_C$$

Here the correct solution must be chosen using engineering judgement.

The data required by the program is read in from a set of three data cards. The data cards are organized as follows:





## First Data Card

Column 1	1,2, or 3 code to determine hull form:  1 indicates series 58 form 4165 2 indicates series 58 form 4166 3 indicates series 58 form 4173
11-20	PO-Assumed auxiliary load (WATTS) or starting point load if several incremented values are to be investigated. If PO is specified as zero, the first iteration will use a value of PO=10 ; F Format.
21-30	Vehicle length, ft; F Format
31-40	Velocity increment in knots for speed verses power calculation: F Format
41-45	Number of iterations to perform in speed power calculation; I Format
51-60	Correction to $C_f$ due to hull roughness; F Format. Usually between $0.5 \times 10^{-3}$ and $1.2 \times 10^{-3}$

## Second Data Card

Column 1-10	Overall propulsion system efficiency. F Format  $= PC \times \eta_{\text{drivetrain}} \times \eta_{\text{motor}} \times \eta_{\text{Battery Conversion}}$
11-20	Factor to account for appendage drag; F Format.  $= 2.3 \left[ 1 + \frac{S_t}{S} \right]$
21-30	Current velocity increment in Knots - if opposing current



21-30 (continued)

+ if assisting current

F Format

31-40      Number of iterations to perform  
the optimum speed calculation using  
incremented values of  $V_C$ ; F Format

### Third Data Card

Column 1-5	Code to determine which value of $C_t$ to use in the optimum speed calculation in sea water. Must be less than IV. If the velocity increment for the speed power curve is 0.5 and this value is 3 then the $C_t$ at a velocity of 2 knots will be used in the optimum speed calculation. I Format.
10-15	Same code as above but determines $C_t$ for fresh water optimum speed Calculation. I Format
21-25	Number of iterations to perform in the assumed auxiliary power loop. Iteration will start at 10 watts if P0 is specified in data as zero and will be incremented by 5 watts for each iteration. Optimum speed calculations are then calculated for each auxiliary power increment.

A listing of the program with comments added for clarity is presented in table A10-1.



### A10.2 Sample Output from Speed versus Power and Optimum Speed Calculation Program.

The sample output presented in Table A10-2 is for the form 4165 equivalent envelope volume equivalent form presented in Appendix II with assumed auxiliary loads of 10, 12 and 17 watts with various opposing and assisting current velocities.

The first two pages of output are the resistance versus power figures in sea water and fresh water, respectively. The next six pages are the optimum velocities at the assumed auxiliary loads for the various opposing and assisting current velocities in sea and fresh water, respectively.

Choosing the correct speed through the water for the robot involves a good deal of engineering judgment. The conditions for the calculated optimum speed to be correct are very specific, but actual operation is not that way. These figures give the designer a target, however, which can be useful in making the decision. Other factors, such as minimum maneuvering speed, should be considered. It is also wise to assume a condition which is as adverse as might be reasonably expected in operation. This will yield a vehicle which will operate fairly well at most conditions and best at the most adverse condition.

In a very sophisticated design, the optimum speed calculated data could be used by the robot to allow the



vehicle to operate at near optimum velocity all the time. This would, however, require the vehicle to be able to measure both its speed through the water and the current velocity all the time so it could properly adjust its speed. This type of control is considered far too advanced to be given realistic consideration at this point in development, however.

In some cases, though, less sophisticated variations of this procedure could be used if the current was measured in the area of operation and then the computer programmed to alter the vehicle speed accordingly on various legs of the mission.

#### A10.3 Dry Weight Estimate.

The final phase of sizing the vehicle is to develop a method for estimating the dry weight of the vehicle. The output of the computer program presented in Appendix V listed the fresh water and salt water displacement for the pressure hull. In a vehicle of this type, the pressure hull provides a majority of the buoyancy for the vehicle.

To estimate the vehicle's dry weight, an estimate of the buoyancy of the remaining volume inside the envelope not enclosed by the pressure hull must be determined.

For submerged neutral buoyancy, the following must be true:





Robot Weight = Buoyancy

The buoyancy can be broken down into two parts.

First, the buoyancy of the pressure hull and, second, the buoyancy of everything else.

$$B = B_{PH} + B_R$$

also  $B_R = \nabla_R (\rho g)$

where  $\nabla_R$  is the volume of all the wet components in the hull. The concept of permeability,  $\mu$ , is useful in estimating this volume.

Permeability is a measure of the portion of a volume which could be filled with water. For example, an empty container has a permeability of 1.0. If an object is placed in the container, it will occupy some of the volume and the volume of water the container could hold will be reduced. A permeability of 0.9 would mean the container could only be filled with 90 per cent of the water it would hold if the object were not inside. Conversely, the volume of an object inside a container can be determined as follows:

$$\text{Object Volume} = \text{Container Volume} (1 - \mu).$$

For the robot, a reasonable value for the permeability of the flooded volume is 0.6. This value can vary



considerably according to the equipment contained in the wet volume, but 0.6 seems a reasonable estimate. With  $\mu$  determined, the volume occupied by equipment in the wet part of the envelope is as follows:

$$V_R = [V_E - (\text{Total Enclosed Pressure Hull Volume})] (1-\mu).$$

The estimated dry weight of the robot is then as follows:

$$W = \text{Pressure Hull displacement} + (\rho g) V_R$$

This weight estimate is very rough at this point and is considerably affected by the assumed value of  $\mu$ . A low estimate of  $\mu$  will yield a high estimate of the total vehicle weight. This can, however, be viewed as a conservative estimate. As the design progresses, the value of  $\mu$  can be refined to improve this overall weight estimate.

This analysis has not taken the weight or buoyancy of the propeller and appendages into account. However, the buoyancy of these parts is small in comparison with the remaining buoyancy and is not felt to seriously affect the estimate.

#### A10.4 Summary.



The previous discussion has presented a systematic method for estimating and calculating the size of a candidate robot vehicle. The various sections of this method can be used successively and refined with each iteration. The impact of pressure vessel volume and dimensions on the vehicle's performance can be easily investigated. This allows a rough look at various configurations without going into a great deal of detail. This routine has proved a useful tool in making trade off decisions.



TABLE A10-1 SPEED VERSUS POWER AND OPTIMUM SPEED CALCULATIONS PROGRAM LISTING

```

USER=VANCE 050 15420 JOINT COMPUTED FACILITY, WIT
C
C PROGRAM TO DETERMINE SPEED VS POWER AND OPTIMUM SPEED
C FOR A SHIPAVING CE SERIES 58 FORMS 4165, 4173, OR 4166.
C
C COVERED BY B, VTC1, VTC2, VTC3, CMFLX, JETA, CSQRT, CEXP, CLOG, CDRF
C I VD, L, VVTSW, VVJSTW, KDS, KDF
C DATA VI/8, K/5/
C
C 57 CONTINUE
C
C ITHUTP IS A CODE TO SPECIFY THE SERIES 58 FORM
C IF ITHUTP IS SPECIFIED AS 0 THEN THE PROGRAM WILL STOP. THIS IS
C THE METHOD TO USE TO TERMINATE THE PROGRAM.
C ITHUTP = 1 IS FOR FORM 4165
C ITHUTP = 2 IS FOR FORM 4166
C ITHUTP = 3 IS FOR FORM 4173
C
C PO IS THE ASSUMED AUXILIARY LOAD IN WATTS OR IT CAN BE THE
C STARTING AUXILIARY LOAD IF A RANGE OF AUXILIARY LOADS ARE TO BE
C INVESTIGATED
C IS PO IS SPECIFIED AS 2780 THEN THE OPTIMUM SPEED CALCULATION WILL
C USE A VALUE OF 100 FOR THE FIRST ITERATION ASSUMED AUXILIARY LOAD.
C
C VINC INDICATES THE SIZE OF THE SPEED INCREMENT USED IN CALCULATION
C THE DRAG VS SPEED IN KNOTS
C IVC IS THE NUMBER OF CTELS TO PERFORM IN THE DRAG VS SPEED
C CALCULATION.
C THE DRAG VS SPEED CALCULATION WILL START AT A SPEED OF ONE KNOT IN
C ALL CASES
C
C DCF IS THE CORRECTION FACTOR TO THE FRICTIONAL RESISTANCE
C COEFFICIENT DUE TO SURFACE ROUGHNESS USUALLY HAS A VALUE BETWEEN
C .4 AND .6 AND 1.1, 3-00.
C

```





TABLE A10-1 contd.

```

USER=RUNCE      069 15422      JOINT COMPUTER EFFICIENCY, *IT
      READ (K1,100) IHULTP,PO,L,VINC,IV,DCE
      IF(IHULTP.EQ.0) GO TO 888
      100 FORMAT (15,5X,3E10.5,15,5X,F10.5)
C
C EFFCA = OVERALL EFFICIENCY ASSUMED FOR THE OPTIMUM SPEED CALCULATION.
C EFFCI = PC * TRANSMISSION EFFICIENCY * MOTOR EFFICIENCY *
C BATTERY ENERGY CONVERSION EFFICIENCY.
C
C APENFT = THE APPENDAGE FRACTION
C APENFT = 1 + 2.3 * (WETTED SURFACE APPENDAGES/ WETTED SURFACE
C OF THE ENVELOPE)
C
C VINC = SIZE OF THE CURRENT VELOCITY STEP IN KNOTS USED IN THE
C OPTIMUM SPEED CALCULATION.
C TVC = NUMBER OF STEPS TO PERFORM FOR THE CURRENT VELOCITY IN THE
C OPTIMUM SPEED CALCULATION.
C
      READ (K1,101) EFFCA,APENFT,VCINC,IVC
      101 FORMAT (3E10.5,I5)
C
C ICTS = CODE NUMBER TO DETERMINE WHICH VALUE OF CT TO USE IN THE
C OPTIMUM SPEED CALCULATION IN SALT WATER. THIS VALUE MUST BE
C LESS THAN THE VALUE OF IV. A VALUE OF ICTS = 0 WITH A VALUE OF
C VINC = .5 MEANS THE VALUE OF CT AT A SPEED OF 2 KNOTS WILL BE
C USED IN THE OPTIMUM SPEED CALCULATION.
C ICTE = SAME CODE AS ICTS BUT FOR THE FRESH WATER OPTIMUM SPEED
C CALCULATION.
C
C IPO = NUMBER OF STEPS TO PERFORM IN THE AUXILIARY POWER LOOP.
C A VALUE OF 0 MEANS THE ASSUMED AUXILIARY LOAD WILL BE ONLY
C THAT ENTERED IN PC. IF IPO IS GREATER THAN 0 THE AUXILIARY LOAD WILL
C BE INCREMENTED BY 5 WATTS AND A SERIES OF OPTIMUM SPEED CALCULATIONS
C PERFORMED AT THE VARIOUS POWERS.

```



TABLE A10-1 contd.

```

USER=XXXXX  160 15420  JOINT COMPUTER FACILITY, MIT
C
      READ (K,102) ICTS,ICTP,IPC
      102 FORMAT (15,5X,15,5X,15)
C
C 101 IS THE SQUARE ROOT OF -1 TIMES THE SQUARE FOOT OF 3. IT IS USED
C IN THE "CRIT" SPEED CALCULATION.
      CRIT = (3.,1-.321)
C CALCULATE THE HULL PARAMETERS
C IF IHLTP = 1 THEN FORM IS 4165
      IF (IHLTP.EQ.1) GO TO 10
      30 TO 20
C
C DELCF IS THE RESIDUAL RESISTANCE WHICH IS CONSTANT FOR A
C PARTICULAR HULL FORM + DCF.
      10 DELCF = .07E-03 + DCF
C S IS THE WETTED SURFACE OF THE ENVELOPE
      S = .231 * (I**2.)
      30 TO 1
C IF IHLTP = 2 THEN FORM IS 4166
      20 IF (IHLTP.EQ.2) GO TO 30
      30 TO 40
C
      20 DELCF = .08E-03 + DCF
      S = .26 * (I**2.)
      30 TO 1
C IF IHLTP = 3 OR GREATER THEN FORM IS 4170
      40 DELCF = .13E-03 + DCF
      S = .34 * (I**2.)
      1 CONTINUE
C CORRECT FRESH AND SALT WATER CONSTANTS
C
C VISCS IS THE KINEMATIC VISCOSITY OF SALT WATER.
      VISCS = 1.26E-05

```



TABLE A10-1 contd.

```

USER=PUNCH      56 15420      JOINT COMPUTER FACILITY, MIT
C
C KVISFW IS THE KINEMATIC VISCOSITY OF FRESH WATER.
C
C      KVISFW = 1.21E-05
C
C ROFW IS THE DENSITY OF SALT WATER IN SLUGS PER CUBIC FOOT
C
C      ROFW = 1.09
C
C ROFW IS THE DENSITY OF FRESH WATER IN SLUGS PER CUBIC FOOT.
C
C      ROFW = 1.94
C
C VKTS IS THE VEHICLE SPEED IN KNOTS.
C      VKTS = 1.
C THESE STATEMENTS WRITE THE OUTPUT HEADINGS.
C      *PITS (X0,640)
C      *PITS (X0,305) INULP,L
C DO 200 I=1,NV
C      VEPS IS THE VEHICLE SPEED IN FEET PER SECOND.
C      VEPS = 1.689 * VKTS
C DENLW IS THE REYNOLD'S NUMBER BASED ON THE ENVELOPE LENGTH AND
C SPEED IN SALT WATER.
C      DENLW = (VEPS*L)/KVISFW
C CF IS THE FRICTIONAL RESISTANCE AND IS COMPUTED BY JACKSON'S FORMULA.
C      CF = .472/(#LOG10(REYNW)**2.58)
C CT IS THE TOTAL RESISTANCE COEFFICIENT AND IS THE SUM OF CF AND DELCP.
C      CT = CF + DELCP
C PT IS THE APPENDED ENVELOPE'S RESISTANCE IN POUNDS.
C      PT = .5 * ROFW * S * (VEPS**2.) * CT * ADEWPT
C WEP IS THE EQUIVALENT APPENDED HULL'S HORSE POWER.
C      WEP = (PT*VEPS)/550.

```



TABLE A10-1 contd.

```

USER=BRUCE      266 15422      JOINT COMPUTER FACILITY, MIT

      WRITE (K0,300) VKTS,VFPS,CT,PT,EHP
C  VEHICLE VELOCITY IS INCREMENTED BY VINCL FOR THE NEXT DRAG CALCULATION.
      VKTS = VKTS + VINCL
C  THIS STEP DETERMINES THE VALUE OF CT TO USE IN THE OPTIMUM SPEED
C  CALCULATION.
      IF (J.EQ.ICT5) CT0 = CT
200 CONTINUE
C  THE FOLLOWING CALCULATIONS COMPUTE THE RESISTANCE OF THE
C  ENVELOPE IN FRESH WATER
C  THESE STATEMENTS WRITE THE OUTPUT HEADINGS.
      WRITE (K0,640)
      WRITE (K0,310) IHUTP, L
      VKTS = 1.0
      DO 210 K = 1,IV
      VFPS = 1.689 * VKTS
C  REYNOLD IS THE REYNOLD'S NUMBER BASED ON THE ENVELOPE LENGTH AND SPEED
C  IN FRESH WATER.
      REYNLD = (VFPS*L)/KVISEW
      CF = .472/(ALOG10(REYNLD)**2.58)
      CT = CF + DELCF
      PT = .5*POW*(VFPS**2.)*CT + APENFT
      EHP = (PT*VFPS)/550.
      WRITE (K0,300) VKTS,VFPS,CT,PT,EHP
C  VEHICLE VELOCITY IS INCREMENTED BY VINCL FOR THE NEXT DRAG CALCULATION.
      VKTS = VKTS + VINCL
C  THIS CARD DETERMINE THE VALUE OF CT TO USE IN THE OPTIMUM SPEED
C  CALCULATION.
      IF (K.EQ.ICT5) CT0F = CT
210 CONTINUE
C  CALCULATE KE.C
C  KDS IS A COEFFICIENT WHICH WHEN MULTIPLIED BY THE VELOCITY CUBED
C  GIVES THE POWER SUPPLIED FROM THE ENERGY STORAGE SYSTEM FOR THE
C  PROPULSION SYSTEM.

```





TABLE A10-1 contd.

```

USER=BUNCE      266 15422      JOINT COMPUTER FACILITY, MIT

      VDS = (.6779*POSW*S*CTO*APENFT) / ZFICA
C KDF IS THE SAME AS KFS BUT IS FOR FRESH WATER.
      KDF = (.6779*FOFW*S*CTO*APENFT) / EFOA
C DETERMINE THE OPTIMUM SPEED
C THE OPTIMUM SPEED CALCULATIONS ARE PERFORMED ACCORDING TO THE
C METHOD DESCRIBED IN APPENDIX IX.
C THE OPTIMUM SPEED IS DEFINED AS THE SPEED WHICH GIVES THE LONGEST
C VEHICLE RANGE POSSIBLE WITH THE PARAMETERS ASSUMED.
C THE OPTIMUM SPEED CALCULATION WILL BE PERFORMED FOR SEVERAL VALUES OF
C AUXILIARY LOAD IF DESIRED BY SPECIFYING THE VALUE OF M AND PO.
C M IS AN INDEX TO DETERMINE THE NUMBER OF ITERATIONS TO PERFORM FOR THE
C OPTIMUM SPEED CALCULATION USING VARIOUS VALUES OF THE AUXILIARY LOAD.
      I = 0
C TEST PO. IF IT WAS READ IN AS ZERO THEN THE FIRST VALUE USED IN
C THE OPTIMUM SPEED CALCULATION FOR THE AUXILIARY LOAD WILL BE 10.
C IF PO WAS READ IN AS NON ZERO THEN THE AUXILIARY LOAD LOOP WILL
C START WITH THE SPECIFIED AUXILIARY LOAD.
      IF (PO.LE..001) GO TO 220
      GO TO 230
220 CONTINUE
      PO = 10.
215 M = M + 1
230 CONTINUE
C VC IS THE OPPOSING CURRENT VELOCITY TO THE SUBMARINE'S DIRECTION.
C VC IS POSITIVE IF ACTING IN THE SAME DIRECTION AS THE SUBMARINE'S
C MOTION.
C PERFORM THE OPTIMUM SPEED CALCULATION IN SALT WATER.
      VC = 0.
C VTO IS THE OPTIMUM VELOCITY OVER GROUND IN FEET PER SECOND.
      VTO = (PO/(2.*KDS))**.33333
C THESE STATEMENTS WRITE THE OUTPUT HEADINGS.
      WRITE (NO,641) INHUTP,L
      WRITE (NO,325) PO,VTC

```



TABLE A10-1 contd.

```

USER=EUNCE      266 15422      JOINT COMPUTER FACILITY, MIT

DO 400 N = 1, TVC
  VC = VC + VCINC * 1.689
  VCO = (PO/KDS)** .33333
  Y = VC/VCO
  Y3 = Y**3.
  TMX3 = 2. - Y3
  CMX3 = 1. - Y3
  VCO2 = VCO/2.
  IF (VC.EQ.VCO) GO TO 411
  AR = VCO2 * (TMX3 + 2. * SQRT(OMY3))** .333333
  BR = VCO2 * (TMX3 - 2. * SQRT(OMY3)) ** .333333
  VIC = AR + BR + .5*VC
  WRITE (K0,320) VC,VIC
  GO TO 400
411 CONTINUE
  CDRT = CSORT(CMPLX(OMX3,0.))
  A = VCO2 * CEYF((CLOG(TMX3+2.*CDRT))/3.)
  B = VCO2 * CEYF((CLOG(TMX3-2.*CDRT))/3.)
  C VTO1, VTO2, VTO3 ARE THE THREE ROOTS OF THE CUBIC EQUATION IF
  C X HAS A VALUE GREATER THAN ONE. IF Y IS GREATER THAN ONE THEN THESE
  C WILL BE THREE SOLUTIONS FOR THE OPTIMUM SPEED. THEY WILL ALL BE REAL
  C AND TWO OF THEM SHOULD BE EQUAL. ENGINEERING JUDGEMENT MUST BE USED
  C TO SELECT THE CORRECT VALUE.
  VTO1 = A + B + .5*CMPLX(VC,0.)
  VTO2 = ((A+B)/2.)+((A-B)/2.)*JPT3+ (.5*CMPLX(VC,0.))
  VTO3 = ((A+B)/2.)-((A-B)/2.)*JPT3 + (.5*CMPLX(VC,0.))
  WRITE (K0,330) VC,VTO1,VTO2,VTO3
400 CONTINUE
C THE PROGRAM NOW PERFORMS THE SAME CALCULATION FOR THE OPTIMUM SPEED
C BUT THIS TIME THE VEHICLE IS ASSUMED OPERATING IN FRESH WATER.
VC = 0.
VTO = (PO/(2.*KDF))** .33333
C THESE STATEMENTS WRITE THE OUTPUT HEADINGS.

```



TABLE A10-1 contd.

```

USER=BUSCE      266 15422      JOINT COMPUTER FACILITY, MIT

WRITE (K0,641) IHULTP,L
WRITE (V0,321) PC,VTO
DO 415 J = 1,IVC
VC = VC + VCINC * 1.689
VCO = (V0/KDF) **.33333
Y = VC/VCO
V3 = Y**3.
TMX3 = 2. - X3
CMX3 = 1. - Y3
VCO2 = VCO/2.
IF (VC.GT.VCO) GO TO 421
AB = VCO2 * (TMX3 + 2. * SQRT(CMX3))**.333333
BB = VCO2 * (TMX3 - 2. * SQRT(CMX3)) **.333333
VTO = AB + BB + .5*VC
WRITE (K0,320) VC, VTO
GO TO 415

421 CONTINUE
CDRT = CSQRT(CMPLX(CMX3,0.))
A = VCO2 * CEXP((CLOG(TM3+2.*CDRT))/3.)
B = VCO2 * CEXP((CLOG(TM3-2.*CDRT))/3.)
VTO1 = A + B + .5*CMPLX(VCO,0.)
VTO2 = ((A+B)/2.)+((A-B)/2.)*JRT3+.5*CMPLX(VCO,0.)
VTO3 = ((A+B)/2.)-((A-B)/2.)*JRT3 + (.5*CMPLX(VCO,0.))
WRITE (K0,330) VC,VTO1,VTO2,VTO3

415 CONTINUE
IF (PC.GE.4.) PC = PC+5.
IF (PC.LE.1.001) PC = 5.
C THIS STEP DETERMINES IF THE PROGRAM SHOULD CALCULATE OPTIMUM
C SPEED FOR ANOTHER ASSUMED AUXILIARY LOAD.
240 IF (M.IT.IPO) GO TO 215
C THE FOLLOWING CARDS ARE THE OUTPUT FORMAT CARDS.
C
C

```



TABLE A10-1 contd.

```

6000=SUVEC 160 17520 JOINT COMPUTE FACILITY, MIT

(40 FORMAT ('1', '//////////'))
641 FORNAT ('1', '//////////10X', 'OPTIMUM VELOCITIES ARE FOR FORNAT',
1 1Y, '12', 'LENGTH', F6.3, ' FT', '///',
210Y, 'ALL VELOCITIES ARE OVER SPOWIP', '///',
310Y, 'SPOWIP THROUGH THE WATER = V OPTIMUM', '///',
410Y, 'ALL VELOCITIES ARE IN FEET PER SECOND', '///')
3 5 FORNAT ('1X', 'THE FOLLOWING DATA IS CALCULATED FOR FULL FLOW',
11Y, 'TYPE', '12.2Y', 'LENGTH =', F7.3, '10X', 'THE REM WATER SPEED VS',
21Y, 'POWER DATA IS AS FOLLOWS', '///', '10Y', 'V KNOTS', '11Y', 'V FPS',
31Y, 'CT', '16X', 'FT', '15Y', 'END', '///')
310 FORNAT ('1Y', 'F7.3, 10Y, F7.3, 10Y, F7.3, 10Y, F7.4)
310 FORNAT ('10X', 'THE FOLLOWING DATA IS CALCULATED FOR FULL FLOW',
11Y, 'TYPE', '12.2Y', 'LENGTH =', F7.3, '10X', 'THE REM WATER SPEED VS',
2 POWER DATA IS AS FOLLOWS', '///', '10Y', 'V KNOTS', '11Y', 'V FPS', '15Y',
3 CT', '16Y', 'FT', '15Y', 'END', '///')
325 FORNAT(
1 10X, 'IN SEA WATER WITH AN AUXILIARY LOAD OF', '1X', '5.1', ' WATTS',
2 ' WE CALCULATE THE FOLLOWING', '///', '10Y', 'OPTIMUM SPEEDS FOR',
3 ' OPPOSING CURRENT VELOCITIES INDICATED', '///',
410Y, 'WITH ZERO CURRENT THE',
5 OPTIMUM VELOCITY IS', F7.3, '2Y', 'FEET PER SECOND', '///')
220 FORNAT('10Y', 'FOR A CURRENT VELOCITY =', F5.2, ' THE OPTIMUM',
1 VELOCITY IS', F8.3, '///')
330 FORNAT('10X', 'FOR A CURRENT VELOCITY =', F6.2, 'THE OPTIMUM',
1 VELOCITIES ARE AS FOLLOWS', '///', '20X', 'V OPT 1 =', F12.4, '4X', '1',
211.4, '20X', 'V OPT 2 =', F12.4, '4Y', '1', F11.4, '20X', 'V OPT 3 =',
3 F12.4, '4Y', '1', F11.4, '///')
321 FORNAT('10', 'IF FEESH WATER WITH AN AUXILIARY LOAD OF', F5.1, '2Y',
1 WATTS, WE CALCULATE THE FOLLOWING', '///',
2 10Y, 'OPTIMUM SPEEDS FOR OPPOSING CURRENT VELOCITIES INDICATED',
1///, '1X', 'WITH ZERO CURRENT THE',
3 OPTIMUM VELOCITY IS', F10.5, '2Y', 'FEET PER SECOND', '///')
642 FORNAT('11')

```





TABLE A10-1 contd.  
 REFERENCE 63 13420 JOINT COMPUTER FACILITY, WIT

TO C 7  
 RE C-1000  
 C-1000 (2, 400)  
 C-1000  
 BY  
 C-1000 \* 1000 (10) NO 1000



TABLE A10-2 SAMPLE OUTPUT FROM SPEED VERSUS POWER  
AND OPTIMUM SPEED CALCULATION PROGRAM.

THE FOLLOWING DATA IS CALCULATED FOR HULL FORM TYPE 1 LENGTH = 9.300

THE SEA WATER SPEED VS POWER DATA IS AS FOLLOWS.

V KNOTS	V FPS	CT	RT	EHP
1.00	1.689	0.5025E-02	0.479	0.0015
1.50	2.533	0.4709E-02	1.010	0.0047
2.00	3.376	0.4504E-02	1.716	0.0105
2.50	4.222	0.4354E-02	2.593	0.0199
3.00	5.067	0.4238E-02	3.634	0.0335
3.50	5.911	0.4143E-02	4.935	0.0520
4.00	5.755	0.4064E-02	6.195	0.0761
4.50	7.600	0.3996E-02	7.709	0.1065
5.00	3.445	0.3936E-02	9.376	0.1440
5.50	9.269	0.3884E-02	11.195	0.1891



TABLE A10-2 contd.

THE FOLLOWING DATA IS CALCULATED FOR HULL FORM TYPE 1 LENGTH = 9.300  
 THE FRESH WATER SPEED VS POWER DATA IS AS FOLLOWS.

V KNOTS	V FPS	CT	RT	EHP
1.00	1.689	0.4989E-02	0.463	0.0014
1.50	2.533	0.4677E-02	0.977	0.0045
2.00	3.373	0.4474E-02	1.652	0.0102
2.50	4.222	0.4326E-02	2.511	0.0193
3.00	5.067	0.4210E-02	3.520	0.0324
3.50	5.911	0.4117E-02	4.684	0.0503
4.00	6.756	0.4038E-02	6.001	0.0737
4.50	7.600	0.3971E-02	7.469	0.1032
5.00	8.445	0.3912E-02	9.085	0.1395
5.50	9.289	0.3860E-02	10.847	0.1832



TABLE A10-2 contd.

OPTIMUM VELOCITIES ARE FOR FCPM TYPE 1 LENGTH 9.300 FT.

ALL VELOCITIES ARE OVER GROUND.

SPEED THROUGH THE WATER = V OPTIMUM - V CURRENT

ALL VELOCITIES ARE IN FEET PER SECOND.

IN SEA WATER WITH AN AUXILIARY LOAD OF 10.0 WATTS, WE CALCULATE THE FOLLOWING  
OPTIMUM SPEEDS FOR OPPOSING CURRENT VELOCITIES INDICATED.

WITH ZERO CURRENT THE OPTIMUM VELOCITY IS 1.967 FT PER SECOND

FOR A CURRENT VELOCITY = -0.84 THE OPTIMUM VELOCITY IS 1.647

FOR A CURRENT VELOCITY = -1.69 THE OPTIMUM VELOCITY IS 1.564

FOR A CURRENT VELOCITY = -2.54 THE OPTIMUM VELOCITY IS 1.693

FOR A CURRENT VELOCITY = -3.39 THE OPTIMUM VELOCITY IS 1.956





TABLE A10-2 contd.

OPTIMUM VELOCITIES ARE FOR FCM TYPE 1 LENGTH 9.300 FT.

ALL VELOCITIES ARE OVER GROUND.

SPEED THROUGH THE WATER =  $V_{OPTIMUM} - V_{CURRENT}$

ALL VELOCITIES ARE IN FEET PER SECOND.

IN FRESH WATER WITH AN AUXILIARY LOAD OF 10.0 WATTS. WE CALCULATE THE FOLLOWING  
OPTIMUM SPEEDS FOR OPPOSING CURRENT VELOCITIES INDICATED.

WITH ZERO CURRENT THE OPTIMUM VELOCITY IS 1.98786 FEET PER SECOND

FOR A CURRENT VELOCITY = -0.84 THE OPTIMUM VELOCITY IS 1.667

FOR A CURRENT VELOCITY = -1.69 THE OPTIMUM VELOCITY IS 1.580

FOR A CURRENT VELOCITY = -2.53 THE OPTIMUM VELOCITY IS 1.704

FOR A CURRENT VELOCITY = -3.38 THE OPTIMUM VELOCITY IS 1.964



TABLE A10-2 contd.

OPTIMUM VELOCITIES ARE FOR FORM TYPE 1 LENGTH 9.300 FT.

ALL VELOCITIES ARE OVER GROUND.

SPEED THROUGH THE WATER = V OPTIMUM - V CURRENT

ALL VELOCITIES ARE IN FEET PER SECOND.

IN SEA WATER WITH AN AUXILIARY LOAD OF 12.0 WATTS, WE CALCULATE THE FOLLOWING  
OPTIMUM SPEEDS FOR OPPOSING CURRENT VELOCITIES INDICATED.

WITH ZERO CURRENT THE OPTIMUM VELOCITY IS 2.067 FT PER SECOND

FOR A CURRENT VELOCITY = 0.84 THE OPTIMUM VELOCITY IS 2.564

FOR A CURRENT VELOCITY = 1.69 THE OPTIMUM VELOCITY IS 3.171

FOR A CURRENT VELOCITY = 2.53 THE OPTIMUM VELOCITY IS 3.847

FOR A CURRENT VELOCITY = 3.38 THE OPTIMUM VELOCITIES ARE AS FOLLOWS,

V OPT 1 =	0.4566E 01	I 0.0000E 00
V OPT 2 =	0.1534E 01	I 0.0000E 00
V OPT 3 =	0.4661E 01	I 0.0000E 00



TABLE A10-2 contd.

OPTIMUM VELOCITIES ARE FOR FORM TYPE 1 LENGTH 9.300 FT.

ALL VELOCITIES ARE OVER GROUND.

SPEED THROUGH THE WATER = V OPTIMUM - V CURRENT

ALL VELOCITIES ARE IN FEET PER SECOND.

IN FRESH WATER WITH AN AUXILIARY LOAD OF 12.0 WATTS. WE CALCULATE THE FOLLOWING  
OPTIMUM SPEEDS FOR OPPOSING CURRENT VELOCITIES INDICATED.

WITH ZERO CURRENT THE OPTIMUM VELOCITY IS 2.08884 FEET PER SECOND

FOR A CURRENT VELOCITY = 0.84 THE OPTIMUM VELOCITY IS 2.595

FOR A CURRENT VELOCITY = 1.69 THE OPTIMUM VELOCITY IS 3.192

FOR A CURRENT VELOCITY = 2.53 THE OPTIMUM VELOCITY IS 3.856

FOR A CURRENT VELOCITY = 3.38 THE OPTIMUM VELOCITIES ARE AS FOLLOWS,

V OPT 1 = 0.4593E 01 I 0.0000E 00

V OPT 2 = 0.1629E 01 I 0.1652E-05

V OPT 3 = 0.4645E 01 I 0.1652E-05



TABLE A10-2 contd.

OPTIMUM VELOCITIES ARE FOR FORM TYPE 1 LENGTH 9.300 FT.

ALL VELOCITIES ARE OVER GROUND.

SPEED THROUGH THE WATER = V OPTIMUM - V CURRENT

ALL VELOCITIES ARE IN FEET PER SECOND.

IN SEA WATER WITH AN AUXILIARY LOAD OF 17.0 WATTS, WE CALCULATE THE FOLLOWING  
OPTIMUM SPEEDS FOR OPPOSING CURRENT VELOCITIES INDICATED.

WITH ZERO CURRENT THE OPTIMUM VELOCITY IS 2.321 FT PER SECOND

FOR A CURRENT VELOCITY = 0.84 THE OPTIMUM VELOCITY IS 2.811

FOR A CURRENT VELOCITY = 1.69 THE OPTIMUM VELOCITY IS 3.404

FOR A CURRENT VELOCITY = 2.53 THE OPTIMUM VELOCITY IS 4.055

FOR A CURRENT VELOCITY = 3.38 THE OPTIMUM VELOCITIES ARE AS FOLLOWS,

V OPT 1 =	0.4769E 01	I 0.0000E 00
V OPT 2 =	0.2022E 01	I 0.0000E 00
V OPT 3 =	0.4430E 01	I 0.0000E 00





TABLE A10-2 contd.

OPTIMUM VELOCITIES ARE FOR FCP\* TYPE 1 LENGTH 9.300 FT.

ALL VELOCITIES ARE OVER GROUND.

SPEED THROUGH THE WATER = V OPTIMUM - V CURRENT

ALL VELOCITIES ARE IN FEET PER SECOND.

IN FRESH WATER WITH AN AUXILIARY LOAD OF 17.0 WATTS. WE CALCULATE THE FOLLOWING  
OPTIMUM SPEEDS FOR OPPOSING CURRENT VELOCITIES INDICATED.

WITH ZERO CURRENT THE OPTIMUM VELOCITY IS 2.34599 FEET PER SECOND

FOR A CURRENT VELOCITY = 0.34 THE OPTIMUM VELOCITY IS 2.835

FOR A CURRENT VELOCITY = 1.69 THE OPTIMUM VELOCITY IS 3.427

FOR A CURRENT VELOCITY = 2.53 THE OPTIMUM VELOCITY IS 4.097

FOR A CURRENT VELOCITY = 3.38 THE OPTIMUM VELOCITIES ARE AS FOLLOWS,

V OPT 1 =	0.4790E 01	I 0.0000E 00
V OPT 2 =	0.2070E 01	I 0.0000E 00
V OPT 3 =	0.4400E 01	I 0.0000E 00



## REFERENCES

- [1] Ballard, R. D. and Emery, K. O., Research Submersibles in Oceanography, Washington D. C.: Marine Technology Society, 1970.
- [2] Terry, Richard D., The Deep Submersible, North Hollywood, California: Western Periodicals Co., 1966.
- [3] "Alvin, 6000 ft. Submergence Research Vehicle", SNAME Transactions, Vol. 74, 1966.
- [4] Covey, Charles W., "Aluminaut", Underseas Technology, Sept. 1964.
- [5] Rind, H., "Parametric Analysis of Submersibles", Marine Technology Society Journal, Vol. 6, No. 5, Sept. - Oct. 1972.
- [6] "Technical Description of Curv III", Proto Power Management Corp., Sept. 1976.
- [7] Vados, J. R., "International Status and Utilization of Undersea Vehicles", NOAA, U. S. Department of Commerce, 1976.
- [8] Francois, R. E. and Nodland, W. E., "Unmanned Arctic Research Submersible (UARS), System Development and Test Report", APL/UW Report 7219, Sept. 1972.
- [9] "OSR System Vol. 1 development of Ocean Space Robot for Measurement of Oceanographic Parameters", Japan Society for the Promotion of Machine Industry, Nov. 1974.
- [10] Johnson, H. A., Verderese, A. J. and Hansen, R. J., "A Smart Multi-Mission Unmanned Free Swimming Submersible", Naval Engineer's Journal, April 1976.
- [11] "Robot Submarine", Unpublished paper; Summary of the First Generation MIT Robot Submarine.
- [12] M.I.T. Sea Grant Report No. 75-12, (Ocean Engineering Summer Laboratory), 1975.
- [13] M.I.T. Sea Grant Report No. 76-3, (Ocean Engineering Summer Laboratory), 1976.



## REFERENCES (Cont'd.)

- [14] Nowak, David, An Analysis and Design of the Propulsion System of a Small Robot Submersible, Unpublished Master's Thesis, Cambridge, Massachusetts: MIT Department of Ocean Engineering, May 1974.
- [15] Keller, G., Automatic Control of a Computer Piloted Submersible, Unpublished Master's Thesis, Cambridge, Massachusetts, MIT Department of Ocean Engineering, Sept. 1976.
- [16] Carmichael, Bruce H., "Underwater Drag Reduction Through Choice of Shape", AIAA Paper No. 66-657, 1966.
- [17] Parsons, J. S. and Goodson, R. E., "The Optimum Shaping of Axisymmetric Bodies for Minimum Drag", Purdue University Automatic Control Center, Report No. ACC-72-5, June 1972.
- [18] Gertler, M., "Resistance Experiments on a Systematic Series of Streamlined Bodies of Revolution for Application to the Design of High-Speed Submarines". DTMB Report C-297, 1950.
- [19] Jackson, H. A., Class Notes from Submarine Design Course, Professional Summer at MIT, 1976.
- [20] Lindgren, H., Jung, I., and Hillander, H., "Contra-rotating Propellers Analysis and Overall Arrangement", STAL-LAVAL Technical Information Letter 22.8.67, May 1967.
- [21] Tejsen, S., "A Comparison of Contra-rotating Propellers with other Propulsion Systems, Results of Model Experiments", Marine Technology, Jan. 1972.
- [22] Steele, T. W., "Propulsion Machinery Considerations for Contra-rotating Propeller Systems", Marine Technology, Oct. 1970.
- [23] Oosterveld, M. W. C. and Van Oossanen, P., "Ship Research Activities in the Netherlands", International Shipbuilding Progress, July 1972.
- [24] Van Gunsteren, L. A., "Ring Propellers and Their Combination with a Stator", Marine Technology, Oct. 1970.



## REFERENCES (Cont'd.)

- [25] Van Manen, J. D. and Oosterveld, M. W. C., "Analysis of Ducted Propeller Design", SNAME Transactions, 1972.
- [26] Oosterveld, M. W. C., Wake Adapted Ducted Propellers, Wageningen, Netherlands: Publication 345 Netherlands Ship Model Basin, 1972.
- [27] Van Manen, J. D. and Oosterveld, M. W. C., Series of Model Tests on Ducted Propellers, Wageningen, Netherlands: Netherlands Ship Model Basin, 1972.
- [28] Oosterveld, M. W. C., "Model Tests with Decelerating Nozzles", International Shipbuilding Progress, June 1966.
- [29] Van Manen, J. D., "Recent Research on Propellers in Nozzles", International Shipbuilding Progress, August 1957.
- [30] Oosterveld, M. W. C., Design and Economical Considerations on Shipbuilding and Shipping, Wageningen, Netherlands: Report on the Post Graduate Course, 1969.
- [31] Meyerhoff, L. and Hill, J. G., "Ducted Propeller Applications for Modern Ships", SNAME Transactions, 1972.
- [32] Beveridge, John L., "Hydrodynamic Performance of a Proposed Cruising Ducted Propeller for Submarines", NSDRC Report No. 3374, April 1971.
- [33] Triantafyllou, M., "Diagrams for Optimum B-Series Propeller Design", MIT Department of Ocean Engineering Project Number 13-712, 1975.
- [34] "Energy Systems of Extended Endurance in the 1-100 Kilowatt Range for Undersea Applications", Committee on Undersea Warfare National Research Council, 1968.
- [35] "Proceedings of the Underwater Propulsion Conference", Sponsored by the Undersea Warfare Weaponry Program Advisory Group, August 26 - 27, 1974.
- [36] Morse, E. M., "Zinc-Oxygen Battery System", Nineteenth Annual Power Sources Conference, 1965.





## REFERENCES (Cont'd.)

- [37] Wagner, O., "Metal-Air (Oxygen) Batteries", Twenty-fifth Annual Power Sources Conference, May 16-17-18, 1967.
- [38] Bartosh, S., "Capabilities of Mechanically Rechargeable Zinc-Air Batteries", Twenty-fifth Annual Power Sources Symposium Proceedings, May 23-24-25, 1972.
- [39] Heronemus, W. and Kidd, G., Some Deep Sea Vehicle Personnel Hulls and Energy Storage Subsystems, Massachusetts University School of Engineering, Thesis-UM-70-7, 1970.
- [40] Berju, K., Daniels, E. and Stohlein, E., "Characteristics of Lead-Acid and Silver-Zinc Batteries in the Deep Ocean Environment", Marine Electrochemistry Symposium, 1972.
- [41] Leveau, Carl W., "Aluminum and Its Use in Naval Craft", Naval Engineer's Journal, April 1965.
- [42] Comstock, John B., ed., Principles of Naval Architecture, New York: SNAME, 1967.
- [43] Abkowitz, Martin A., Stability and Motion Control of Ocean Vehicles, Cambridge, Massachusetts: MIT Press, 1972.
- [44] Kritz, Jack, "Dopplar Sonar Navigator for Work Submersibles", 1970 Offshore Technology Conference, Houston, Texas, April 22-24, 1970.







Thesis  
B848

Bunce

171164

A proposed preliminary design for a second generation of the M. I. T. robot, data collecting, submarine.

2 NOV 77  
JAN 23 78  
23 APR 87

DISPLAY  
25275  
29763  
33350

Thesis  
B848

Bunce

171164

A proposed preliminary design for a second generation of the M. I. T. robot, data collecting, submarine.

thesB848

A proposed preliminary design for a seco



3 2768 002 07913 9

DUDLEY KNOX LIBRARY